N 70 14573
NASA-CR-72520

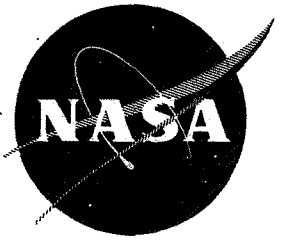

DEVELOPMENT AND EVALUATION OF CONTROLLED VISCOSITY COATINGS FOR SUPERALLOYS

by
R. B. Grekila, J. W. Chapman, D. M. Mattox

WESTINGHOUSE RESEARCH LABORATORIES
Materials and Materials Processing Ceramics and Glasses Dept.
Pittsburgh, Pa. 15235

Prepared for

NATIONAL AERONAUTICS AND SPACE ADMINISTRATION

Technical Management
NASA Lewis Research Center
Cleveland, Ohio
Materials & Structures Division
Contract NAS3-10486

R. E. Oldrieve, Project Manager
H. B. Probst, Research Advisor

August 31, 1969

NOTICE

This report was prepared as an account of Government-sponsored work. Neither the United States, nor the National Aeronautics and Space Administration (NASA), nor any person acting on behalf of NASA:

A.) Makes any warranty or representation, expressed or implied, with respect to the accuracy, completeness, or usefulness of the information contained in this report, or that the use of any information, apparatus, method, or process disclosed in this report may not infringe privately-owned rights; or

B.) Assumes any liabilities with respect to the use of, or for damages resulting from the use of, any information, apparatus, method or process disclosed in this report.

As used above, "person acting on behalf of NASA" includes any employee or contractor of NASA, or employee of such contractor, to the extent that such employee or contractor of NASA or employee of such contractor prepares, disseminates, or provides access to any information pursuant to his employment or contract with NASA, or his employment with such contractor.

DEVELOPMENT AND EVALUATION OF CONTROLLED VISCOSITY COATINGS FOR SUPERALLOYS

by
R. B. Grekila, J. W. Chapman, D. M. Mattox

WESTINGHOUSE RESEARCH LABORATORIES
Materials and Materials Processing Ceramics and Glasses Dept.
Pittsburgh, Pa. 15235

Prepared for

NATIONAL AERONAUTICS AND SPACE ADMINISTRATION

Technical Management
NASA Lewis Research Center
Cleveland, Ohio
Materials & Structures Division
Contract NAS3-10486

R. E. Oldrieve, Project Manager
H. B. Probst, Research Advisor

August 31, 1969

FOREWORD

This is the final report of work performed under NASA Contract No. NAS3-10486 by the Research Division, Westinghouse Electric Corporation, Pittsburgh, Pennsylvania 15235. It summarizes all effort performed under the Contract during the period 1 June 1967 through 23 November 1968.

The contract was initiated under Project No. YOG-2139, and was under the technical surveillance of the NASA-Lewis Research Center, Cleveland, Ohio 44135. R.E. Oldrieve and Dr. H.B. Probst were Project Manager and Research Advisor respectively. Their helpful suggestions and cooperation are gratefully acknowledged.

The following people contributed to the experimental work and writing of the report: R.B. Grekila (Principal Investigator), J.W. Chapman, C. Hirayama, D.M. Mattox, J. Siedel, S. Way and W.E. Young, of the Westinghouse Electric Corporation.

TABLE OF CONTENTS

DEVELOPMENT AND EVALUATION OF CONTROLLED VISCOSITY COATINGS FOR SUPERALLOYS
(NAS3-10486)

ABSTRACT

The feasibility of developing glass-based protective coatings for superalloys, TD-Nickel, IN-100 and WI-52, was demonstrated. The ability of the coatings to protect superalloys from oxidation was investigated by exposures of coated discs to a temperature of 1149°C (2100°F) at velocities up to 20,000 rev/min and by exposures to thermally cycled combustion products at velocities from 0 to 400 ft/sec. Three types of coatings (glass, crystallized glass, and two-phase admixtures) were developed and evaluated. The ability of the coatings to successfully recover from impact by limited viscous flow and subsequent rehealing was determined. One promising coating was developed for IN-100 for use at 1038°C (1900°F) but not at 1149°C (2100°F). Other coating substrate combinations were suitable for less stringent environments.

LIST OF TABLES

LIST OF FIGURES

List of Figures (Continued)

List of Figures (Continued)

I. SUMMARY

Glass coatings were investigated as oxidation protective coatings for the superalloys TD-Nickel, IN-100 and WI-52 for turbine blade applications. Glasses were considered desirable since due to their continuous viscosity-temperature characteristics it seemed feasible to produce a coating which would by flowing reheal a coating penetrated by airborne contamination and at the same time be viscous enough not to flow off the blade at the high blade velocities.

Glasses were developed which coated the alloy well but did not have high enough viscosities. Two other approaches were pursued which were based on producing coatings comprised of crystalline and glassy phases. In one case crystals were nucleated and grown in the glass by carefully established heating schedule and in the other, they were mechanically incorporated in the glass slurry and fused as a mixture on the metal.

The coatings were applied by conventional porcelain enamelling techniques. Pretreatment schemes were developed for the various alloys to facilitate enameling. The glasses were melted, quenched in water, ground to a fine particle size and applied to the metals by spraying in an aqueous suspension with binder. In the case of the mechanically filled systems a crystalline additive was introduced to the glass slurry prior to spraying.

The coated alloys were placed in ovens at various temperatures to bring about fusion of the powdered glass coatings. The crystallized glass or glass ceramic coatings were produced by a post heat treatment of certain fused coatings whose compositions had been designed for this crystallization. Crystallization was not allowed to go to completion. The better coatings were preliminarily screened in a 1149°C (2100°F) torch test and/or a 6 hour oxidation test at the same temperature. The best coatings after these tests were further subjected to 20 one hour cyclic oxidation tests. The surviving coatings were subjected to four more 20 hour cycles.

After this test only four coating systems merited further evaluation. This included one glassy coating and one crystallized glass coating on TD-Nickel and a mechanically, crystal-filled, glass on both TD-Nickel and IN-100. The samples were cyclically tested in a centrifugal spin test at 1149°C (2100°F) for 6 hours and cyclically tested in a turbine simulator at 1038°C (1900°F) for a maximum of 100 hours. This latter temperature was chosen when after the spin tests it became apparent the coatings would not survive the higher temperature.

Of the four systems the pure glass coating alone offered 100 hour oxidation protection at 1038°C (1900°F) in the turbine simulator. None of the coatings offered 100 hour oxidation protection in an oxidation furnace at 1149°C (2100°F). The concept of obtaining high viscosity by crystallizing the glass did not appear promising because of the appreciable growth or dissolution rates of the crystallized phases in these temperature ranges. Glass crystal admixtures apparently failed because of the inherent weakness of the bond between the non reactive additive and the substrate. None of the glasses are therefore suitable for turbine blades or vanes. The lower temperature results indicate possible suitability for combustor can or similar application.

From a compositional viewpoint, the most interesting aspect of the coating development was that good, adherent, thermal shock resistant coatings were produced from glasses in which a large disparity in thermal expansion occurred. In the best glass the ratio of the coefficient of the metal to the glass was 3:1. This indicates a very strong chemical bond which overcomes the mechanical stress due to this mismatch with superalloys or TDNi. It was also found that several glasses with relatively close expansion match to TDNi either failed to adhere or to remain adherent during oxidation testing. In the program, glasses which match the expansion of refractory metals (and with high sag temperature) and some which match iron or steel were produced. Both could be successfully applied to typical substrates with corresponding thermal expansion (T-222 alloy and iron) but neither coated material was evaluated for oxidation protection, etc. Several patent applications for the more unique glasses were submitted (possible solder glasses, refractory metal coating layers, etc.) - but no successful coatings for use on TDNi at temperatures above 1900°F were found.

II. INTRODUCTION

Turbine blades are subjected to many deleterious influences in gas turbojet environments. In particular, one degrading influence is the reaction of the blade metal with the ambient gases (particularly oxygen) at the elevated operating temperatures. Since little can be done by way of altering the combustive mixture of gases, ways of protecting the metal are needed.

Oxidation resistant coatings on the metals are the logical solution. In ordinary turbojet environments, air-borne particulate contamination is present; and at the high blade velocities involved can produce coating removal upon impact. One solution to this problem is to have the coating possess flow properties, such that, in the event a small portion of the coating is removed, the cavitated region is filled and healed by flow of the coating.

The properties required of such a coating are that it have high temperature stability, be oxidation resistant, be capable of viscous flow and be applicable to the base metal. Such properties are uniquely those of inorganic glasses. Unlike crystalline materials, glasses have continuous viscosity characteristics from temperatures where they are rigid to temperatures where they are very fluid. This means that in theory a glass composition can be tailored so that at the use temperature the glass will have the desired viscosity, i.e., a viscosity where flow healing is possible, but not so fluid that the coating flows off the blade under the action of the centrifugal forces at high velocities. Since inorganic glasses are generally oxides, they are very stable toward oxidation. Finally the technology for coating glasses on metals has long been understood and is the basis for conventional porcelain enameling.

The scope of the current project confined our interest to glass compositional systems which were known to yield high viscosities, namely the silicates. Compositional modifications were made to achieve a compromise between high viscosity and applicability.

The following report describes a research program wherein high viscosity glassy coatings were developed for application to various superalloys and tested in simulated turbojet environments.

III. COATING COMPOSITION DEVELOPMENT

A. Coating Background

In developing glass coatings for the superalloys, two sets of criteria had to be considered. The first dealt with the rheological properties of the coating. The second dealt with the effects of composition on adherence. Normally the most important property in adherence is the expansion match of coating to metal. Glass coatings usually have or are selected to provide a slightly lower expansion which leave them in compression once applied. This stressed condition is desirable since glasses are far superior in compressive strength. With larger expansion mismatches the coating thickness must be reduced to minimize the interfacial stress. A limitation proposed by the application procedure is that the temperature of application, and consequently the viscosity, must be such that the coating may be fused below the temperature at which the metal deforms.

Another compositional factor is less well understood. In the enameling of ferrous materials, small amounts of oxides (CoO, NiO, CdO and Fe_2O_3) promote adherence. It was not known whether these materials or some other additive would help in the development of adherence in the superalloys.

B. Metal Properties

Three superalloys, IN-100, WI-52, and TD-Ni, were procured from various suppliers during the period of the contract. TD-Ni was obtained from E. I. DuPont de Nemours in nominal 60 mil sheets, while WI-52 and IN-100 were obtained from the Misco Division of the Howmet Corporation as 1" x 2" x .100" castings. The 4" diameter spin discs of WI-52 and IN-100 were also obtained from Misco as 60 mil castings, while the 4" spin discs of TD-Ni were machined from the 60 mil sheet stock.

The chemical compositions of the three materials are listed in Table I. The linear thermal expansions of these materials were measured by the Materials Testing and Evaluation Laboratory at the Westinghouse Research Laboratories. The thermal expansions of the superalloys are shown in Figure 1 with coefficients of linear thermal expansion.

C. Composition Background

Certain well known working properties of glasses have been defined in terms of their viscosity. The annealing temperature is the temperature which corresponds to a viscosity of 10^{13} poises, and is the point at which internal stresses are relieved in a matter of minutes. The aerodynamic shear requirements in this program require that any glassy material contemplated as a coating have a viscosity of 10^{11} poises at the use temperature. This number is calculated using the formula in Appendix A, and is the viscosity required for a coating to flow to half its original thickness in 100 hours in a centrifugal spin test at 20000 rpm. The tendency to speak interchangeably about temperature and viscosity must be recognized at this point since, for any given glass, the logarithm of viscosity is linearly related to the reciprocal of temperature reduced by a constant.

To achieve the desired viscosity three approaches to the coating problem were considered; pure glassy coatings, crystallized glass coatings, and mechanically filled, glass-crystal admixtures. These three phases of development will be discussed separately.

C.1 Phase I. Glass Coatings

At present the only stable glass known to have an annealing temperature above 1000°C (1832°F) is fused silica. Unfortunately this material has a thermal expansion coefficient near zero. Alumino-silicate glasses were the best candidates for this investigation in view of their known high viscosity and generally higher melting temperatures. Modifications of this system were made to achieve favorable expansion matches, in high viscosities as measured by sag point (J. Am. Ceram. Soc. 45,113,1962) and good adherence.

Glasses were thus investigated in the system SiO_2--MO--R_2O_3--TO_2--A_2O, where M refers to Mg^{2+} and Ca^{2+}; R to Al^{3+}, Cr^{3+}, and Fe^{3+}; A to K^+ and Rb^+; and T to Zr^{4+} and Th^{4+}. The range of compositions were: SiO_2, 65 to 80 mole percent; A_2O, 5 to 15 mole percent; and MO, R_2O_3, and TO_2 concentrations adjusted to obtain a stable glass of highest annealing temperature. Systematic compositional changes were then made by adjusting the concentrations in the direction of highest softening temperature which could be applied without damage to the substrates.

Modifications were made according to the following guidelines: The addition of alkali will decrease the high and low temperature viscosities with larger alkali ions being less effective than smaller ions; the addition of CaO or MgO will decrease the high temperature viscosity more than the low temperature viscosity; the addition of ZnO or BaO will decrease the low temperature viscosity more than the high temperature viscosity; and the addition of CoO, NiO, CdO and Fe_2O_3 will promote adherence. Generally, high viscosities are associated with low thermal expansions and high softening temperature as a result of additive modifications within the same glass structural system.

Unfortunately all of these composition "guide lines" are only that; and compositions still must be prepared since glass science has not yet progressed to the point that properties may be precisely predicted from compositions. Thus the problem was to get the right combination of thermal expansion with high and low temperature viscosities.

Approximately 30 compositions were prepared in this phase of glass development. The softening temperatures were rapidly determined from the sag points at which temperature the viscosity is approximately 10^{10} poises. The thermal expansion coefficients of the glasses were also measured.

The target for the first part of this program was to develop a glass composition which would have a sag point above 700°C and a

thermal expansion lower than that of the metal to be coated. The data of Table II show that many glasses were developed with properties close to those desired.

The approach used to apply the glasses was derived from the art of porcelain enameling. A porcelain enamel coating is essentially a thin layer of glass applied to a metal as a powder and fused at a temperature and time such that the powder melts and forms a continuous and adherent glassy layer.

In order to form a uniform and reproducible coating, four application and/or fusion methods were investigated with glasses of proven enameling ability. These were as follows:

1. Gravity dipping from a slip plus furnace fusion.
2. Air spraying from a slip plus furnace fusion.
3. Plasma spraying with simultaneous fusion.
4. Air spraying from a slip plus induction fusion.

Gravity dipping did not produce a uniform coating due to the inherent presence of a "trailing edge". Plasma spraying would have been an ideal solution as the glass would have been applied and fused without the heat distorting the substrate, but the low gas velocities of the available equipment prohibited the glass powder from flowing and forming a uniform coating. Induction heating was impractical with TD-Ni since the material is ferromagnetic and above its Curie temperature there are significant changes in its inductive requirements. Air spraying techniques and subsequent furnace fusion were then employed and uniform and reproducible coatings obtained.

The glasses applied as coatings to the superalloys were ball-milled in porcelain jar mills with water and a suspending agent to form a -200 mesh slip. Larger particle sizes would not form a uniform thin coating, while smaller particle sizes tended to craze before final firing. The method of slip preparation is shown in Table III.

In general the development of an acceptable bond between a glass and a metal depends first on the glass wetting the metal and then

on both a mechanical interlocking and a controlled reaction between the glass and the metal at the interface. The degree of adherence also depends on minimizing the glass thickness to produce a low stress level at the interface.

In many cases a treatment of the metal prior to enameling promotes better adherence than an untreated substrate. The pre-treatments that were investigated included roughening the surface by both sand-blasting and acid etching, applying an oxide film to the metal prior to coating by pre-firing in an air atmosphere, and plating a chromium layer on the surface as a protective layer. In all cases the metal was cleaned by washing with cleanser and cleaning with acetone followed by methanol prior to pre-treatment to remove dirt and grease.

The success or failure of the glass to the metal substrate bond was determined by the amount of glass adhering to the metal after metal deformation, the resistance of the coating to 649°C (1200°F)-to-water-quench-thermal-shock and the visual appearance of the coating. The results of the above pretreatments indicated that the "as-cast" condition of WI-52 and IN-100 gave satisfactory adherence and hence they were only cleaned* prior to coating. A pre-oxidation cycle was found beneficial to TD-Ni in that the thin oxide film that was formed increased the ability of the glass to wet the substrate. The metal pre-treatment techniques that were employed for all subsequent applications are indicated below:

Metal	Pre-Treatment
TD-Ni	Clean and Pre-oxidize at 871°C for 3 minutes
WI-52	Clean the "as-cast" material*
IN-100	Clean the "as-cast" material*

* If the surface of the casting was changed by subsequent metal finishing, a light 60 mesh sandblast was used.

The glasses that were developed for the contract were applied as 5 mil thick coatings to pre-oxidized 1" x 2" x .060" TD-Ni panels. Glasses that formed acceptable coatings on TD-Ni were then evaluated as 5 mil coatings on IN-100 and WI-52. The glass composition numbers that are indicated on Table II were modified by the addition of a letter designating the metal when they are evaluated as a superalloy coating. For example, Glass 3 becomes T-3, I-3, or W-3 when it is a coating on TD-Ni, IN-100, or WI-52. The glasses were fused in an air atmosphere for 3 minutes at their optimum furnace fusion temperatures. The fusion temperatures were selected from the relationship between sag point temperature and application temperature that was developed after numerous trials and which is depicted in Fig. 2. It should be noted that the application temperatures were ambient furnace temperatures and not sample temperatures. The optimum application temperatures that were used are included in the glass composition data on Table II.

The coatings were evaluated visually to determine the wetting of the glass to the metal, the presence of pinholes, and the ability of the glass to resist devitrification. The coatings were also evaluated for adherence and thermal shock resistance. The adherence test was the typical industrial pressure deformation method in which the metal is deformed by 1250 lb of pressure exerted on a 1" circular die. The adherence is then judged by the degree of glass adhering to the deformed metal. These evaluations were limited in value as all the samples failed due to the severity of the test. The thermal shock resistance was evaluated by the appearance of the coating after a 704°C for 2 minutes to water quench cycle. The results of this investigation are summarized on Fig. 3 in the Phase I-Preliminary Evaluation Section.

The preliminary evaluation eliminated a large number of coating systems. The coating systems that were rejected were not compatible with the substrate. This incompatibility was due either to the glass not wetting the substrate sufficiently to form an adherent and uniform coating, or the inability of the glass to react with the substrate to the proper degree that would enable it to form an adherent coating.

The 13 coating systems that were selected for further evaluation are underlined in the Phase I - Preliminary Evaluation Section shown in Fig. 3.

C.2 Phase II. Crystallized Glass Systems

At this phase of the glass composition development it was clear that the rehealing properties were achieved while the viscosity properties objectives as indicated in centrifugal testing were not being attained and that more composition development was necessary.

One way of achieving high viscosity coatings is to incorporate particulate material in the viscous glassy matrix. This produces an effective viscosity which is higher than the glass, while the glass phase will still flow and permit the rehealing processes. The inclusions may be brought about in two ways. They may be mechanically added or developed in situ by controlled crystallization. One drawback to this latter technique is that once crystallization has proceeded to some predetermined level it must be arrested so that there will be a glassy phase present.

Initial trials were made with a base glass having the approximate composition $7SiO_2$-$3Na_2O$-$3Al_2O_3$-$4CaO$. This composition was selected since the corresponding crystalline phase melts at about 1160°C (2120°F). The glass was doped with up to 5% fluorine, which acts both as a nucleating agent and as a flux. The latter imparts a lower viscosity in the glassy state thereby enhancing coatability. The controlled crystallization was made at heat treating temperatures which were determined for each glass system and which are indicated in Table II. The major crystal phases in the first system were $CaSiO_3$ and $NaAlSiO_4$. Other systems, such as $2MgO \cdot SiO_2 + Na_2O \cdot Al_2O_3 \cdot 6SiO_2$, were also prepared to crystallize forsterite, $2MgO \cdot SiO_2$, which has an expansion coefficient of 10×10^{-6}/°C.

Table II summarizes additional glass compositional work done in the CaO-Al_2O_3-SiO_2 system. Compositions 61 through 67, except 62 represent attempts to produce crystallizing glasses in the CaO-Al_2O_3-SiO_2

system with TiO_2 as the nucleating agent. The principal phase expected was anorthite ($CaAl_2Si_2O_8$). With the exception of 66 the type of crystallization that took place was unsuitable due to gross density differences between the glass and crystallized material. Composition 66 crystallized very rapidly from the surface while retaining its dimensional stability. This rapid uncontrolled crystallization prevented consideration as a coating.

Glasses were next investigated in the high melting $CaO-Al_2O_3$ glass system. Small amounts of SiO_2 stabilize this as a glass system. Compositions 68, 69, and 70 represent approximately similar $CaO:Al_2O_3$ ratios with small variations in the SiO_2 content. These adjustments controlled the amount of initial crystallization but at 1150°C crystallization proceeded completely. The glass system has a linear expansion coefficient of approximately 7.5×10^{-6}/°C.

Numbers 71 through 77 represent various compositions in this system which have the same liquidus but different crystallizing phases. The glasses were tested by making bars, crystallizing them and testing them for sagging between knife edges at 1150°C. Number 72 crystallized homogeneously with a rather coarse grain structure at 1150°C. The appearance of the sample indicated it to be a glassy crystalline admixture and this merited consideration as a coating.

The previously mentioned candidate glasses that were developed for glass-ceramic coatings were applied to TD-Ni panels as glass coatings and then heat-treated to form the desired degree of crystallinity. This procedure was necessary in order to apply the very refractory crystalline coatings below the melting temperature of the metal. The method of slip preparation, application, and fusion of the glass coating was similar to that previously described for glass coatings. These specimens were then visually evaluated to determine the coatability of the glass. The application temperatures of these coatings are indicated in Table II. All of the glasses that were investigated as coatings except T-72 were capable of forming adherent 5 mil coatings on TD-Ni. T-72 appeared to

be a promising composition in the preliminary development work, but could not be applied to the substrate due to the temperature limitations imposed by the metal.

The glass coatings were heat-treated for 1 hour at three different temperatures in order to obtain varying degrees of crystallization. This procedure was required in order to qualitatively determine the amount of crystalline material required to obtain the desired viscosity and the amount of glassy material required to adhere to the substrate.

The heat-treating temperatures for the materials that were investigated varied from 800°C to 1100°C. These temperatures do not correspond to the optimum crystallization temperatures that were determined for the bar form of the pure glasses due to the change in the glass composition caused by the reaction with the metal during application. Table II indicates the optimum crystallization temperature of each coating. The Phase II - Preliminary Evaluation Section in Fig. 3 shows the results that were obtained.

In general, most of the coatings were very poor due to crazing induced during formation of the crystal phase. A second weakness of these coatings is the reappearance of the glassy phase above the optimum crystallization temperature, and below the use temperature. This indicates that the crystalline material would not be stable at the intended use temperature. The best crystallized coating appeared to be T-54 which does not craze or spall during crystallization and does not have a reappearance of the glassy phase when the hold temperature is increased above the full crystallization temperature. The 13 crystallized systems that are underlined in the Phase II - Preliminary Evaluation Section of Fig. 3 as well as one non-crystallized sample of each system were selected for further evaluation. A crystallized sample of coating T-54 was submitted for metallographic examination.

C.3 Phase III - Mechanically Filled, Glass-Crystal Admixtures

The controlled crystallization technique has certain serious limitations in that the glass compositions must correspond closely to that of the crystal. More often this composition is not in the glass forming region. The type of crystal phase which one may obtain by controlled crystallization is therefore limited. However, it is possible to embed a crystal phase in a glassy matrix by the fusion of a glass-crystal mixture. In this instance the crystal phase must be a finely powdered material. The range of possible combinations is wider in this method. There are also certain inherent limitations in this technique. Two of the most serious are (1) homogeneous distribution of embedded crystal may not be obtained; (2) the volume of crystal phase may be of the order of 50% at most. A distinct advantage, however, is that the crystal may be selected for its expansion coefficient and melting point.

The oxides or metals that were then investigated as additions to Glass 23-1 were MgO, Ni, SiO_2, $Al(OH)_3$, Cr, Cu, W, Cr_2O_3, CaO, NiO, ZrO_2 and TiO_2. The above materials were added in varying percentages to a water slip of the base glass as -325 mesh particles and stirred thoroughly to ensure a homogeneous mixture. Table IV indicates the variety of mechanically filled glass systems that were evaluated as high viscosity glass coatings.

The admixtures were applied to two different surface conditions of TD-Ni panels. The admixtures were either applied to pre-oxidized TD-Ni as a 5 mil thick film or applied as a 3 mil thick film to TD-Ni panels ground-coated with a fused 2 mil thick film of Glass 23-1. The purpose of the ground coat was to eliminate the poor adherence that is possible when non-reactive oxides or metal particles are in contact with the substrate.

The coatings were generally fused at 1316°C (2400°F) or 1427°C (2601°F) for 5 minutes in an air atmosphere and evaluated visually to determine the suitability of the coating for TD-Ni. Initial additions were generally made at the 25 volume percent level and varied up or down

according to the coating that was obtained. The coating results are shown in the Phase III - Preliminary Evaluation Section in Fig. 3.

In general, several additives were found suitable for producing high viscosity coatings on both pre-oxidized and ground-coated TD-Ni. TiO_2, ZrO_2, and SiO_2 were excellent coatings at both the 25 and 50 volume percent, while $Al(OH)_3$, NiO, CoO, and Cr metal additions were excellent coatings at the 25 volume percent level. Excellent coatings were formed from both reactive and non-reactive materials. Reactive materials, such as SiO_2, combined with the base glass to form a clear coating. Non-reactive materials, such as ZrO_2, formed opaque coatings which consisted of particles of the oxide or metal bonded by the glassy phase. The increase in the bulk viscosity of these coatings cannot be measured quantitatively but the increase can be shown by the increase in both the fusion temperature and time that were needed to form the coatings. The sixteen systems which produced acceptable coatings are underlined in the Phase III - Preliminary Evaluation Section of Fig. 3. These samples were selected for further evaluation. A 25% NiO addition on pre-oxidized TD-Ni (T-11) and a 50% SiO_2 addition on ground coated TD-Ni (T-94) were submitted for metallographic examination.

IV. TEST APPARATUS AND PROCEDURES

Candidate coating systems which passed the preliminary evaluation were subjected to progressively more severe test environments. The coating systems were examined after each series of tests and unsuitable systems were eliminated. The tests which were conducted are as follows. Six hour furnace oxidation at 1149°C, (2100°F), 1 hour torch at 1149°C, 1 hour centrifugal spin rig at 1149°C, 100 hour cyclic furnace oxidation at 1149°C, 6 hour cyclic centrifugal spin rig at 1149°C, and 100 hour turbine simulator at 1038°C (1900°F). Full range viscosity measurements were performed on four promising Phase I coating materials.

A. Six Hour Furnace Oxidation

A six hour furnace oxidation test at 1149°C was used as a preliminary screening test for all coating systems. The purpose of the test was to quickly eliminate coating systems that would not be capable of protecting the metal for longer times and more severe enviornments. The 1" x 2" samples of the 13 Phase I systems, 13 Phase II systems, and 16 Phase III systems were prepared with a 5 mil thick coating in the manner previously described in Sec. C.1. Candidate coating systems were evaluated in both the "as-coated" and room temperature impacted conditions. Six room temperature impacts were made on the samples with a modified Gardner Drop Weight Impact tester. The test apparatus was modified by using a one-eighth inch diameter ball affixed to a 123 gm weight. The weight drove the ball into the sample. The impact levels that were obtained varied from 0.23 in.-lb to 5.67 in.-lb.

The specimens were then attached to a Hastelloy plate with platinum wire and rapidly inserted into a furnace preheated to 1149°C. After six hours in the furnace the specimens were rapidly extracted and allowed to cool. Figure 4 shows the sample holder and Fig. 5 is a cut-away view of the oxidation furnace.

B. One Hour Torch Test

A one hour torch test at 1149°C was used as a preliminary screening test for the 13 Phase I coating systems to observe the effects of low gas velocities on the coatings. This test was not used for Phase II and Phase III when it became apparent that the test did not discriminate between coatings. Two samples each of the 13 Phase I systems were prepared with a 5 mil thick coating in the manner previously described in Sec. III - C.1.

As shown in Fig. 6 two 1" x 2" impacted and plain panels of a given coating system were mounted on a stainless steel holder, and two chromel-alumel thermocouples were loosely attached to the back surface of the specimen. The specimens were slowly inserted into the furnace (about 200°C per minute temperature rise) and placed in front of the swirl burner flame. The specimens were retained in the furnace for one hour at a temperature of 1149°C, and then they were slowly extracted from the furnace and cooled to room temperature (about 111°C per minute cooling). Nominally identical test procedures were followed for specimens of each of the thirteen coating systems tested.

C. Centrifugal Spin Test

A centrifugal spin test at 20,000 rev/min and 1149°C was used as a preliminary screening test and as a final evaluation of selected coating systems. The purpose of the test was to simulate the drag forces occurring in a turbine at the stationary blade surfaces. The apparatus consisted of a furnace chamber, a burner, and a retractable vertical air driven rotating one inch shaft. The test samples, four inch discs coated only on the top side, were bolted to the hot-end of the shaft. The fuel used in the evaluation was natural gas. Oxidizing conditions were obtained by exceeding the 17:1 stoichiometric weight ratio of air to gas. The average excess air, by Orsat analyses, was 2%. Figures 7 and 8 show the inside of the furnace and the furnace assembled with the spin rig in place and the burner retracted for ignition. After ignition the burner is slid on locating bolts up to the end plate and fastened in place. An assembly drawing of the swirl burner is shown in Fig. 9. The

spinner drive consists of an air turbine, Model W-1, supplied by the Metal Removal Company. It is intended for hand grinding operations and is rated at 3/4 horsepower turning at 25,000 rpm. Guaranteed maximum runout is 0.005" and the air requirement was about 25 CFM at the working pressure of 90 psig. Calculated air friction horsepower with the 4" diameter disc shown is nearly negligible and no trouble was experienced in obtaining the required speeds of 20,000 rev/min. The disc surface temperature was measured at three radial positions on the rotating disc and found to vary only 60°C from the center to the edge of the disc. An analysis of the stress in the rotating spinning disc is given in Appendix B.

The effect of the centrifugal spin rig on glass coatings was evaluated early in the contract period. Since no contract glasses were yet available, two available glasses of differing viscosities were applied to one side of TD-Ni discs. The discs were exposed at 1149°C and spun at a speed of 20,000 rev/min for approximately 30 minutes. It appeared that in the coating systems explored, the spin rig was capable of discriminating between coating viscosities.

Two promising Phase I coatings (T-23 and T-25) were evaluated at 1149°C for one hour at 20,000 rev/min. T-23 was impacted prior to the test at an impact level of 5.67 in.-lb while T-25 was evaluated in the "as-coated" condition. The initial 5 mil thick coatings were applied in the normal manner to the 4" diameter x .060" thick discs. The results are discussed in Sec. V.C.

D. 100 Hour Furnace Oxidation

The 100 hour test consisted of 20 one-hour and 4 twenty-hour exposures to 1149°C in a controlled oxidizing atmosphere. The oxidizing atmosphere was obtained by excess air in the combustion products of Diesel fuel grade No. 2. The first thermal cyclings indicated the initial compatibility and degree of adherence between the coating and the substrate in the prepared test samples. Thermal cyclings after continued hot oxidation indicated the effect on adherence by changes at the

interface and in the coating structure. The continued exposure to hot oxidation indicated the time dependent high temperature properties of the coating and the coating to substrate interactions.

The self-healing, by viscous flow, of coatings superficially damaged by particle impact was also tested. For this purpose, three specimens from the five prepared from each of the first 16 systems were ballistically impacted. Specimen Nos. 1, 2, and 3 were impacted at room temperature, at 927°C, and at 1149°C respectively. The remaining two were made in an electric furnace, and the impact damage was controlled by the pellet velocity.

The initial sixteen systems were tested at 1149°C in the oxidizing furnace for a total of 20 one hour cycles. From the sixteen systems, the best six were further tested at 1149°C in the oxidizing furnace for an additional total of 80 hours comprising four 20 hour cycles.

E. Cyclic Centrifugal Spin Test

Four promising coating systems from the cyclic oxidation results were evaluated in the centrifugal spin rig at 1149°C for a maximum of six 1 hour cycles. The tests were made in the apparatus previously described in Sec. IV.C, at speeds up to 20,000 rev/min. While this test duplicated the effect obtained by oxidation testing, the primary purpose of the spin test was to subject the coating to viscous deformation by centrifugal forces acting parallel to the disc and radially from its center.

The self-healing evaluation of superficially impacted coatings at elevated temperature in conjunction with the spin test required the construction of an air driven pellet impeller. This device consisted of a barrel bored to accommodate a nominal 3/16 inch pellet. The barrel was attached at one end to an air source, and the pellet was positioned by means of a retractable pin 3 inches from the muzzle. The elevated temperature tests were made by placing the impeller muzzle in an opening

in the furnace wall 9 inches from the panel. The desired degree of coating damage was obtained at an air pressure of 3 psi. However probably due to gas turbulence, a pressure of 10 psi was necessary in the spin test to produce the same degree of damage. By means of a camera and a stroboscope it was possible to determine the muzzle velocity of the pellets. At 3 psi pressure the velocity was 29.0 ft/sec and at 10 psi pressure a velocity of 63.5 ft/sec was obtained. From the average pellet weight of 7.75×10^{-4} pounds the impact levels for 29.0 and 63.5 ft/sec velocities were calculated to be 0.0101 and 0.0485 ft-lbs respectively.

F. One Hundred Hour Cyclic Turbine Simulator

As the name implies, this test was designed to simulate a gas turbine environment. The drag forces upon the stationary coating were simulated by a flow of hot combustion products and excess air at an average temperature of 1038°C, at a velocity of 400 ft/sec, and at a pressure of 5 atmospheres absolute. The samples were positioned in the test passage of the turbine simulator in a vertical plane 30° to the direction of the gas stream in order to simulate the drag and pressure forces on turbine blades. The test was conducted in six-one hour cycles, four-six hour cycles, and additional daily cycles for a total of 76 hours. Systems were constantly evaluated and unsatisfactory systems were eliminated.

A holder was designed for testing five specimens simultaneously. The holder and samples were placed in the retractable supporting frame (Fig. 10) by which means the samples were introduced into the test section of the passage and positioned at 30° to the gas stream. The test section had a rectangular opening to accommodate the 2 x 4-1/2 inch opening of the retractable supporting frame. The inside diameter of the existing passage was six inches, and a transition sleeve was placed in front of the test section to change the 6 inch circular path of the gas stream to a 2 x 4-1/2 inch rectangular path at the test section. The gas stream temperature was monitored by 33 thermocouples. Figure 11 shows a typical

test section, thermocouple probes, sample supporting frame and its retraction mechanism. Three standard passages and some of the control instrumentation are shown in Fig. 12. The middle passage (No. 2) was used in the final evaluation.

In order to obtain a minimum gas flow to 400 ft/sec (24,000 ft/min) it was necessary to determine first the effective opening at the test section. From an effective opening of 0.0487 ft^2 it was established that the volume flow was 1170 ft^3/min at 1038°C and 5 atmospheres pressure. When adjusted to room temperature and standard pressure, this flow became 1320 ft^3/min or 1.76 lb/sec air. The requisite conditions were obtained by the compressor delivering a minimum of 1.76 lb/sec air. The simulator was fired by Diesel oil grade No. 2, and highly oxidizing conditions were obtained since the air flow far exceeded the 14:1 stoichiometric weight ratio of air to oil. Calculations from air and oil flows as well as from Orsat analyses established that the percent excess air was 220 $\pm$ 15.

V. TEST RESULTS AND DISCUSSION OF RESULTS

A. Six Hour Oxidation Tests at 1149°C

The 13 Phase I, 13 Phase II, and 16 Phase III coating systems underlined in Fig. 3 were evaluated after the six hour exposure period to qualitatively determine the ability of the coating to cover sharp edges, resist spalling, and protect the metal from oxidation. The coatings were also evaluated for their stability and ability to resist flow. These results are shown in Fig. 3.

A general summary of the Phase I glass coating systems that have been developed indicates that the coating at the sharp edges is insufficient to protect the metal from oxidation, that the impact marks will reheal, that spalling will destroy the coating integrity of most systems, and that the viscosity is too low to withstand high aerodynamic shear forces. If the edge coverage is ignored, however, several of the glassy coating systems were promising. The most promising systems are T-13, T-22-2, T-23, I-23, T-24, T-25, I-25, and T-29.

In general, the Phase II, glass-ceramic coatings were not protective at 1149°C for six hours. The crystal phase was not stable at this temperature and the coating integrity was destroyed. The crystal phase tended to return to the glassy state and the coating tended to collapse and become wrinkled. The inherent poor adherence of the crystal phase to the substrate also caused thermal spalling.

The 900°C crystallized coating of T-54 appeared to be the only system that overcame the above mentioned difficulties. The crystal phase was stable at the 1149°C and the coating was not prone to thermal spalling.

Seven of the Phase III, mechanically filled glass systems on TD-Ni appeared to be promising. Varying metal pretreatments and volume percent additions of NiO, SiO_2, TiO_2 and ZrO_2 protected TD-Ni from

oxidation for the duration of the test. These coating systems were also spall resistant and did not appear to have such a low viscosity at 1149°C (2100°F) that the impact marks completely rehealed. The most promising systems were T-92, T-93, T-94, T-119, T-121, T-123 and T-127.

B. One Hour Torch Test at 1149°C

One hour torch tests were run on Phase I coating systems. All specimens were visually examined after the test to qualitatively determine the ability of the coating to cover sharp edges, resist spalling and protect the metal from oxidation. The coatings were also evaluated for their ability to resist flow and their stability as coatings.

Two coating systems (T-15-1 and T-24) resulted in considerable spalling of the coating on the impacted specimens after the specimens were cooled to room temperature. For all the coating systems tested, the impact cracks appeared to be re-fused before the substrate metal had a chance to oxidize. Most of the specimens tested (with the exception of T-13) showed a tendency of slight edge creeping, and this effect was greater when the original edges contained spots of sharp discontinuity or imperfection. These results were similar to the oxidation results and the same systems were considered to be the most promising.

C. One Hour Centrifugal Spin Rig Test at 1149°C

Two of the Phase I coating systems, T-23 and T-25, were subjected to centrifugal spin at 20,000 rev/min and 1149°C for one hour. As shown in Figs. 13a and 13b the T-23 disc lost most of the coating except at the center region where temperature was about 30 to 60°C lower than the outer edge Fig. 13a. T-25 behaved similarly except for center spalling after the disc was taken out of the furnace Fig. 13b. There was also evidence that the glass on both discs had flowed during the spinning cycle, indicating that the viscosity was lower than desirable.

D. Full Range Viscosity Measurement of Candidate Glasses

Four of the most promising Phase I glasses were sent to the Hartford Division of the Emhart Corporation for full range viscosity measurements (concentric cylinder and fiber elongation methods). These glasses were 13-1, 22-2, 23-1, and 25. Glass 25 could not be evaluated due to the temperature limitations of the testing equipment and 23-1 devitrified during the slow heating rate. The viscosity-temperature relationships for the three glasses are plotted in Fig. 14 which indicates that the log viscosities of Glasses 13-1, 22-2, and 23-1 at the 1149°C (2100°F) test temperature are 4.3, 4.0, and 5.4 poises. Although the viscosity of Glass 25 at 1149°C cannot be measured, the sag point temperature indicates that it would be considerably higher than Glass 23-1. It is apparent however, that the viscosity of these glasses is too low for turbine blade coatings unless they react with the substrate to such a degree that their chemical composition and hence their viscosity is altered.

E. One Hundred Hour Cyclic Furnace Oxidation at 1149°C

A total of sixteen systems were cyclically tested by 20 one-hour cycles at 1149°C. These systems are underlined in Fig. 3. The samples were visually evaluated at the end of each cycle for spall resistance, coating continuity, coating stability, and metal protection. These results are shown in Fig. 3. The weight loss was taken every five hours and the samples were then photographed. Figures 15 and 16 show the samples after 20 hours exposure while Table V indicates the weight loss data. On the basis of appearance, spall resistance, glassy phase, and weight loss systems I-25, T-54, T-92, T-93, T-94, and T-119 were selected for further evaluation by exposure to an additional four 20-hour cycles.

After these four cycles I-25, T-54, and T-94 were selected for continued evaluation. The weight loss data and sample appearance are shown in Figs. 17-20 and Table VI. Figure 3 indicates the overall test results. Since more samples of IN-100 became available at this time,

one new coating substrate combination (I-94) was included for further testing in the spin rig and turbine simulator.

A general observation of the coating systems that have been developed indicates that they cannot protect the metal from oxidation for one hundred hours at 1149°C. The coatings are prone to spalling after long interaction with the substrates at these temperatures. Glass 25 on IN-100 (System I-25) appeared to be the best system as it protected the metal for 80 hours.

F. Cyclic Centrifugal Spin Rig at 1149°C

Four systems (I-25, T-54, I-94, and T-94) were tested as coated discs for a total of six one-hour runs at 1149°C and velocities from 20,000 to 3,000 rpm. They were weighed and photographed after each run. With the exception of I-25 the other three systems had failed after two one-hour runs regardless of spin velocity.

It was found necessary to reduce the spin velocity in the case of Systems I-25 and I-94. The disc specimen for I-94 developed visible cracks after coating application. The disc specimen for I-25 cracked during the first one-hour run at the requisite velocity of 20,000 rpm. The cracks in both systems were practically identical in that they emanated from each of the three bolt holes in each disc. Since the tangential tensile stresses are at a maximum in the region of the bolt holes caution was exercised by reducing the speed to approximately 3,000 rpm. Even at the reduced speed, some of the cracks had propagated to within a 1/4 inch from the outer edge of the disc by the end of the sixth one-hour run.

The results of the spin and impact tests indicated that the best coating system was I-25. Nevertheless, at 1149°C and at a spin velocity of only 3,000 rpm about one-third by weight of the glass coating and oxide were lost after a total of six hours of testing.

Table VII shows the weight change with each one-hour run. Selected photographs illustrating the effect of the testing are shown in Figs. 21, 22, 23, and 24. Figure 3 indicates the overall results of this test.

G. One Hundred Hour Turbine Simulator at 1038°C (1900°F)

The four coating systems under consideration (I-25, T-54, T-94, and I-94) were tested in the turbine simulator at 1038°C for a total of 100, 4, 24, and 6 hours respectively.

The samples were screened in four tests. In Test No. 1 for Systems I-25 and I-94, and in Test No. 2 for Systems T-54 and T-94 the coatings were evaluated after 6 one-hour runs. The two best systems I-25 and T-94 were then further screened in Test No. 3 by three six-hour runs. Test No. 4 was then conducted on the best system, I-25, for an additional 76 hours of cyclic testing time. Figure 3 indicates the overall test results.

Test No. 1

The five samples of I-25 and I-94 were positioned, throughout the testing in the order of I-94, I-94, I-25, I-25 and I-25 from left to right facing down-stream (front). After a total of six hours at 1038°C, I-25 was hardly affected by the impingement of the gas stream. The only exception was on the front surfaces (the surfaces facing the gas stream) which showed slight rippling in the coating. The rippling effect was absent in the back, indicating that the viscosity of (Glass No. 25) may be too low to withstand the velocity (400 ft/sec) and density (5 atm abs.) of the impinging hot gases. The I-94 coatings were much more affected by this impingement as indicated by the fact that even the back surface underwent extensive rippling while shielded from direct gas impingement. Figure 25 shows the extent of this rippling on the back surface of the I-94 samples (the two samples at the right).

Test No. 2

The five samples of Systems T-54 and T-94 were tested in the same manner as Test No. 1. The samples were positioned in the order of T-54, T-54, T-94, T-94 and T-94. Figures 26a and 26b show before and after effects on the one-hour run. The coatings of System T-94 showed rippling in front and back. The coatings of System T-54 on the other

hand, were smooth but changed in color from white toward green. The appearance of the coatings after the 2nd and 3rd runs showed a progressive change in structure. The ceramic or crystalline phase increased at the expense of the glassy phase. Apparently a volume change accompanied this structure change with the resultant flaking of the coating after the third and fourth runs as shown in Fig. 37a. This figure also shows that the initial rippling of the T-94 coatings on the subsequent exposure had been more violently disturbed. At this stage, the two specimens of T-54 were removed. In their place, two spare specimens from T-94 were used so as to maintain the same gas flow patterns for the remaining three specimens of T-94. The results of the six one-hour runs on the three specimens are shown in Fig. 28. The texture became rougher, with little coating remaining on the leading-edge, and some of the coating at the trailing-edge spalled off.

Test No. 3

In this test, the three I-25 specimens from Test No. 1 and two specimens of T-94 from Test No. 2 were used. The specimen holder from Test No. 1 was used again so that specimens for the I-25 systems (3, 4 and 5 positions) were not disturbed. Figures 29a and 29b show the results of the first six-hour run, and Figs. 30a and 30b show the results of the third six-hour run. At this stage all specimens were tested for a total of 24 hours. The general appearance of the T-94 specimens (in positions 1 and 2) was poor. The coatings of I-25 were only slightly affected. The ripples in front became more pronounced, and the glass at the leading edges became thinner. The coatings in the back showed some random rippling which was attributed to the deflection and scatter of the gas stream from specimen to specimen.

Test No. 4

The evaluation of the three specimens for I-25 was continued in Test No. 4 for an additional 76 hours. In this test, periodic weighings were made of each specimen. The weight changes are summarized

in Table VIII. A spare specimen of I-25 was placed in position 1, and a bare IN-100 panel was placed in position 2 of the holder. Figures 31a and 31b show the final effect of the simulator testing at 1038°C (1900°F). The specimens as shown in Fig. 31a are from left to right I-25 (dummy sample) IN-100, I-25, I-25, and I-25. The first I-25 specimen and IN-100 received 76 hours testing and the last three specimens were tested for a total of 100 hours. A more detailed view of the effects of the test is shown in Fig. 32a of a representative specimen of I-25 and Fig. 33, the IN-100 specimen.

Visual and metallographic examination of the I-25 specimens which have been simulator tested up to a total of 100 hours indicated that the coating, Glass No. 25, is stable to long exposure to 1038°C. The fact that the simulated drag and pressure forces caused the coating to ripple indicated that the viscosity of the glass at 1038°C was too low. The ideal compromise of a viscosity which allows for self-healing and yet capable of resisting the drag and pressure forces was not obtained for 1038°C.

H. Metallographic Examination of Selected Test Specimens

A number of test specimens, including both IN-100 and TD-Ni, were sectioned, etched and examined photographically at 500X. The center line Knoop Hardness Numbers (KHN) at either 25 or 100 gm impression loads were also determined. The specimens that were examined, the mounting and etching techniques, the KHN for the coatings and substrates, and the photomicrographs at 500X are shown in Tables IX-X and Figs. 34-44.

The coated TD-Ni specimens that were examined (T-54, T-94, and T-119) do not exhibit any metallurgical change after exposure to either 1038°C (1900°F) or 1149°C (2100°F). The KHN indicates the coating does not change the hardness of the material.

In general the micrographs indicate a very low degree of reaction between the coatings and TD-Ni in both the as-coated and exposed samples.

It would appear that the coatings protected TD-Ni from oxidation until they spalled from the metal and that the limited reaction at the interface caused the adherence of the coating to be low enough to allow the low expansion coatings to spall from a majority of the metal. The appearance of the coatings on TD-Ni before and after exposure reveals the temperature instability of the glass-ceramic, Figs. 34,35, two-phase admixture, Figs. 36-39, systems as well as the reduction in the coating thickness of the tested samples.

The IN-100 specimens that were examined, I-23, I-25, I-94, and bare IN-100, Figs. 40-44) showed a considerable metallurgical change in the complex multi-phase substrate. Coated specimens indicated that the complex intermetallic and carbide phases disappeared at interface during long-term exposure at 1149°C (Figs. 40b, 41b), but not during short-term exposure at 1149°C (Fig. 42a), or long-term exposure at 1038°C (Fig. 42b). There was no evidence of oxide penetration into the substrate for any of the coated specimens. The uncoated IN-100 specimen, which received only 76 hours exposure at 1038°C, showed oxide penetration into the substrate as well as the disappearance of the secondary phases (Fig. 44). The KHN of the uncoated sample decreased at the oxide-metal interface to 262 while the coated sample remained relatively high at 367 to 396. This indicates chromium diffusion from the uncoated specimen at the interface. This has been borne out by electron microprobe.

It should be noted that both the high center-line KHN and visual examination of the as-coated I-25 system show that there is a high degree of reaction between Glass 25 and IN-100 at the interface and that this system is not prone to thermal spalling. The photomicrographs of System I-25 (Fig. 42b) shows that the IN-100 was adequately protected by Glass 25 from hot corrosion for the 100 hour turbine simulator test at 1038°C. A difference in the coating thickness between the front and back of the specimens indicates that the coating was fluid enough to be affected by the gas velocity and hence might not protect the substrate at higher temperatures, longer times, and higher gas velocities.

VI. COATING OF NASA EROSION SPECIMENS WITH GLASS 25

A. IN-100 Specimens

A total of ten 4" x 1" x 0.25" IN-100 erosion bars to be coated with glass 25 were received from NASA-Lewis. The corners and edges of the top three inches of each specimen were rounded to facilitate the application of the coating. The same top three inches of each specimen was then lightly blasted with 60 mesh grit to prepare the surface for glass coating.

A 5 mil coating of glass 25 was applied to the top three inches of each specimen by air spraying from a -200 mesh water slurry. The powder coating was fused in an air atmosphere at 1286°C (2350°F) for four minutes followed by a three minute fusion at 1315°C (2400°F). The double fire at two different temperatures and times was necessary in order for the glass to form a stable coating without excessive metal distortion or incipient metal melting. If the coating contained small pinholes after the initial firing they were filled with slip and covered on the second firing. Samples that were not satisfactory were sand-blasted to remove the coating and reprocessed. In general the coatings were uniform, but some pinholes were still evident due to the nature of the metal oxide that was formed during fusion. The details of the application and fusion procedures for the IN-100 specimens are shown in Table III.

B. B-1900 Specimens

A total of ten 4" x 1" x 0.25" B-1900 specimens to be coated with glass 25 were received from NASA-Lewis. The corners and edges of these specimens were also rounded to facilitate the application of the coating. Since this material had not been investigated during the contract period, a metal pretreatment had to be determined that would

allow the application of glass 25. Sandblasting and pre-oxidation were tried without success as the glass spalled on cooling with both of these methods. A 60 second HNO_3:HF:H_2O etch appeared to give the best results as the glass film was uniform and adherent.

A 5 mil coating of glass 25 was then applied to the top three inches of each specimen by air spraying from a -200 mesh water slurry. The powder coating was fused in an air atmosphere at 1315°C (2400°F) for four minutes. The higher temperature and single fire was possible since the specimens were not prone to metal deformation or incipient metal melting. Five acceptable specimens were produced in this manner. The other five specimens were not acceptable due to non-wetting of the glass film on the metal oxide. These specimens were sandblasted and reprocessed without success. The details of the application and fusion procedures for the B-1900 specimens are shown in Table III.

VII. SUMMARY OF RESULTS

Of the three approaches toward high viscosity, oxidation-protective coatings, pure glass coatings appeared to be the best. Even the two phase admixture which looked promising proved to be a hybrid case where the second phase entered the glass network.

It cannot be concluded that there was a unique aspect of the testing conditions which caused failure in the coatings. In every instance the deterioration of the coating was controlled by rate processes. Consequently, we effectively examined the kinetics of the failure mechanism under progressively more severe conditions.

The mode of attack for the coatings was typically oxidation at a weak site. Ideal bonding is achieved when the minimum amount of oxide necessary is present at the interface to provide a compositioned gradient from the oxidic glass to the metal. Thus, if the coating is thin and does not offer much of a barrier, or if there is a pinhole site, oxidation proceded at rates varying increasingly with temperature. As the oxide builds up, the glass-to-metal bond is weakened because of the poor adherence of the metal oxide interface. The local failure of the coating exposes an even larger area to attack and the rate of deterioration increases. The rate of attack is to a degree effected by the viscosity of the glass. Consequently, we expected and observed a slower rate of attack in the high viscosity coatings. The ratio of attack were greatest at the edges because of the weakness of the glass to metal bond at the sharp edges.

Because of the low gas velocities in the torch test, this test did not prove to be very discriminating for the glass systems tested and was abandoned in favor of the spin and turbine simulator tests.

The coatings which survived the oxidation testing proved to be the most viscous glass (No. 21 on IN-100) and the glass which resulted from the reaction and dissolution of the SiO_2 particles in the 23-1 glass. These results are consistent with rate controlled and viscosity effected reactions. Particulate SiO_2 could not be introduced in glass 25 because it would raise the fusion temperature and this temperature was already the maximum possible temperature wherein IN-100 would not distort. The glass ceramic results will be discussed later.

As was expected, as the conditions of the test became more severe and the time of test longer, the rate of attack and the degree of deterioration increased. Only the most viscous glass systems survived the early phases of the testing. The effect of centrifugal testing was to thin the coatings which shortened the time for breakdown of the coating barrier. At 2100°F the coating life times were so short that comparisons were meaningless. Therefore, turbine simulator testing was carried out at 1900°F.

The results of this testing showed glass 25 able to protect IN-100 for 100 hours from oxidation. However, the viscosity of the coating proved to be too low as evidenced by rippling in the glasses.

The glass ceramic approach failed by two different mechanisms, both time controlled factors. At 2100°F the crystalline material reverted to the glassy phase whose viscosity is by nature too low for consideration. Thus, the coating thinned to the point where it offered no protection. At 1900°C the glassy phase continuously crystallized until the final coating was all crystalline. This produced wrinkling and overall instability.

Common to all these modes of failure, in all systems, is the fact that at some point in time the coatings are providing the required protection. It can therefore be seen, that in the necessary trade off of viscosity for applicability, lifetimes have been sacrificed. Greater lifetimes could be realized if higher application temperatures were permissible.

VIII. CONCLUSIONS

1. Glass enamel coatings may be applied to TD-Nickel, IN-100 and WI-52. Strong adherence is achieved in spite of large thermal expansion mismatches.
2. A silicate based glass coating offered 100 hour oxidation protection in a turbine simulator at 1900°F.
3. Long term oxidation protection at 1900°F and greater appears unlikely because of the substrates restrictions on application temperature.
4. Coating attack typically began at edges where pinhole free coating and good adherence is difficult to achieve.

APPENDIX A

THEORY OF DEFORMATION OF A GLASS COATING

The deformation in a thin viscous layer on the surface of a rapidly rotating disk may be investigated by the Navier-Stokes equations written up in cylindrical coordinates. The inertia terms may be neglected if a body force is introduced having the potential

$$\Omega = -\frac{1}{2} r^2 \omega^2 \rho \tag{1}$$

Thus

$$F_r = -\frac{\partial \Omega}{\partial r} = r\omega^2\rho \tag{2}$$

The inertia force F_r acts in the radially outward direction at all points. We keep in mind that velocities relative to the disk are very low compared to $r\omega$.

Let v_r, v_z, v_φ be velocity components in the radial, axial and azimuthal directions relative toaxes fixed in the disk. The problem may be treated as one of slow viscous flow, without inertia forces, if we include the body force F_r.

The equilibrium equations without the inertia terms are as follows:

$$\left.\begin{aligned}
\mu\left[\frac{\partial^2 v_r}{\partial r^2} + \frac{1}{r}\frac{\partial v_r}{\partial r} - \frac{v_r}{r^2} + \frac{1}{r^2}\frac{\partial^2 v_r}{\partial \varphi^2} - \frac{2}{r^2}\frac{\partial v_\varphi}{\partial \varphi} + \frac{\partial^2 v_r}{\partial z^2}\right] &= -\frac{\partial}{\partial r}(p+\Omega) \\
\mu\left[\frac{\partial^2 v_\varphi}{\partial r^2} + \frac{1}{r}\frac{\partial v_\varphi}{\partial r} - \frac{v_\varphi}{r^2} + \frac{1}{r^2}\frac{\partial^2 v_\varphi}{\partial \varphi^2} + \frac{2}{r^2}\frac{\partial v_r}{\partial \varphi} + \frac{\partial^2 v_\varphi}{\partial z^2}\right] &= \frac{1}{r}\frac{\partial}{\partial r}(p+\Omega) \\
\mu\left[\frac{\partial^2 v_z}{\partial r^2} + \frac{1}{r}\frac{\partial v_z}{\partial r} + \frac{1}{r^2}\frac{\partial^2 v_z}{\partial \varphi^2} + \frac{\partial^2 v_z}{\partial z^2}\right] &= \frac{\partial}{\partial z}(p+\Omega)
\end{aligned}\right\} \tag{3}$$

Conservation of mass for incompressible flow gives,

$$\frac{\partial v_r}{\partial r} + \frac{v_r}{r} + \frac{1}{r}\frac{\partial v_\varphi}{\partial \varphi} + \frac{\partial v_z}{\partial z} = 0 \qquad (4)$$

Stress components are

$$\left.\begin{aligned} p_{rr} &= -p + 2\mu\frac{\partial v_r}{\partial r} \quad ; \quad p_{r\varphi} = \mu\left(r\frac{\partial}{\partial r}\frac{v_\varphi}{r} + \frac{1}{r}\frac{\partial v_r}{\partial \varphi}\right) \\ p_{\varphi\varphi} &= -p + 2\mu\left(\frac{1}{r}\frac{\partial v_\varphi}{\partial \varphi} + \frac{v_r}{r}\right) \quad ; \quad p_{\varphi z} = \mu\left(\frac{\partial v_\varphi}{\partial z} + \frac{1}{r}\frac{\partial v_z}{\partial \varphi}\right) \\ p_{zz} &= -p + 2\mu\frac{\partial v_z}{\partial z} \quad ; \quad p_{zr} = \mu\left(\frac{\partial v_r}{\partial z} + \frac{\partial v_z}{\partial r}\right) \end{aligned}\right\} \qquad (5)$$

The hydrostatic pressure p is the average of the negative values of the viscous tensile stresses p_{rr}, $p_{\varphi\varphi}$, p_{zz}. Quantity μ is dynamic viscosity and ρ is density.

We have a simplification for the rotating disk system because of radial symetry. This leads to the conditions

$$v_\varphi = 0$$

$$\frac{1}{r}\frac{\partial}{\partial \varphi}(\text{all quantities}) = 0$$

$$p_{r\varphi} = p_{\varphi z} = 0$$

The simplified equations take the form:

$$\left.\begin{aligned} \mu\left[\frac{\partial}{\partial r}\left\{\frac{1}{r}\frac{\partial}{\partial r}(r v_r)\right\} + \frac{\partial^2 v_r}{\partial z^2}\right] &= \frac{\partial p}{\partial r} - r\omega^2\rho \\ \mu\left[\frac{1}{r}\frac{\partial}{\partial r}\left(r\frac{\partial v_z}{\partial r}\right) + \frac{\partial^2 v_z}{\partial z^2}\right] &= \frac{\partial p}{\partial z} \end{aligned}\right\} \qquad (6)$$

$$\frac{1}{r}\frac{\partial}{\partial r}(r v_r) + \frac{\partial v_z}{\partial z} = 0 \tag{7}$$

$$\left.\begin{aligned} p_{rr} &= -p + 2\mu \frac{\partial v_r}{\partial r} \\ p_{\varphi\varphi} &= -p + 2\mu \frac{v_r}{r} \\ p_{zz} &= -p + 2\mu \frac{\partial v_z}{\partial z} \end{aligned}\right\} \tag{8}$$

$$p_{zr} = \mu\left(\frac{\partial v_r}{\partial z} + \frac{\partial v_z}{\partial r}\right) \tag{9}$$

Here, use has been made of Equation 1, and also some partial derivative identities have been introduced.

Since we deal with a very thin layer we may assume also

$$\frac{\partial p}{\partial z} = \frac{\partial p}{\partial r} = 0 \tag{10}$$

$$p = p_0 = \text{const.}$$

The equations to be solved are then,

$$\frac{\partial}{\partial r}\left(\frac{1}{r}\frac{\partial}{\partial r}(r v_r)\right) + \frac{\partial^2 v_r}{\partial z^2} = -\frac{r\omega^2\rho}{\mu} \tag{11}$$

$$\frac{1}{r}\frac{\partial}{\partial r}(r v_r) + \frac{\partial v_z}{\partial z} = 0 \tag{12}$$

and the stresses are given by Equations 8 and 9.

Here ω is angular velocity in radians/sec, ρ is density in gm/cm^3, μ is viscosity in poises, and r and z are cylindrical coordinate distances in cm.

The boundary conditions are as follows:

$$v_z = 0 \quad \text{at} \quad z = 0 \tag{13}$$

$$v_r = 0 \quad \text{at } r = 0 \text{, and at } z = 0 \tag{14}$$

Since $\partial v_z/\partial r$ is very small compared to $\partial v_r/\partial z$, the boundary condition for shear stress p_{rz} at z = h is equivalent to

$$\left(\frac{\partial v_r}{\partial z}\right)_{z=h} = 0 \tag{15}$$

Consideration of the Equation (11) leads one to a formulation of a solution for v_r as follows, when h is constant:

$$v_r = \frac{\omega^2 \rho}{\mu}\left(hrz - \frac{rz^2}{2}\right) \tag{16}$$

This expression satisfies Equation (11) and boundary conditions (14) and (15). The z-component, v_z, is found by integration of Equation (12) with use of (16) and boundary condition (13):

$$v_z = -\frac{\omega^2 \rho}{\mu}\left(hz^2 - \frac{z^3}{3}\right) \tag{17}$$

The shear stress p_{rz} is given by

$$p_{rz} = \omega^2 \rho (hr - rz) \tag{18}$$

At the surface z = h we have

$$(v_z)_{z=h} = -\frac{2}{3}\frac{\omega^2 \rho h^3}{\mu} \tag{19}$$

It is of interest that v_z is independent of r. If we start with h uniform, then h remains uniform, although it decreases with time. Since v_z at z = h is actually dh/dt, we have from Equation (19):

$$\frac{dh}{dt} = -\frac{2}{3}\frac{\omega^2 \rho h^3}{\mu} \tag{20}$$

Integration of this equation, with use of the condition $h = h_o$ at t = o, gives

$$\frac{1}{h^2} - \frac{1}{h_o^2} = \frac{4}{3}\frac{\omega^2 \rho}{\mu} t \tag{21}$$

Let t* be the time required until $h = 0.5\ h_o$. We find for t*

$$t^* = \frac{9}{4}\frac{\mu}{\omega^2 \rho h_o^2} \tag{22}$$

A numerical example may be taken with

$\mu = 10^{10}$ poises
$\omega = 2000$ rad/sec
$\rho = 2.76$ gm/cm^3
$h_o = 0.015$ cm

For this example

$$t^* = \frac{9}{4} \times \frac{10^{10}}{4 \times 10^6 \times 2.76 \times 0.015^2} = 9.08 \times 10^6 \text{ sec}$$

or t* = 105 days.

The tensile stresses in the glass layer are calculated from the expressions given previously:

$$\left.\begin{aligned} p_{rr} &= -p + 2\mu \frac{\partial v_r}{\partial r} = -p + 2\omega^2\rho\left(hz - \frac{z^2}{2}\right) \\ p_{\varphi\varphi} &= -p + 2\mu \frac{v_r}{r} = -p + 2\omega^2\rho\left(hz - \frac{z^2}{2}\right) \\ p_{zz} &= -p + 2\mu \frac{\partial v_z}{\partial z} = -p - 2\omega^2\rho\left(2hz - z^2\right) \end{aligned}\right\} \quad (23)$$

A previous assumption was that p was constant. We should have merely assumed that p was independent of r. To determine the dependence of p on z, use can be made of the equation of equilibrium in the z-direction:

$$\mu\left\{\frac{1}{r}\frac{\partial}{\partial r}\left(r\frac{\partial v_r}{\partial r}\right) + \frac{\partial^2 v_z}{\partial z^2}\right\} = \frac{\partial p}{\partial z} \quad (24)$$

substitution for v_r and v_z then gives

$$\frac{\partial p}{\partial z} = -\omega^2\rho\left(2h - 2z\right) \quad (25)$$

$$\therefore \quad p = -\omega^2\rho\left(2zh - z^2\right) + p_o \quad (26)$$

where p_o is the value of p at the surface z = o. If we introduce the expression for p (Eq. 26) into the last of Equations (23) we now find

$$p_{zz} = -\omega^2\rho\left(2zh - z^2\right) - p_o \quad (27)$$

When z = h the tensile stress p_{zz} should be

$$\left(p_{zz}\right)_{z=h} = -p_a \quad (28)$$

where p_a is atmospheric pressure. Therefore

$$-p_2 = -\omega^2 \rho h^2 - p_a \tag{29}$$

and

$$p_c = p_a - \omega^2 \rho h^2 \tag{30}$$

APPENDIX B

ANALYSES OF STRESSES IN A SPINNING DISC

The case of the rotating disc of uniform thickness has been treated in standard texts on strength of materials. It is customary to assume an elemental volume from the disc and to set up balanced forces including normal and tangential components. When the resulting equation is solved and the proper boundary conditions applied, for example the radial stress must be zero at the periphery and the edge of the center hole assuming that such a hole is present, the following expressions result:

for radial stress

$$\sigma_r = \frac{\gamma V^2}{g} \left(\frac{3 + \mu}{8}\right)\left(1 + \alpha^2 - X^2 - \frac{\alpha^2}{X^2}\right) \qquad (1)$$

and for tangential stress

$$\sigma_t = \frac{\gamma V^2}{g} \left(\frac{3 + \mu}{8}\right)\left[1 + \alpha^2 - \left(\frac{1 + 3\mu}{3 + \mu}\right) X^2 + \frac{\alpha^2}{X^2}\right] \qquad (2)$$

where γ = density of the material

V = peripheral velocity

g = gravitational constant

μ = Poisson's ratio

α = a/b (inner and outer radii - fixed values)

X = r/b (r is a radius varying between a and b)

As pointed out above, the radial stress vanishes, at the edges and becomes a maximum at the point $r = \sqrt{ab}$. At this point the maximum radial stress becomes equation (1) with the right hand parentheses

value reduced to $(1 - \alpha)^2$. Similarly the maximum tangential stress occurs at the inner or hole edge of the disc at the point r = a or X = α and equation (2) becomes:

$$\sigma_t)_{max} = \frac{\gamma V^2}{g} \left(\frac{3 + \mu}{4}\right)\left[1 + \left(\frac{1 - \mu}{3 + \mu}\right)\alpha^2\right] \qquad (3)$$

It will become apparent that the tangential stress in the disc will always be higher than the radial and that failure should begin at the edge of the hole and propagate along a radius

The equations were solved for a 4" diameter disc currently used in the spinner experiments. This disc has a 1/2" diameter center hole and rotates at 20,000 RPM. The maximum radial stress occurs at 0.71" from the center and has a value of 5,230 psi. The maximum tangential stress is 10,700 psi if yielding has not occurred and as mentioned previously, is found at the edge of the hole. It drops rapidly along the radius reaching 2,380 psi at the outer edge of the disc. The tangential and radial stress curves are shown in Figure 81. Some distortion of the curves would occur locally as a result of the fastening screws.

The calculated stresses in the disc suggested that the properties of the three materials, i.e. IN-100, WI-52, and TD-Nickel should be checked at the proposed operating temperature. Tables of properties of nickel base alloys are given in the International Nickel Company Bulletin A-393 and from there, curves of ultimate and yield stresses were plotted as shown in Figures 82 and 83 and extrapolated to 2100°F. No problems would be expected with IN-100 or TD-Nickel but some yielding of WI-52 might occur at the mounting hole. Presently, even without cooling, however, this area runs about 75°C below test temperature so that a yield strength of 15,000 psi may be expected.

Since it is planned to spin the discs for long intervals, a property of more significance is the 100 hour rupture strength, shown in Figure 84. These curves indicate that some cracking at the hole may be expected for all three alloys and may be particularly serious for

WI-52 although the extrapolation in this case is a little questionable. There is even some doubt that the average stress (approximately 4,700 psi) or even the stress at the periphery (2,380 psi) could be permitted. Only TD-Nickel looks reasonably safe. In case of rupture during the test, reinforcement of the disc at the hole with a thicker area or hub may be indicated. An alternative would be intentional cooling. If the disc were cooled, particularly in the region of the hole a thermal gradient would result which would itself introduce stresses. For example, the following relation is available for tangential stress in a disc:

$$\sigma_t = \alpha E \left[-t + \frac{1}{b^2}\int_o^b trdr + \frac{1}{r^2}\int_o^r trdr\right]$$

It is only necessary to determine the temperature t as a function of the radius r and to perform the integration. This stress would then be superimposed on the other stresses. Under some conditions the thermal stress would be negative at the periphery, tending to reduce the total tangential stress in the hottest region (the radial stress would still be zero) and would add in the cooler region of the hole where the permissible stresses are now higher and hub reinforcing would be possible.

Table I

CHEMICAL COMPOSITIONS OF TD-Ni, WI-52, AND IN-100

A. TD-Ni

Chemical Analysis (wt. %)

Heat No.	C	Ti	Fe	Cr	Co	Cu	S	ThO_2	Ni
2404	.004	<.001	<.01	.01	<.01	.005	.0034	2.4	Balance
2311	.0044	<.001	.005	.003	.008	.005	.0034	2.5	Balance

B. IN-100

Chemical Analysis (wt. %)

Heat No.	C	Mn	Si	S	Cr	Fe	Co	Mo	Al	Ti	Zr	B	Cu	V	Ni
UA004	.17	<.1	<.1	.003	9.70	.16	15.30	3.00	5.45	4.28	.07	.015	<.1	1.04	Balance
RU202	.16	<.1	<.1	.003	10.75	.22	14.95	3.12	5.46	4.68	.067	.015	-	.81	Balance

C. WI-52

Chemical Analysis

Heat No.	C	Mn	Si	P	S	Cr	Ni	W	Fe	Cb+Ta	Co
RF246	.49	.22	.35	.010	.017	21.45	.36	10.8	1.70	1.75	Balance
RF223	.48	.17	.22	.015	.013	21.05	<.1	11.2	2.08	2.18	Balance
RF226	.47	.19	.38	.010	.012	20.50	.16	11.0	2.06	1.77	Balance

TABLE II

COATING COMPOSITIONS

COMPOSITION OF GLASSES (mole %)

Sample No.	Sag Pt. °C	$\alpha \times 10^{-6}$/°C	K_2O	Na_2O	SiO_2	Al_2O_3	MgO	CaO	ZnO	BaO	Miscellaneous
2	840	4.8	---	12.5	75	12.5	---	---	---	---	
3	> 910	10.3	12.5	----	75	12.5	---	---	---	---	
5	775	7.9	8.8	----	77.9	2.2	11.1	---	---	---	
6	530	----	9	10	70	6	5	---	---	---	
8-1	612	----	7	6	76	6	5	---	---	---	$2ThO_2$
8-2	695	7.8	7	6	70	6	5	---	4	---	$2ThO_2$
9	> 910	10	11.5	----	75	10.5	---	---	---	---	$1CoO, 2Fe_2O_3$
11-1	583	10.0	7	10	70	3	---	---	---	7	$3ZrO_2$
13-1	632	10.1	10	3	77	2	5	3	---	---	
13-2	576	9.4	4	7	75	2	---	4	---	5	3CdO
14-1	588	8.3	7	4	75	2	---	4	---	5	3CdO
14-2	586	11.3	10	5	75	3	---	5	---	2	
15-1	683	8.6	10	----	77	2	5	6	---	---	
15-2	687	9.2	7	6	71	6	5	---	4	---	$1ThO_2$
17	730	6.0	7	----	80	2	2	6	---	---	1NiO, 2CoO
18	673	8.0	7	6	71	6	2	---	4	---	$1ThO_2$, 1NiO, 2CoO
19-1	595	9.7	7	5	73	3	2	5	2	---	3CdO
19-2	663	6.9	---	3	77	2	5	3	---	---	$10Rb_2O$
20-1	730	6.4	---	----	77	3	---	10	---	---	$10Rb_2O$
20-2	660	8.0	10	----	75	2	---	---	---	13	
21-1	650	8.8	10	----	70	2	---	5	---	13	
21-2	650	9.0	10	----	70	2	---	---	---	18	
22-1	625	10.2	10	----	70	----	---	10	---	10	
22-2	678	8.1	7	----	68	2	---	10	3	10	
23	706	7.7	7	----	68	5	---	10	---	10	
24	844	6.8	12	----	75	10	---	3	---	---	
25	831	5.5	9	----	75	10	---	6	---	---	
26	707	7.2	8	3	70	6	4	5	4	---	
27	660	7.6	10	3	70	4	4	5	4	---	
28	778	7.4	12.3	----	74.1	9.9	---	3.7	---	---	
29	745	7.0	12	----	74	8	---	---	3	3	
30	742	6.0	10	----	74	8	---	---	3	5	

TABLE II (continued)
COATING COMPOSITIONS
CRYSTALLIZED GLASS COMPOSITIONS

Sample No.	Nominal Composition, Part By Weight								Sag Point °C	α ($\times 10^{-6}$/°C)	Comments	Application Temp (°C)	Crystallization Temp (°C)
	SiO_2	Na_2O	NaF	CaO	CaF_2	Al_2O_3	TiO_2	BaF_2					
32	36.96	16.37	-----	19.75	-----	26.92	-----	-----	692	9.73	Glass	----	----
33	36.96	16.37	-----	12.37	10.27	26.92	-----	-----	592	9.18	Homogeneously crystallized at 700°C	1240	1000
34	36.96	16.37	-----	16.06	5.14	26.92	-----	-----	626	10.16	Did not crystallize homogeneously	----	----
35	48.06	9.87	11.05	-----	-----	33.91	-----	-----	647	-----	Did not crystallize	----	----
36	48.06	-----	24.43	-----	-----	33.91	-----	-----	488	-----	Surface devitrification	----	----
38	36.96	16.37	-----	19.75	-----	21.92	5.00	-----	640	10.61	Homogeneous crystallization at 800°C. Glass very viscous.	1260	1000
38A	Crystallized sample of No. 38								---	13.61		----	----
39	36.96	16.37	----	14.75	----	26.92	5.00	-----	658	-----	Poor crystallization	----	----
40	44.5	16.7	-----	-----	-----	31.4	3.7	3.7	717	-----	High viscosity but glass crystallized homogeneously at 800°C.	----	----
41	44.5	8.54	11.05	-----	-----	31.4	7.4	-----	604	-----	Homogeneous crystallization at 700°C	1371	1000

TABLE II (continued)
COATING COMPOSITIONS
TiO_2 GLASS COMPOSITIONS

Sample No.	Nominal Composition, Parts by Weight									Sag Point °C	Thermal Expansion $\alpha(\times 10^{-6}/°C)$		Application Temp (°C)	Crystallization Temp (°C)
	SiO_2	Na_2O	NaF	CaO	CaF_2	Al_2O_3	TiO_2	BaF_2	K_2O		Glass	Crystallized		
42	46.9	8.54	11.05	---	---	31.4	5.0	---	---	593	8.7	8.7	1427	1000
43	55.55	---	---	.28	10.27	6.94	---	20.89	8.98	680	7.75	8.3	----	----
44	36.96	16.37	---	16.80	4.11	23.92	3.00	---	---	605	10.4	---	1204	1000
45	50.0	8.54	11.05	---	---	28.3	5.00	---	---	582	8.8	8.5	1316	1000
46	40.0	16.37	---	14.75	---	23.88	5.00	---	---	642	12.5	---	----	----
47	36.96	16.37	---	.19.75	---	21.92	7.5	---	---	635	---	---	----	----
48	50.0	12.64	4.06	---	---	28.3	5.0	---	---	670	8.0	8.9	1204	1000
49	40.0	12.64	5.5	20.0	---	20.0	5.0	---	---	600	10.9	13.1	1204	1000
50	40.0	12.64	5.5	20.0	---	20.0	7.5	---	---	591	11.2	12.0	1260	900
51	40.0	10.0	5.5	20.0	---	22.5	5.0	---	---	618	10.0	11.1	1260	900
52	45.0	12.64	5.5	20.0	---	20.0	5.0	---	---	602	10.1	10.6	1260	900
53	43.0	12.64	5.5	20.0	---	20.0	7.5	---	---	593	11.1	13.0	1260	900
54	40.0	12.64	5.5	15.0	---	24.0	5.0	5.0 BaO	---	602	9.4	13.5	1260	900

TABLE II (continued)
COATING COMPOSITIONS
GLASS COMPOSITIONS (wt. %)

Sample No.	SiO_2	Al_2O_3	CaO	TiO_2	Miscellaneous	Comments
61	78.5	3.9	--	--	2.5 K_2O, 12.1 Li_2O 3.0 P_2O_5	Crystallized-redissolved at 1150°C.
62	4.8	40.6	35.2	19.4	--	Did not form glass.
63	37.1	6.9	29.7	26.3	--	Surface crystallization.
64	35.1	30.6	24.0	10.3	--	Crystallized in pouring.
65	35.6	20.2	25.8	18.4	--	Bloated upon crystallizing.
66	39.0	32.3	25.3	5.4	--	Crystallized from surface.
67	40.5	28.1	22.0	9.4	--	Crystallized homogeneously.
68	3.9	50.2	45.9	--	--	Crystallized homogeneously at 1150°C.
69	4.8	48.8	46.4	--	--	Crystallized homogeneously at 1150°C.
70	3.1	49.7	47.2	--	--	Crystallized homogeneously at 1150°C.
71	8.1	58.5	33.4	--	--	Did not form glass.
72	10.0	54.0	36.0	--	--	Crystallized homogeneously at 1150°C. Sag point - 826°C.
73	11.0	28.0	61.0	--	--	Crystallized homogeneously at 1150°C.
74	15.0	30.0	55.0	--	--	Severely attacked crucible causing failure.
75	19.0	30.0	51.0	--	--	Crystallized homogeneously at 1150°C. Sag point - 816°C.

TABLE II (continued)
COATING COMPOSITIONS
GLASS COMPOSITIONS (wt. %)

Sample No.	SiO_2	Al_2O_3	CaO	TiO_2	Miscellaneous	Comments
76	15.0	42.0	43.0	--	--	Severely attacked crucible causing failure.
77	14.0	47.0	39.0	--	--	Would not form glass.
78	11.0	28.0	55.0	--	6.0 MgO	Severely attacked crucible causing failure.

Table III

METHOD OF SLIP PREPARATION FOR GLASSES AND GLASS-CERAMICS

1. Melt glasses, water quench to form frit.

2. Mix frit with water and suspending agent as below:

Frit	100 parts
Water	50 parts
CMC-7H*	.5 parts

3. Mill in ceramic lined saw mills containing ceramic balls for 24-48 hrs. to obtain -200 mesh particle size.

*Hercules Chemical Company, Carboxy Methalcellulose

Table IV

COMPOSITION OF MECHANICALLY-FILLED GLASS SYSTEMS

Additive	Volume Percent Additives to Glass 23-1
MgO	14.5, 25.5, 33.8, 40.5, 45.9, 50.0
Ni	6.3, 12.8, 17.3, 21.5, 25.5, 50.0
SiO_2	25, 50
$Al(OH)_3$	25, 50
Cr	25, 50
Cu	25
W	10, 25
Cr_2O_3	25, 50
CoO	25, 50
NiO	10, 25
ZrO_2	25, 50
TiO_2	25, 50

Table V

EFFECT ON WEIGHT LOSS OF 20 ONE-HOUR CYCLES OF SELECTED SYSTEMS

		Initial Weight	After 5 cycles		After 10 cycles		After 15 cycles		After 20 cycles		Total Change
I-23	1	27.3410	27.1036	-	27.0554	-	-		-		-0.2856
	2	27.1874	27.1178	-	27.0126	-	26.9660	-	26.9408	-	-0.2466
	3	27.7767	27.6067	-	27.5641	-	27.5424	-	27.5316	-	-0.2451
	4	28.0000	27.8111	-	27.6932	-	27.6270	-	27.5697	-	-0.4303
	5	27.5616	27.3771	-	27.1696	-	27.0600	-	27.0151	-	-0.5465
I-25	1	26.7483	26.7514	+	26.7514	0	26.7531	0	26.7516	0	+0.0033
	2	27.3835	27.3870	+	27.3870	0	27.3888	0	27.3878	0	+0.0043
	3	27.7727	27.7727	0	27.7710	0	27.7708	0	27.7684	0	-0.0043
	4	27.4618	27.4643	+	27.4633	0	27.4636	0	27.4611	0	-0.0007
	5	27.2436	27.2411	-	27.2354	-	27.2337	-	27.2305	0	-0.0130
T-13	1	18.5064	18.4184	-	18.3774	-	18.2845	-	17.9069	-	-0.5995
	2	18.5092	18.2612	-	18.1722	-	18.1073	-	17.9593	-	-0.5499
	3	18.3466	18.2647	-	18.2141	-	18.1464	-	17.8406	-	-0.5060
	4	18.3453	18.3067	-	18.2380	-	18.1185	-	17.8015	-	-0.5438
	5	17.4503	17.4060	-	17.3617	-	17.3185	-	17.1983	-	-0.2520
T-23	1	18.6273	18.4801	-	18.2976	-	18.2075	-	17.9240	-	-0.7033
	2	18.7274	18.3829	-	18.2842	-	18.2744	-	18.1917	-	-0.5357
	3	18.5030	17.7718	-	17.7602	-	17.7524	-	17.6825	-	-0.9205
	4	18.6911	18.2330	-	17.9936	-	18.0700	+	18.0355	-	-0.6556
	5	18.6169	17.9660	-	17.9558	-	17.9509	-	17.8693	-	-0.7476
T-24	1	19.2741	18.0062	-	18.0051	-	18.0032	-	18.0019	-	-1.2732
	2	19.4014	18.0765	-	18.0697	-	18.0671	-	18.0636	-	-1.3378
	3	19.0083	17.6996	-	17.6973	-	17.6938	-	17.6934	0	-1.3149
	4	19.3257	18.2087	-	18.1635	-	18.1585	-	18.1440	-	-1.1817
	5	18.8465	18.1159	-	17.7051	-	17.6745	-	17.6670	-	-1.1795
T-25	1	19.2865	19.1708	-	19.0643	-	19.0632	-	19.0623	0	-0.2242
	2	20.1103	17.9725	-	17.9700	-	17.9688	-	17.9682	0	-2.1421
	3	19.1535	18.0012	-	18.0013	0	18.0006	0	18.0006	0	-1.1529
	4	20.0982	19.4178	-	19.0465	-	19.0431	-	19.0411	0	-1.0571
	5	20.3707	18.1421	-	18.1383	-	18.1357	-	18.1341	0	-2.2466
T-22	1	18.5691	18.4230	-	18.1793	-	17.9895	-	17.9650	-	-0.6041
	2	18.5564	18.5364	-	18.5234	-	18.1114	-	17.9634	-	-0.5930
	3	18.7237	18.6715	-	18.6633	-	18.5531	-	18.1466	-	-0.5771
	4	18.5257	18.3628	-	18.3149	-	18.000	-	17.9360	-	-0.5897
	5	17.5544	17.4019	-	17.1418	-	16.9433	-	16.9151	-	-0.6393
T-29	1	18.8000	18.6501	-	18.5774	-	18.4823	-	18.1805	-	-0.6195
	2	17.5237	17.4632	-	17.4321	-	17.3937	-	17.2802	-	-0.2435
	3	17.4951	17.4136	-	17.3794	-	17.3436	-	17.2456	-	-0.2495
	4	19.4242	18.9475	-	18.8853	-	18.8273	-	18.7113	-	-0.7129
	5	19.6789	19.3983	-	19.2860	-	19.1952	-	18.9787	-	-0.7002

Table V (continued)

EFFECT ON WEIGHT LOSS OF 20 ONE-HOUR CYCLES OF SELECTED SYSTEMS

		Initial Weight	After 5 cycles		After 10 cycles		After 15 cycles		After 20 cycles		Total Change
T-92	1	20.4711	20.4171	-	20.4125	-	20.4230	+	20.4200	-	-0.0511
	2	19.6354	19.5502	-	19.5412	-	19.5703	+	19.5771	+	-0.0583
	3	19.9602	19.9116	-	19.9075	-	19.9045	-	19.8851	-	-0.0751
	4	19.8054	19.7026	-	19.6906	-	19.7128	+	19.7194	+	-0.0860
	5	19.3188	19.2029	-	19.1953	-	19.2119	+	19.2124	+	-0.1064
T-121	1	19.0014	18.9816	-	18.6735	-	18.5585	-	18.5767	+	-0.4247
	2	18.5646	18.5107	-	18.3086	-	18.2303	-	18.1293	-	-0.4353
	3	18.3324	18.3093	-	18.1976	-	18.1291	-	18.0491	-	-0.2833
	4	19.7237	19.6660	-	19.5306	-	19.4479	-	19.4254	-	-0.2983
	5	18.9208	18.6428	-	18.5614	-	18.5693	+	18.5869	+	-0.3339
T-123	1	19.6352	19.5717	-	19.5230	-	19.1840	-	19.2387	+	-0.3965
	2	18.9114	18.8196	-	18.7558	-	18.5658	-	18.5939	+	-0.4175
	3	19.5508	19.4218	-	19.3491	-	19.2444	-	19.2984	+	-0.2524
	4	19.6146	19.5575	-	19.4984	-	19.1971	-	19.2283	+	-0.3861
	5	18.5190	18.4635	-	18.4163	-	18.0940	-	18.1466	+	-0.3724
T-127	1	19.0926	18.9457	-	18.8947	-	18.2436	-	18.2970	+	-0.7956
	2	18.0502	17.9245	-	17.7614	-	17.6980	-	17.7387	+	-0.3115
	3	18.6172	18.2014	-	17.9470	-	18.0573	+	18.1085	+	-0.5087
	4	19.3545	19.2422	-	19.1052	-	18.9720	-	19.0275	+	-0.3270
	5	14.7907	14.7409	-	14.5222	-	14.1762	-	14.2205	+	-0.5702
T-94	1	18.9097	18.8622	-	18.8416	-	18.8281	-	18.7687	-	-0.1410
	2	19.6768	19.6418	-	19.6241	-	19.6074	-	19.5889	-	-0.0879
	3	19.7632	19.7130	-	19.6972	-	19.6831	-	19.6630	-	-0.1002
	4	19.2360	19.1891	-	19.1715	-	19.1663	-	19.1383	-	-0.0977
	5	19.3445	19.2964	-	19.2705	-	19.2438	-	19.2214	-	-0.1231
T-119	1	19.1418	19.1475	+	19.1173	-	19.1926	+	19.1879	-	+0.0461
	2	19.5674	19.5720	+	19.5407	-	19.4694	-	19.4507	-	-0.1167
	3	19.1213	19.1255	+	19.0885	-	19.0500	-	18.8196	-	-0.3017
	4	18.5004	18.5130	+	18.4782	-	18.4720	-	18.2200	-	-0.4864
	5	19.6083	19.6125	+	19.5728	-	19.6230	+	19.6330	+	+0.0247
T-93	1	19.6283	19.6044	-	19.6001	-	19.6041	+	19.6072	+	-0.0211
	2	19.2490	19.1958	-	19.1910	-	19.2069	+	19.2115	+	-0.0375
	3	19.2954	19.2470	-	19.2386	-	19.2415	+	19.2336	-	-0.0618
	4	19.8010	19.7518	-	19.7447	-	19.7572	+	19.7599	+	-0.0411
	5	19.1984	19.1566	-	19.1508	-	19.1588	+	19.1584	-	-0.0400
T-54	1	20.0464	20.0428	-	20.0139	-	20.0287	+	19.9862	-	-0.0602
	2	20.1675	20.1635	-	20.1340	-	20.1606	+	20.1493	-	-0.0182
	3	19.8918	19.8910	-	19.8646	-	19.8952	+	19.8076	-	-0.0842
	4	19.6267	19.6230	-	19.5987	-	19.6339	+	19.6030	-	-0.0237
	5	19.4656	19.4630	-	19.4302	-	19.4633	+	19.4351	-	-0.0305

Table VI

EFFECT ON WEIGHT LOSS OF 4 20-HOUR CYCLES OF SELECTED SYSTEMS

		Initial Weight	After 20 hours		After 40 hours		After 60 hours		After 80 hours		Change
I-25	1	26.7494	26.6413	-	26.6003	-	26.4810	-	26.3873	-	-0.3621
	2	27.3974	27.3005	-	27.2585	-	27.2282	-	27.0733	-	-0.3241
	3	27.7650	27.6947	-	27.6014	-	27.5279	-	27.4726	-	-0.2924
	4	27.4567	27.3760	-	27.1235	-	26.9155	-	26.7780	-	-0.6787
	5	27.2173	27.1093	-	27.0180	-	26.9295	-	26.8467	-	-0.3706
T-92	1	20.4255	20.2511	-	20.2764	+	19.9706	-	19.8789	-	-0.5466
	2	19.5807	19.4887	-	19.2515	-	18.8350	-	18.6384	-	-0.9423
	3	19.8951	19.6266	-	19.3576	-	19.1118	-	19.0649	-	-0.8302
	4	19.7280	19.5260	-	19.2075	-	18.8566	-	18.8131	-	-0.9149
	5	19.2032	18.9503	-	18.7392	-	18.5530	-	18.4761	-	-0.7271
T-94	1	18.8252	18.7057	-	18.6989	-	18.6537	-	18.3715	-	-0.4537
	2	19.6007	19.4787	-	19.4114	-	19.3615	-	19.2374	+	-0.3633
	3	19.6694	19.4550	-	19.3302	-	19.0637	-	18.9732	+	-0.6962
	4	19.1225	18.9039	-	18.7045	-	18.5030	-	18.4532	+	-0.6693
	5	19.2748	18.9459	-	18.8556	+	18.5316	-	18.4376	+	-0.8372
T-119	1	19.1880	19.2052	+	19.3639	+	19.4430	+	18.8225	-	-0.3655
	2	19.4416	19.4790	+	19.6355	+	19.7310	+	19.8114	-	+0.3698
	3	18.8140	18.8511	+	18.4930	-	18.6129	+	18.6975	-	-0.1165
	4	18.2349	17.7903	-	17.8831	+	17.9555	+	18.0450	-	-0.1899
	5	19.6340	19.0696	-	19.2827	+	19.4040	+	19.5066	-	-0.1274
T-93	1	19.6150	19.5453	-	19.5011	-	19.4528	-	19.3143	-	-0.3007
	2	19.2166	19.1565	-	19.0393	-	18.9444	-	18.7450	-	-0.4716
	3	19.2317	19.1585	-	19.0795	-	18.9576	-	18.7973	-	-0.4344
	4	19.7601	19.6666	-	19.5842	-	19.3427	-	19.2607	-	-0.4994
	5	19.1618	19.0738	-	18.9515	-	18.7876	-	18.7183	-	-0.4435
T-54	1	19.9868	19.7327	-	18.8684	-	18.1891	-	18.3378	+	-1.6490
	2	20.1379	19.9300	-	18.8366	-	18.1335	-	18.3258	+	-1.8121
	3	19.7909	19.5435	-	17.8966	-	18.0383	-	18.1725	+	-1.6184
	4	19.6048	19.5360	-	17.3996	-	17.5606	+	17.7167	+	-1.8881
	5	19.4313	19.1625	-	17.5262	-	17.7157	+	17.8674	+	1.5639

Table VII

SPIN TEST AT 1149°C

Weight change with each one-hour run.

System	Initial Weight	1	2	3	4	5	6	Total Change
I-25 *	98.4755	98.5336	--	97.8471	--	--	97.6129	-0.8626
T-94	112.3218	112.0515	111.0528	111.1052	111.1165	111.2169	111.1997	-1.2690
T-54	112.9497	111.5162	111.2632	111.2588	111.2224	111.2424	111.1560	-1.7937
I-94 **	101.4299	100.5622	100.0246	99.5408	99.2589	99.0658	98.7303	-2.6996

* After first one-hour run speed was reduced.

** Run at a reduced speed.

Table VIII

WEIGHT CHANGE VS TIME IN TURBINE SIMULATOR AT 1038°C

System I-25 - Glass No. 25 on In-100, Bare In-100

System and Position	Initial Weight	After, hours						Total Change
		24	40	46	65	80	100	
I-25 (5th pos.)	24.3052	23.566	23.2462	23.1522	23.1261	23.0672	22.9782	-1.3270**
I-25 (4th pos.)	24.7229	24.5029	24.4413	24.3631	24.3312	24.2867	24.1453	-0.5776
I-25 (3rd pos.)	24.4664	24.1016	24.0742	24.0138	23.9814	23.9443	23.6946	-0.7718**
(In-100) (2nd pos.)*	26.7994	--	26.8044	26.7463	26.7134	26.6553	26.1248	-0.6746**
I-25 (1st pos.)*	24.1773	--	24.0741	24.0107	23.9455	23.8863	23.7647	-0.4126

* Subtract 24 hours from hours listed.

** Damage to leading and trailing edges resulted in too high weight change.

Table IX

PREPARATION OF METALLURGICAL SAMPLES

A. Mounting

Mounted in aluminum filled epoxy

B. Etchant

IN-100 Samples

Modified Marbles Solution diluted to one-half strength

25 ml. alcohol

25 ml. water

50 ml. conc. hydrochloric acid

10 g. cupric sulfate

TD-Ni Samples

3 parts hydrochloric acid

1 part nitric acid

Diluted with glycerine

Table X

KNOOP HARDNESS TEST OF IN-100 SPECIMENS
25 AND 100 GM. LOAD IMPRESSIONS

Sample Identification		Glass 23-1 on IN-100 as coated System I-23		Glass 25 on IN-100 as coated System I-25		Glass 25 on IN-100 after 100 hour oxidation System I-25		50% SiO_2 on IN-100 after 6 hrs cyclic spin System I-94		Glass 25 on IN-100 after 6 hrs cyclic spin System I-25		Bare IN-100 after 76 hrs simulator test		Glass 25 on IN-100 after 100 hrs simulator test System I-25		Glass 25 on IN-100 after 100 hrs simulator test System I-25	
Distance from Interface (in mils)	Material	Photo H-1901 100 g	25 g	Photo H-1903 100 g	25 g	Photo H-1904 100 g	25 g	Photo H-2360 100 g	25 g	Photo H-2361 100 g	25 g	Photo H-2418 100 g	25 g	Photo H-2419 100 g	25 g	Photo H-2420 100 g	25 g
4	Glass	638	681.5		601										617.5		
3	"		681.5		589										617.5		
2	"	*	638		769						608				571		598
1	"	*	693		742				597**		648		998***	451	537.5		608
Interface																	
1	Metal	429		475		444		491		419		262		367		396	
3	"	422		614		390		429		402		415		402		402	
5	"	415		483		396		454		406		422		396		429	
10	"	444		451		422		396		415		402		396		390	
15	"	447		412		451		415		384		402		409		398	
20	"	396		409		396		409		384		390		429		367	
40	"	422		419		459		409		402		409		436		412	
60	"	406		451		509		---		---		402		415		406	

*Hardness indent caused crack in glass.
**Difficult to read in dark glass.
***Oxide and not glass.

Table XI

KNOOP HARDNESS TEST OF TD-Ni SPECIMENS
25 AND 100 GM. LOAD IMPRESSIONS

Sample Identification		50% SiO_2 on G.C. TD-Ni as coated System T-94		50% SiO_2 on G.C. TD-Ni after 100 hr. Oxidations System T-94		Crystallized Glass 54 on TD-Ni After 4 hr. simulator System T-54		50% SiO_2 on G.C. TD-Ni after 24 hr. Simulator System T-94		50% SiO_2 on G.C. TD-Ni after 6 hr. Cyclic spin System T-94	
Distance from Interface (in mils)	Material	Photo H-1911 100 g.	25 g.	Photo H-1913 100 g.	25 g.	Photo H-2354 100 g.	25 g.	Photo H-2357 100 g.	25 g.	Photo H-2359 100 g.	25 g.
4	Glass	*	*								
3	"	*	*								
2	"	*	*	598				648			
1	"	*	*	586.5		522		522		**	
Interface											
1	Metal	199		185		166		199		172	
3	"	198		193		191		195		172	
5	"	213		189		209		204		181	
10	"	202		204		195		197		179	
15	"	193		202		199		191		175	
20	"	198		197		197		202		172	
40	"	187		191		189		199		183	

*Could not obtain reading in dark glass.
**Glass structure mottled and not in one plane. Hardness impression is not continuous and cannot be measured.

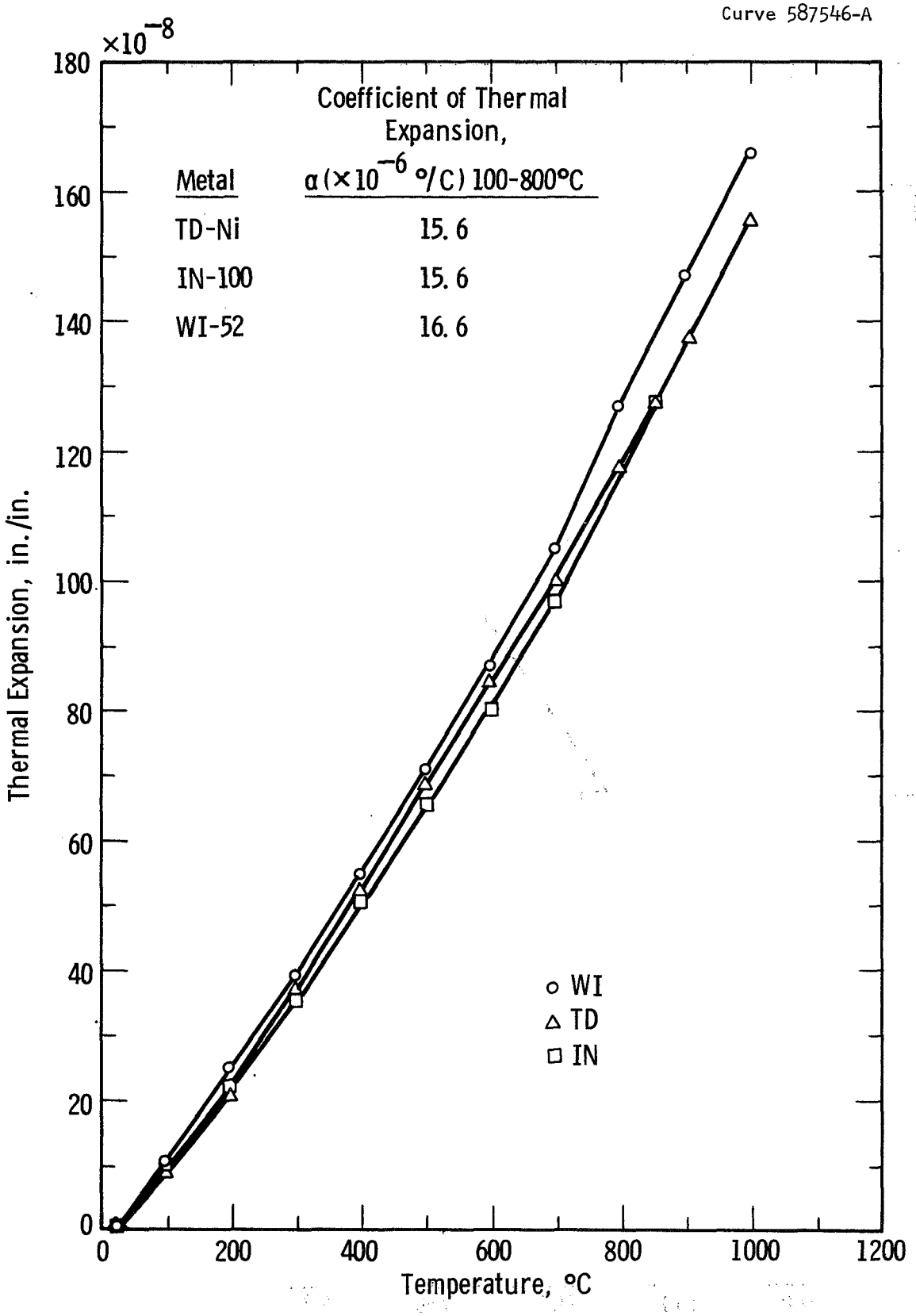

Fig. 1—Thermal expansion of WI-52 from 25°C to 1000°C in argon

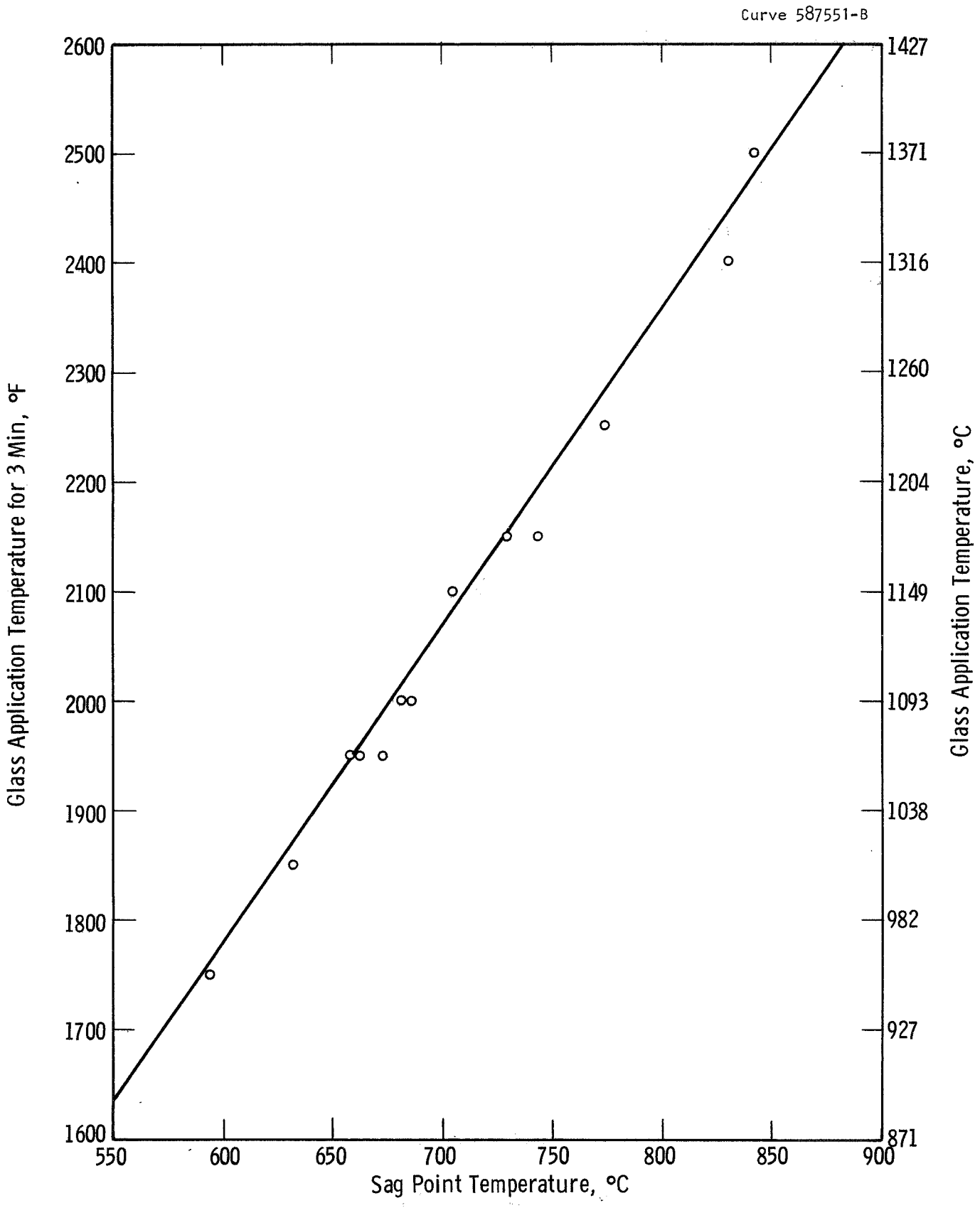

Fig. 2—Sag point temperature vs application temperature for glassy coatings

EVALUATION OF CONTROLLED

PHASE I COATINGS

PHASE II COATINGS

PHASE III COATINGS

PRELIMINARY EVALUATION - GLASS COATINGS

COATING NUMBER	COAT. SYS. GLASS/METAL	GLASS SAG POINT	TH. EXPAN. MISMATCH	FUSEABILITY OF COATING	WETTABILITY TO METAL	FORM. OF CONT. COAT	ADHERENCE	THER. SH. RESIST.	STAB. OF COATING	TOTAL OF 8 TESTS
T-3	3/TD-Ni	3	3	1	—	—	—	—	—	7
T-5	5/TD-Ni	3	2	2	1	1	1	1	1	12
T-6	6/TD-Ni	1	—	2	1	1	1	2	3	11
T-8	8Z/TD-Ni	2	2	2	2	1	1	1	3	14
T-9	9/TD-Ni	3	3	1	—	—	—	—	—	7
T-11	11-1/TD-Ni	1	3	2	2	1	1	1	3	14
T-13	13-1/TD-Ni	1	3	3	3	3	3	3	3	22
I-13	13-1/IN-100	1	3	3	1	1	1	1	1	12
W-13	13-1/WI-52	1	3	3	1	1	1	1	1	12
T-15-1	15-1/TD-Ni	2	3	3	3	3	3	2	3	22
I-15-1	15-1/IN-100	2	3	3	3	1	1	1	3	17
W-15-1	15-1/WI-52	2	3	3	3	1	1	1	3	17
T-15-2	15-2/TD-Ni	2	3	3	3	3	3	2	3	22
I-15-2	15-2/IN-100	2	3	3	3	1	1	1	3	17
W-15-2	15-2/WI-52	2	3	3	3	1	1	1	3	17
T-17	17-1/TD-Ni	2	1	3	2	2	2	1	3	16
T-18	18-1/TD-Ni	2	2	2	1	1	1	1	3	13
T-19-1	19-1/TD-Ni	1	3	2	1	1	1	2	3	14
T-19-2	19-2/TD-Ni	2	1	2	2	2	2	1	3	15
T-20-1	20-1/TD-Ni	2	1	3	3	2	2	1	3	17
T-20-2	20-2/TD-Ni	2	2	2	1	1	2	2	3	15
T-21-1	21-1/TD-Ni	2	3	2	1	1	2	2	3	16
T-21-2	21-2/TD-Ni	2	3	2	1	1	2	1	1	13
T-22-2	22-2/TD-Ni	2	2	3	3	3	3	3	3	22
I-22-2	22-2/IN-106	2	2	3	3	3	3	3	3	22
W-22-2	22-2/WI-52	2	2	3	3	3	3	3	3	22
T-23-1	23-1/TD-Ni	2	2	3	3	3	3	2	3	21
I-23-1	23-1/IN-100	2	2	3	3	3	3	3	3	22
W-23-1	23-1/WI-52	2	2	3	3	3	3	3	3	22
T-24	24/TD-Ni	3	1	3	3	3	3	2	3	21
I-24	24/IN-100	3	1	3	3	1	1	1	3	16
W-24	24/WI-52	3	1	3	3	1	1	1	3	16
T-25	25/TD-Ni	3	1	3	3	3	3	3	3	22
I-25	25/IN-100	3	1	3	3	2	2	2	3	19
W-25	25/WI-52	3	1	3	3	1	1	1	3	16
T-26	26/TD-Ni	2	1	3	3	2	3	1	3	19
T-27	27/TD-Ni	2	2	2	2	1	1	1	3	14
T-28	28/TD-Ni	3	1	2	2	1	1	2	3	15
T-29	29/TD-Ni	2	1	2	2	2	2	2	3	16
I-29	29/IN-100	2	1	3	3	1	1	1	3	16
W-29	29/WI-52	2	1	3	3	1	1	1	3	15
T-30	30/TD-Ni	2	—	2	2	2	1	1	3	13

PRELIMINARY SCREENING TEST - GLASS COATINGS

COATING NUMBER	TORCH TESTS - 2100°F EDGE COVERAGE	SPALL RESISTANCE	METAL PROTECT.	GLASS STABILITY	REHEAL IMPACT	TOTAL TORCH 5 TESTS	6 HOURS OXIDATION - 2100°F EDGE COVERAGE	SPALL RESISTANCE	METAL PROTECT.	GLASS STABILITY	REHEAL IMPACT	TOTAL 6 HR. OX. 5 TESTS	OVERALL AVG. 5 TESTS
T-13	3	3	3	3	2	14	1	3	3	2	3	12	13
T-15-1	1	3	3	1	2	10	2	3	3	2	1	11	10
T-15-2	2	1	3	3	2	12	1	3	3	1	2	10	10
I-22-2	1	3	3	3	2	12	1	2	2	1	1	7	9
I-22-2	2	2	3	3	1	9	1	2	1	2	3	9	9
W-22-2	1	3	3	3	2	12	1	2	1	1	3	8	10
T-23-1	2	3	3	3	3	14	1	3	2	3	2	11	12
I-23-1	2	2	3	2	2	11	2	3	3	3	1	9	10
W-23-1	2	1	3	1	2	9	1	1	3	1	1	7	8
T-24	2	3	3	3	2	13	1	1	3	1	1	7	10
T-25	2	3	3	3	1	12	1	2	3	1	2	9	10
I-25	2	3	3	3	2	13	1	3	2	3	2	11	12

PRELIMINARY EVALUATION - GLASS-CERAMICS ON TD-Ni

	COATING SYSTEM	ABILITY TO FORM GLASS	ABILITY TO XTAL GLASS	SUIT. TYPE OF XTAL	STAB. OF XTAL IN BULK FOR.	ABIL. TO COAT TD-Ni MET.	GLASS SAG POINT	EXPANSION MISMATCH	COAT. OF GLASS TO MET.	ABIL. TO FORM CONT. XTAL	OPT. OF XTAL COMP. TO USE	T. STAB. OF XTAL COAT	TOTAL OF 6 TESTS
T-32	32	YES	NO	—	—	—							
T-33	33	YES	YES	YES	YES	YES	1	1	3	1	2	1	9
T-34	34	YES	YES	NO	—	—							
T-35	35	YES	NO	—	—	—							
T-38	38	YES	YES	YES	YES	YES	2	3	2	1	2	1	11
T-39	39	YES	YES	NO	—	—							
T-40	40	YES	YES	YES	YES	NO							
T-41	41	YES	YES	YES	YES	YES	2	—	1	1	2	2	8
T-42	42	YES	YES	YES	YES	YES	1	1	1	1	1	1	6
T-43	43	YES	YES	YES	YES	NO							
T-44	44	YES	YES	YES	YES	YES	2	2	2	1	2	1	10
T-45	45	YES	YES	YES	YES	YES	1	1	2	1	2	1	8
T-46	46	YES	YES	YES	YES	NO							
T-47	47	YES	YES	YES	YES	NO							
T-48	48	YES	YES	YES	YES	YES	3	1	2	1	3	1	11
T-49	49	YES	YES	YES	YES	YES	2	3	2	1	3	1	12
T-50	50	YES	YES	YES	YES	YES	1	3	3	1	2	1	11
T-51	51	YES	YES	YES	YES	YES	2	2	3	3	2	1	13
T-52	52	YES	YES	YES	YES	YES	2	2	3	2	2	1	12
T-53	53	YES	YES	YES	YES	YES	1	3	3	2	2	1	12
T-54	54	YES	YES	YES	YES	YES	2	3	3	3	2	3	16
T-61	61	YES	YES	NO	—	—							
T-62	62	NO	—	—	—	—							
T-63	63	YES	YES	NO	—	—							
T-64	64	NO	—	—	—	—							
T-65	65	YES	YES	NO	—	—							
T-66	66	YES	YES	NO	—	—							
T-67	67	YES	YES	YES	NO	—							
T-68	68	YES	YES	YES	NO	—							
T-69	69	YES	YES	YES	NO	—							
T-70	70	YES	YES	YES	NO	—							
T-71	71	NO	—	—	—	—							
T-72	72	YES	YES	YES	YES	NO							
T-73	73	YES	YES	YES	NO	—							
T-74	74	NO	—	—	—	—							
T-75	75	YES	YES	YES	NO	—							
T-76	76	NO	—	—	—	—							
T-77	77	NO	—	—	—	—							
T-78	78	NO	—	—	—	—							

PRELIMINARY SCREENING TEST GLASS-CERAMIC COATINGS 6 HOUR OXIDATION - 1149°C (2100°F)

COATING SYSTEM	SPALL RESISTANCE	COATING CONT.	STAB. OF XTAL PHAS.	METAL OXIDATION	EDGE COVERAGE	TOTAL 5 TESTS
32						
33	1	1	1	1	1	5
34						
35						
38	1	1	1	1	1	5
39						
40						
41	1	1	1	1	1	5
42	1	1	1	1	1	5
43						
44	1	1	1	1	1	5
45	1	1	1	1	1	5
46						
47						
48	1	1	1	1	1	5
49	1	1	1	1	1	5
50	1	1	1	1	1	5
51	2	1	2	1	1	7
52	1	1	1	1	1	5
53	1	1	1	1	1	5
54	3	2	3	3	2	13

PRELIMINARY EVALUATION - MECHANICALLY FILLED GLASS SYSTEMS (23-1 BASE GLASS + VOLUME% ADDITIVE ON TD-Ni

	COAT. SYS. FILL METTRE*	ABILITY TO FUSE COAT.	WETTABILITY TO METAL	FORM. OF CONT. COAT.	ADHERENCE	TOTAL OF 4 TESTS
T-79	14.5Ni + O NGC	2	1	1	1	5
T-80	25.5 " "	2	1	1	1	5
T-81	33.8 " "	2	1	1	1	5
T-82	40.5 " "	2	1	1	1	5
T-83	45.9 " "	2	1	1	1	5
T-84	50.0 " "	2	1	1	1	5
T-85	6.3 Ni NGC	2	2	1	1	6
T-86	12.8 Ni NGC	2	2	1	1	6
T-87	17.3 Ni NGC	2	2	1	1	6
T-88	21.5 Ni NGC	2	2	1	1	6
T-89	25.5 Ni NGC	2	2	1	1	6
T-90	50.0 Ni NGC	2	2	1	1	6
T-91	25 Si_3N_4 NGC	3	3	3	3	12
T-92	25 SiO_2 GC	3	3	3	3	12
T-93	50 SiO_2 NGC	3	3	3	2	11
T-94	50 SiO_2 GC	3	3	3	3	12
T-95	25 $Al(OH)_3$ NGC	3	3	3	3	12
T-96	25 $Al(OH)_3$ GC	3	3	3	3	12
T-97	50 $Al(OH)_3$ NGC	1	2	2	1	6
T-98	50 $Al(OH)_3$ GC	2	2	1	1	7
T-99	25 Cr_2 NGC	2	1	1	1	5
T-100	25 Cr_2 GC	2	2	1	1	6
T-101	50 Cr_2 NGC	2	1	1	1	5
T-102	50 Cr_2 GC	2	1	1	1	5
T-103	25 Cu_2 GC	2	1	1	1	5
T-104	25 Cu_2 NGC	2	1	1	1	5
T-105	10 W NGC	1	1	1	1	4
T-106	10 W GC	2	1	1	1	5
T-107	25 W NGC	1	2	1	1	5
T-108	25 W GC	2	1	1	1	5
T-109	25 Cr_2O_3 NGC	2	3	3	2	10
T-110	25 Cr_2O_3 GC	3	3	3	3	12
T-111	50 Cr_2O_3 NGC	1	1	1	1	4
T-112	50 Cr_2O_3 GC	2	2	1	1	6
T-113	25 Co_3O_4 NGC	2	1	1	1	5
T-114	25 Co_3O_4 GC	3	3	3	3	12
T-115	50 Co_3O_4 NGC	2	1	1	1	5
T-116	50 Co_3O_4 GC	2	1	1	1	5
T-117	10 NiO NGC	1	1	1	1	4
T-118	10 NiO GC	2	1	1	1	5
T-119	25 NiO NGC	2	2	2	3	9
T-120	25 NiO GC	1	1	1	1	4
T-121	25 Zr_3O_2 NGC	3	3	3	3	12
T-122	25 Zr_3O_2 GC	3	3	3	3	12
T-123	50 Zr_3O_2 NGC	3	2	2	2	9
T-124	50 Zr_3O_2 GC	2	2	1	1	6
T-125	25 TiO_2 NGC	3	3	3	2	11
T-126	25 TiO_2 GC	3	3	3	2	11
T-127	50 TiO_2 NGC	3	3	3	3	12
T-128	50 TiO_2 GC	2	2	1	1	6

PRELIMINARY SCREENING TEST MECHANICALLY FILLED GLASS SYSTEM 6 HOUR OXIDATION 1149°C (2100°F)

SPALL RESISTANCE	COATING CONT.	COATING STABILITY	REHEAL IMPACTS	EDGE COATING	METAL OXIDATION	TOTAL 6 TESTS
1	1	1	3	2	3	11
2	3	3	2	2	3	15
3	3	2	3	2	3	16
3	3	3	1	2	3	15
1	1	1	3	1	3	10
2	1	1	3	1	3	11
1	1	1	1	1	1	6
2	1	1	2	1	2	9
2	1	1	2	1	2	9
3	3	3	3	2	3	17
3	3	3	3	2	3	17
3	3	3	3	2	3	17
2	2	1	3	2	2	12
3	3	3	2	2	3	16
2	1	1	3	1	2	10
2	1	1	3	1	2	10

*METAL TREATMENT
G.C. - 2 MILS OF 23-1 BASE GLASS AS A GROUND COAT
N.G.C. - NOT GROUND COATED BUT PRE-OXIDIZED

VISCOSITY COATING FOR SUPERALLOYS

100 HOUR FURNACE OXIDATION AT 1149°C (2100°F)

ADVANCED TESTING

	END 20-ONE HOUR CYCLES						END 4 ADDITIONAL 20 HOUR CYCLES						CENTRIFUGAL SPIN TESTS 1149°C (2100°F)					TURBINE SIMULATOR 1038°C (1900°F) END 6-1 HR. CYCLES					END 3-6 HR. CYCLES					END ADDITIONAL 76 CYCLES-HRS.				
	SPALL RESISTANCE	COATING CONT.	COATING STABILITY	WT. LOSS	METAL OXIDATION	TOTAL 5 TESTS	SPALL RESISTANCE	COATING CONT.	COATING STABILITY	WT. LOSS	METAL OXIDATION	TOTAL 5 TESTS	SPALL RESISTAN.	WT. LOSS	RESIST. TO COAT FLOW	COATING STABILITY	TOTAL 4 TESTS	WT. LOSS	RESIST. TO COAT FLOW	COATING STABILITY	RESIST. TO METAL OX.	TOTAL 4 TESTS	WT. LOSS	RESIST. TO COAT. FLOW	COATING STABILITY	METAL OXIDATION	TOTAL 4 TESTS	WT. LOSS	RESIST. TO COAT. FLOW	COATING STABILITY	RESIST. TO METAL OX.	TOTAL 4 TESTS
	1	1	1	1	1	5																										
	1	1	1	1	1	5																										
	1	1	1	1	1	5																										
	2	1	2	2	2	9																										
	1	1	1	1	1	5																										
	1	1	1	1	1	5																										
	3	2	3	3	3	14	2	1	3	2	2	10	3	2	2	3	10	3	3	3	3	12	3	2	3	3	11	3	2	3	3	11
	1	1	2	1	1	6																										
	3	3	1	2	3	12	1	1	1	1	1	5	3	1	2	2	8	1	1	1	1	4*										
	1	1	3	2	2	9*	1	1	1	1	1	5																				
	2	2	3	2	3	12	1	1	1	1	1	5																				
	2	3	3	2	3	14	2	1	3	2	1	9	3	2	1	2	8	3	2	3	3	11	2	1	2	1	6					
ADDITIONAL COATING SYSTEM I-94 50% SiO_2 - GC ON IN-100													1	1	1	1	4	2	1	2	2	7										
	2	1	2	2	1	8*	1	1	1	2*	1	6																				
	1	1	1	1	1	5																										
	1	1	1	1	1	5																										
	1	1	1	1	1	5																										

* SEVERAL SAMPLES OUT OF 5 POOR

* DUE TO EXCESSIVE OXIDATION

* ONLY TESTED 4 HOURS

NOTE:
RATING ON A 3-2-1 WITH 3 INDICATING THE MOST DESIRABLE PROPERTIES IN RELATION TO THE CONTRACT OBJECTIVES

FIG. 3

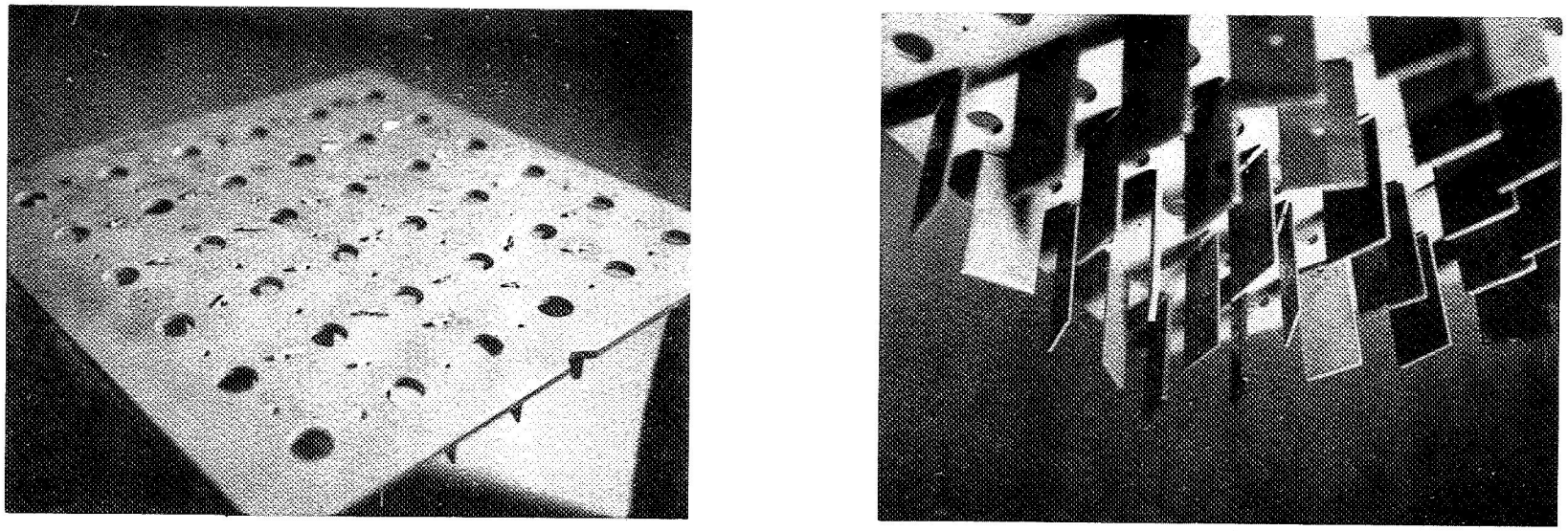

Fig. 4 —Oxidation test specimen holder with test specimens attached

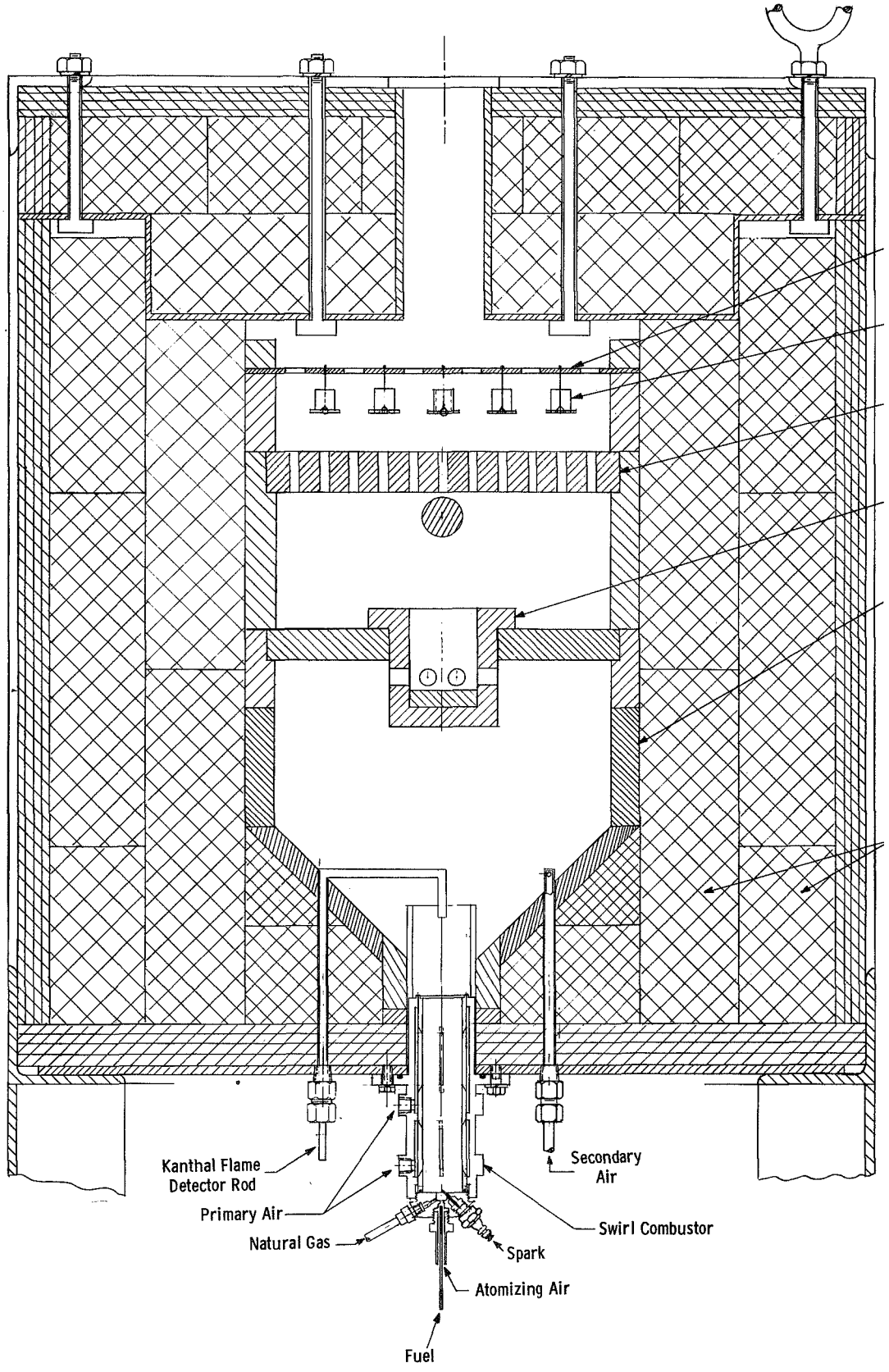

Fig. 5 —Cutaway drawing of the oxidation furnace

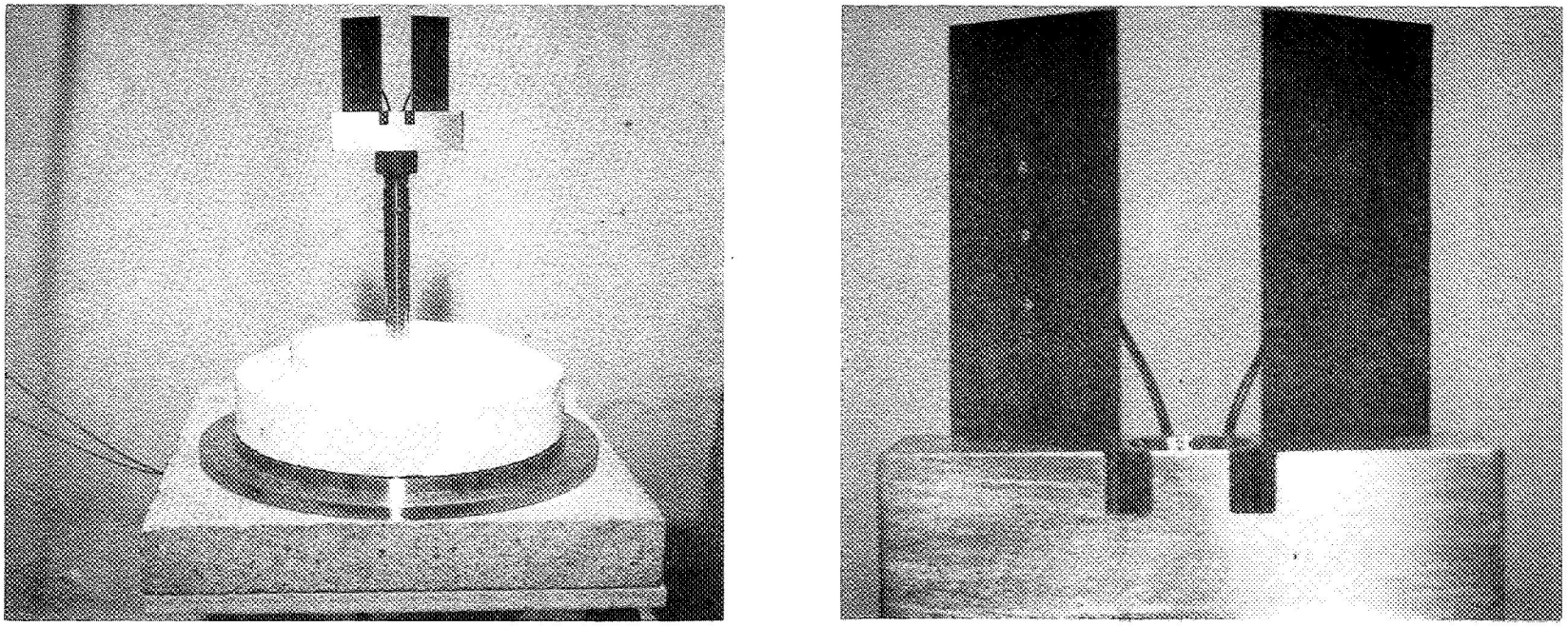

Fig. 6—Torch test specimen holder

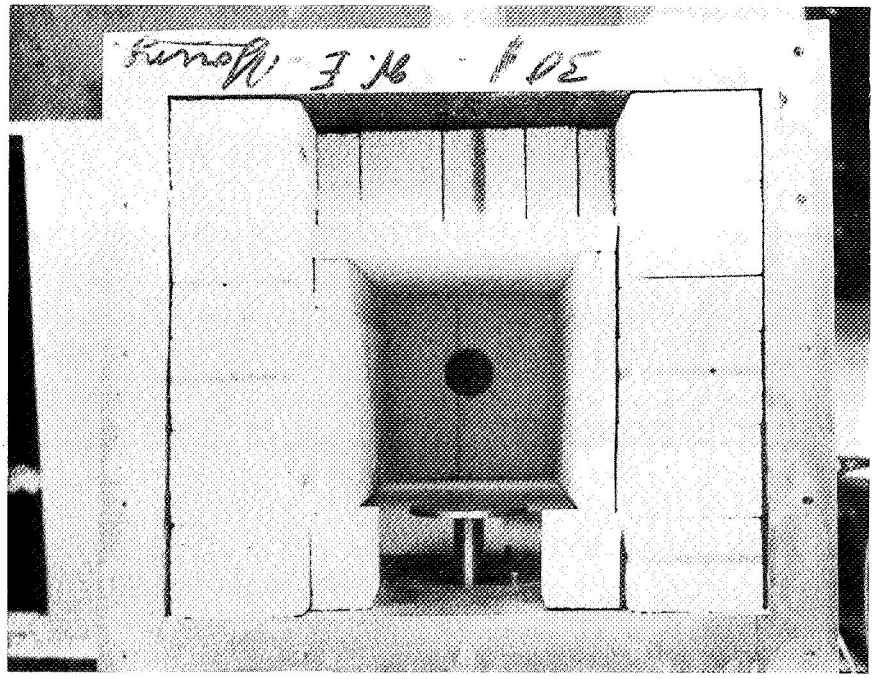

Fig. 7 – Inside of spin rig furnace

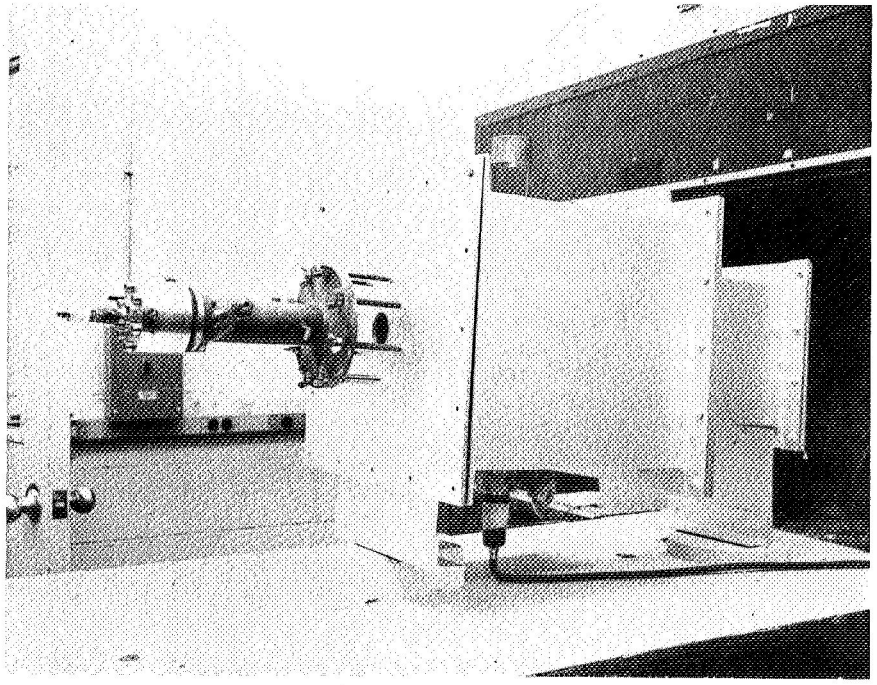

Fig. 8 – Spin rig assembly

	13	3/8-16 x 2 1/2 LG. ALLEN HD. SST. CAPSCR.	6							
	14	1/4-20 x 3/4 " " " " "	6							

○ FURN. BY ENGR.
◉ BUY FR. BUR-MAT CORP. PGH. 21, PA.
△ BUY FR. KEROTEST MFG. CO. PGH. 22, PA

□ BUY FR. UNITED AIRCRAFT PRODUCT CO., DAYTON, OHIO

APPARATUS MHD DEMONSTRATION MODEL # 2
SWIRL BURNER - ASS'Y.

DWG. 413C480 SUB. 1 FINISH CHART

SYM.	ITEM	DESCRIPTION – MATERIAL DIMENSIONS IN INCHES	PAT. NO. OR REF. DWG.	FIN. CH. LINE NO.	STYLE NO.	SYM. GR.	1	2	3	4	5
	1	ITS. # 1 & 2 GR. # 1 DWG. #	413C479				1				
	2	IT. # 3 "	"				1				
	3	IT. # 4 "	"				1				
	4	ITS. # 1 THRU 9 DWG. #	547D434				1				
○	5	DELAVAN NOZZLE #					1				
○	6	"CHAMPION" SPARK PLUG # Y-8					1				
△	7	U-6C 3/8 MALE FLARE X 3/8 IPS KEROTEST FITTING					1				
◉	8	1/2 CU. TO 3/8 M.S.P.S. NIBCO MALE ADAPTER					1				
□	9	METALLIC O'RING # U-2210-02375-SEN					2				
□	10	METALLIC O'RING # U-2210-00937-SEN					1				
	11	6" OF 1/4 O.D. X 5/16 I.D. SOFT CU. TUB.					1				
	12	.190-32 x 1/2 LG. ALLEN HD. SST. CAPSCR.					4				

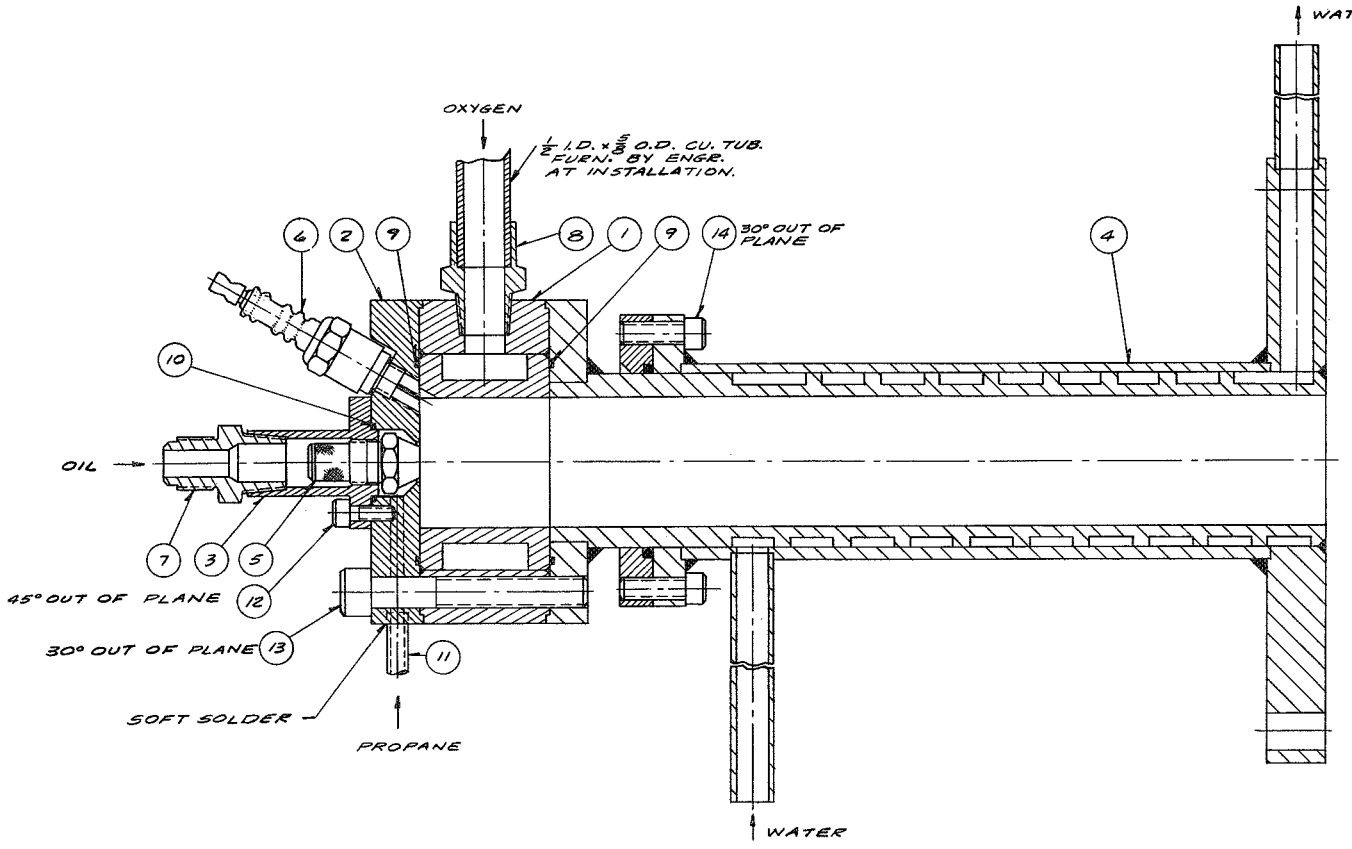

Fig. 9 – Swirl burner

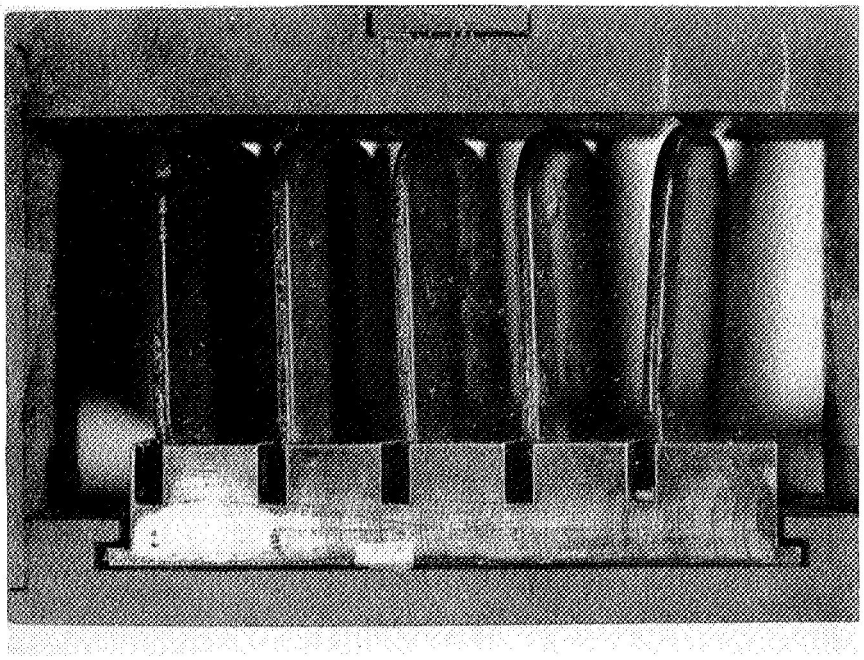

Fig. 10 –Insertion frame and specimen holder

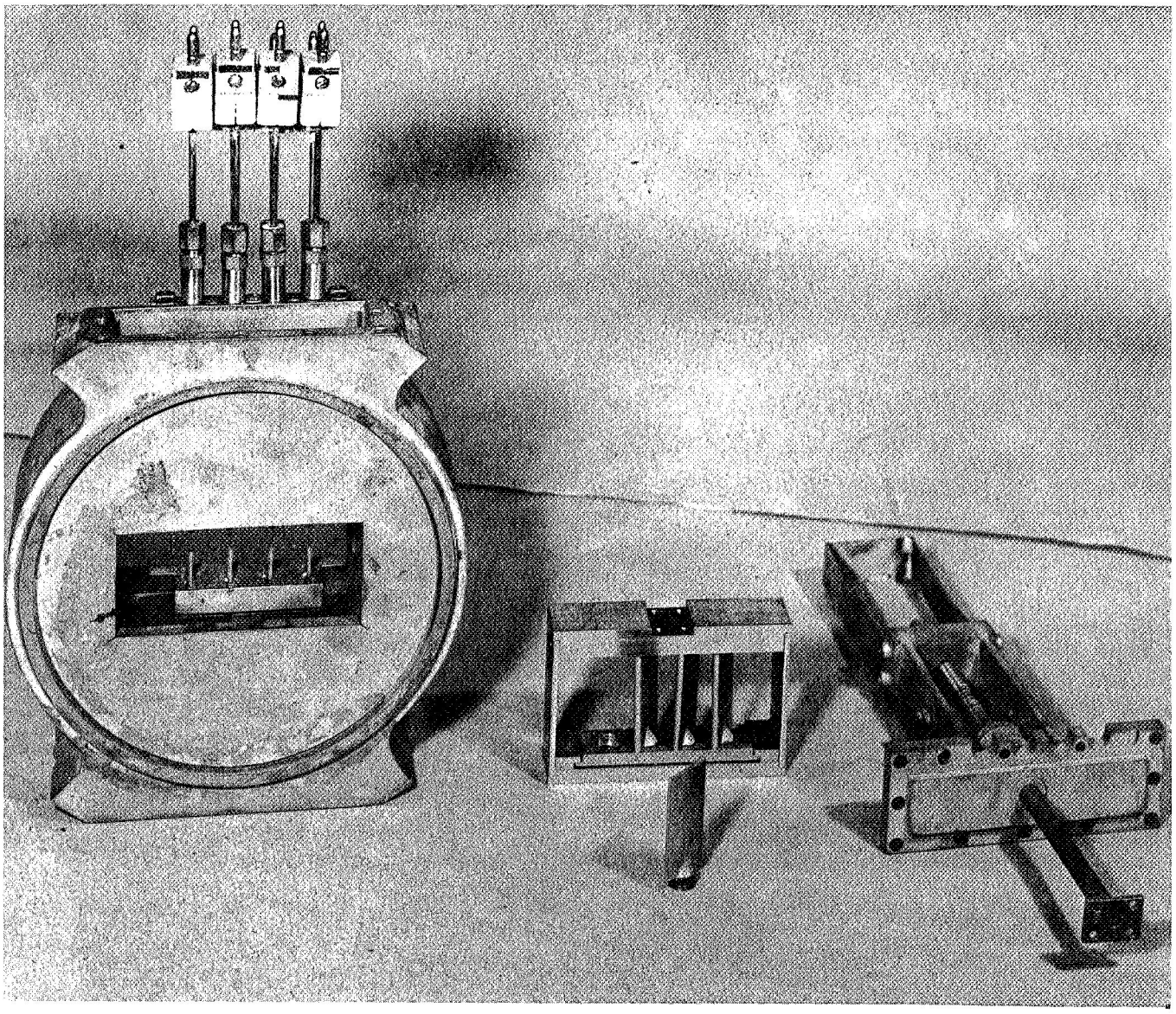

Fig. 11 –Aerodynamic shear test section

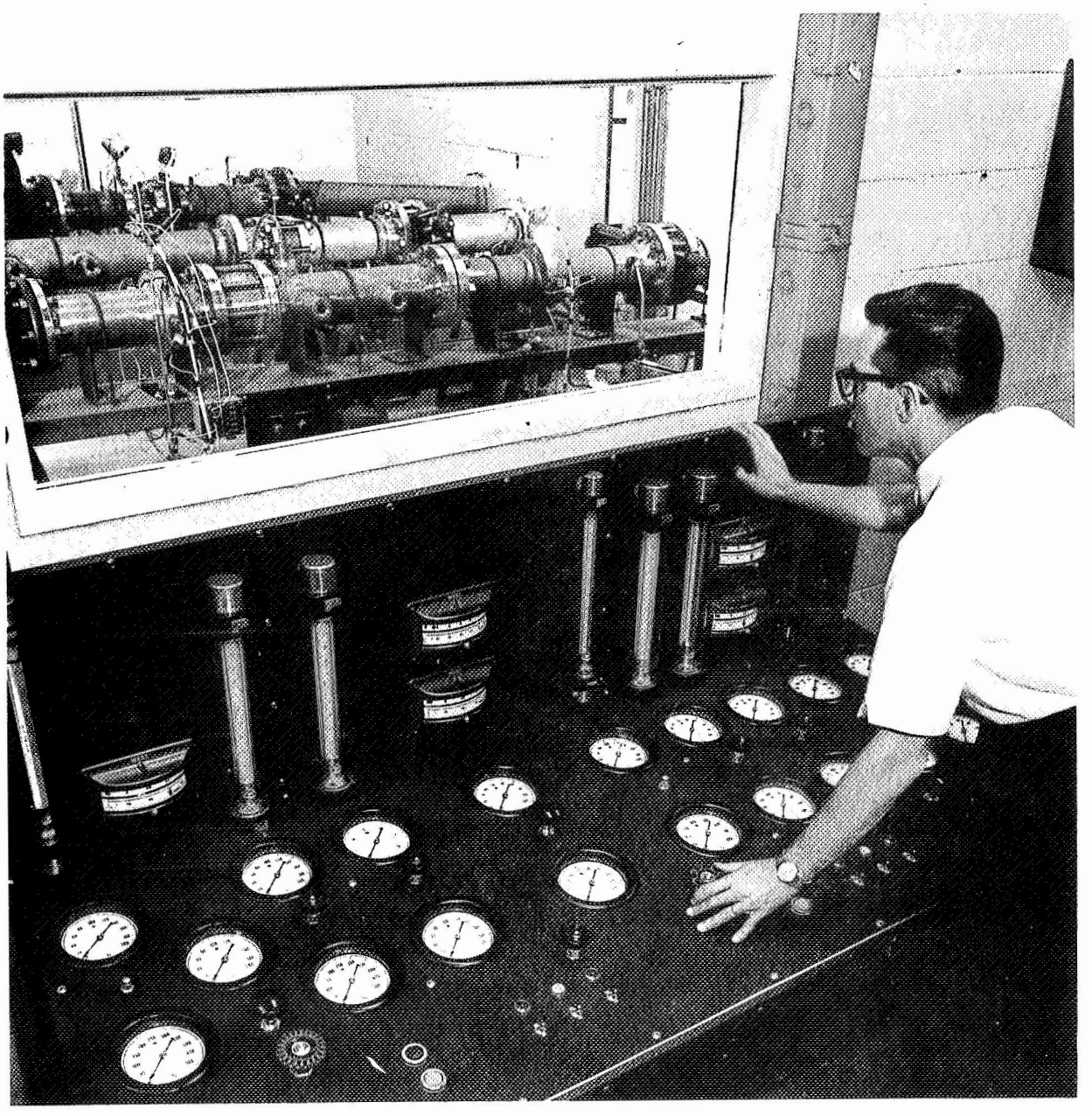

Fig. 12 – Instrumented turbine passages

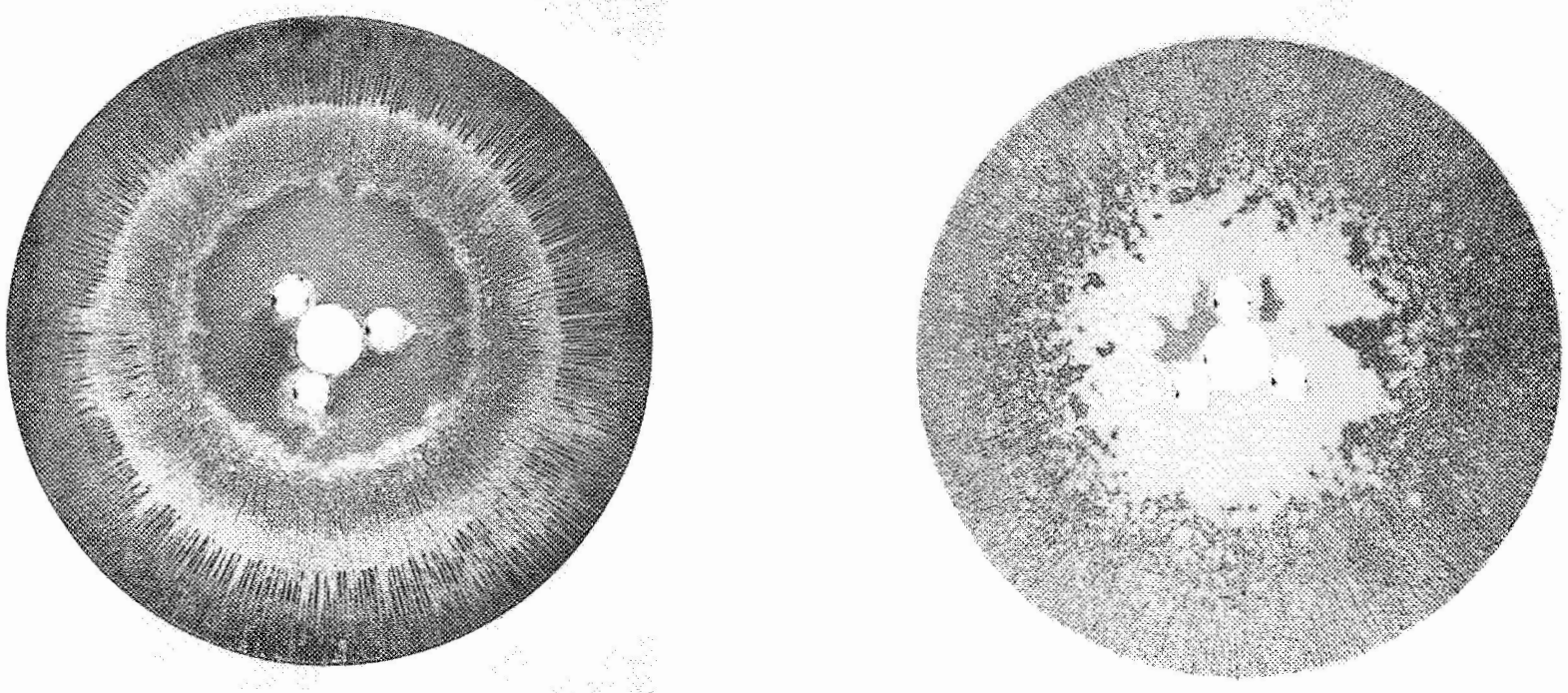

(a) No. 23-1 Coated Disc (T-23)

(b) No. 25 Coated Disc (T-25)

Fig. 13 –Appearance of spin discs after one-hour test at 2100° F

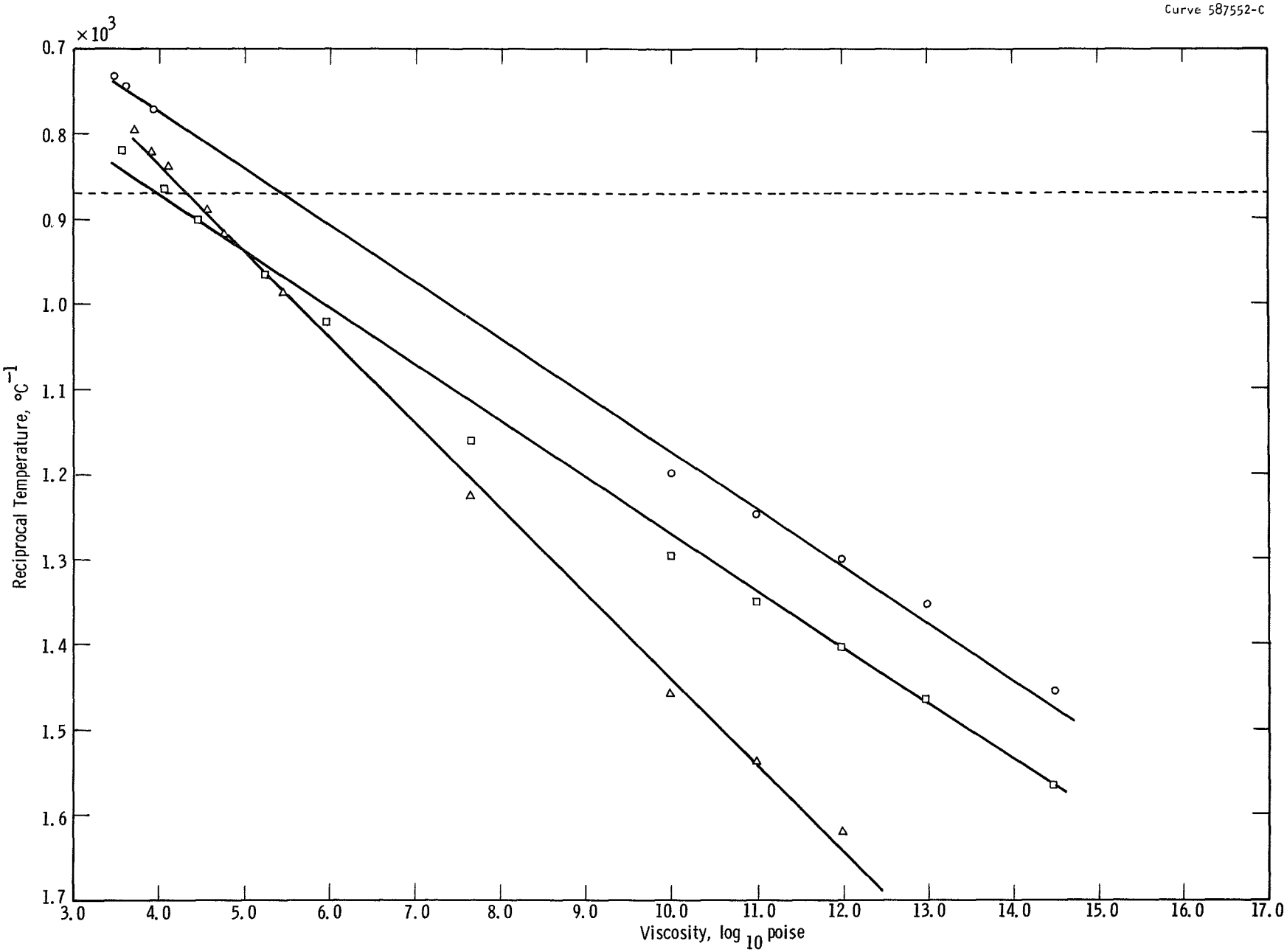

Fig. 14—The viscosity-temperature relationships for Glasses 13-1, 22-2 and 23-1

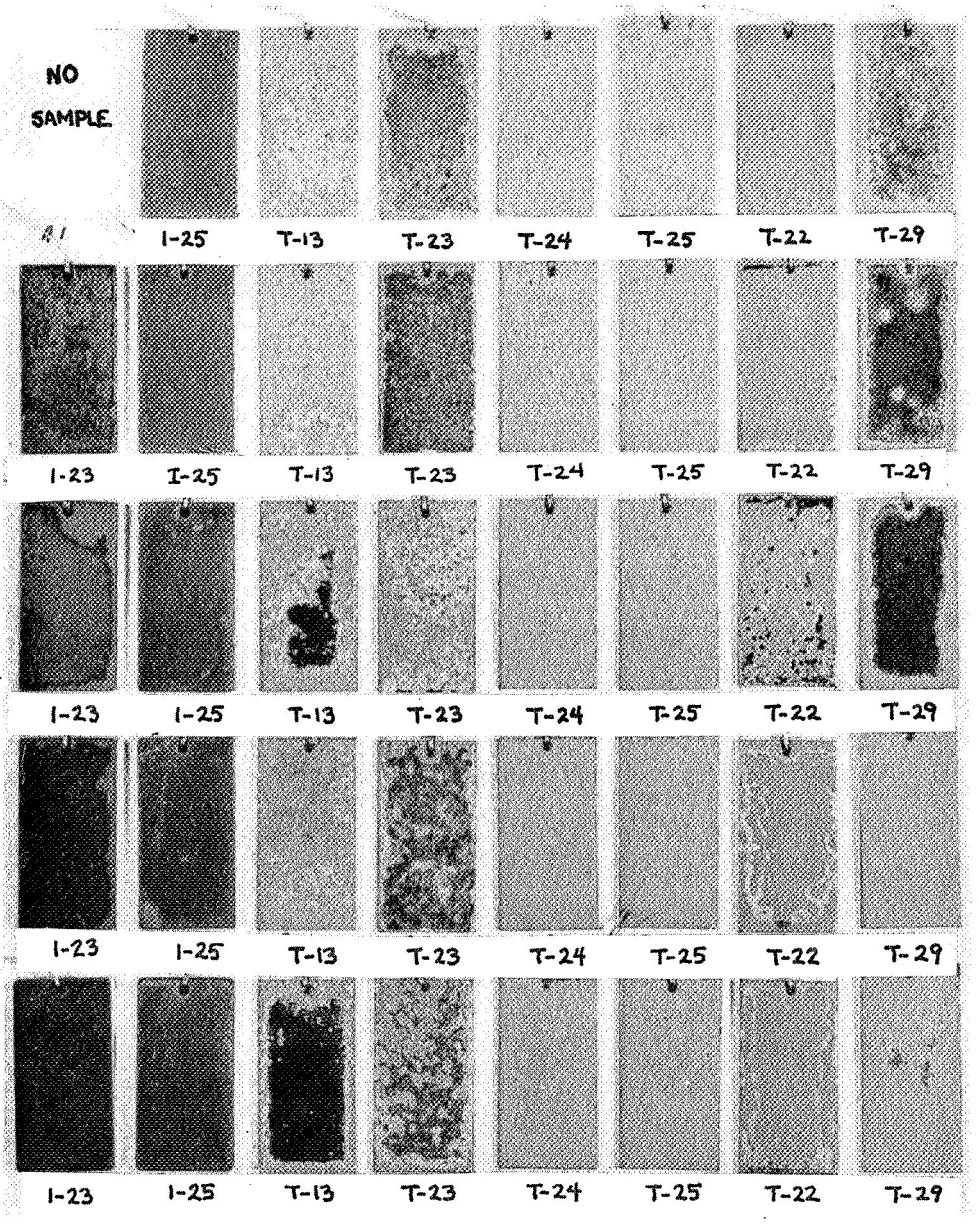

Fig. 15—Selected systems after 20 one-hour cycles 1149°C

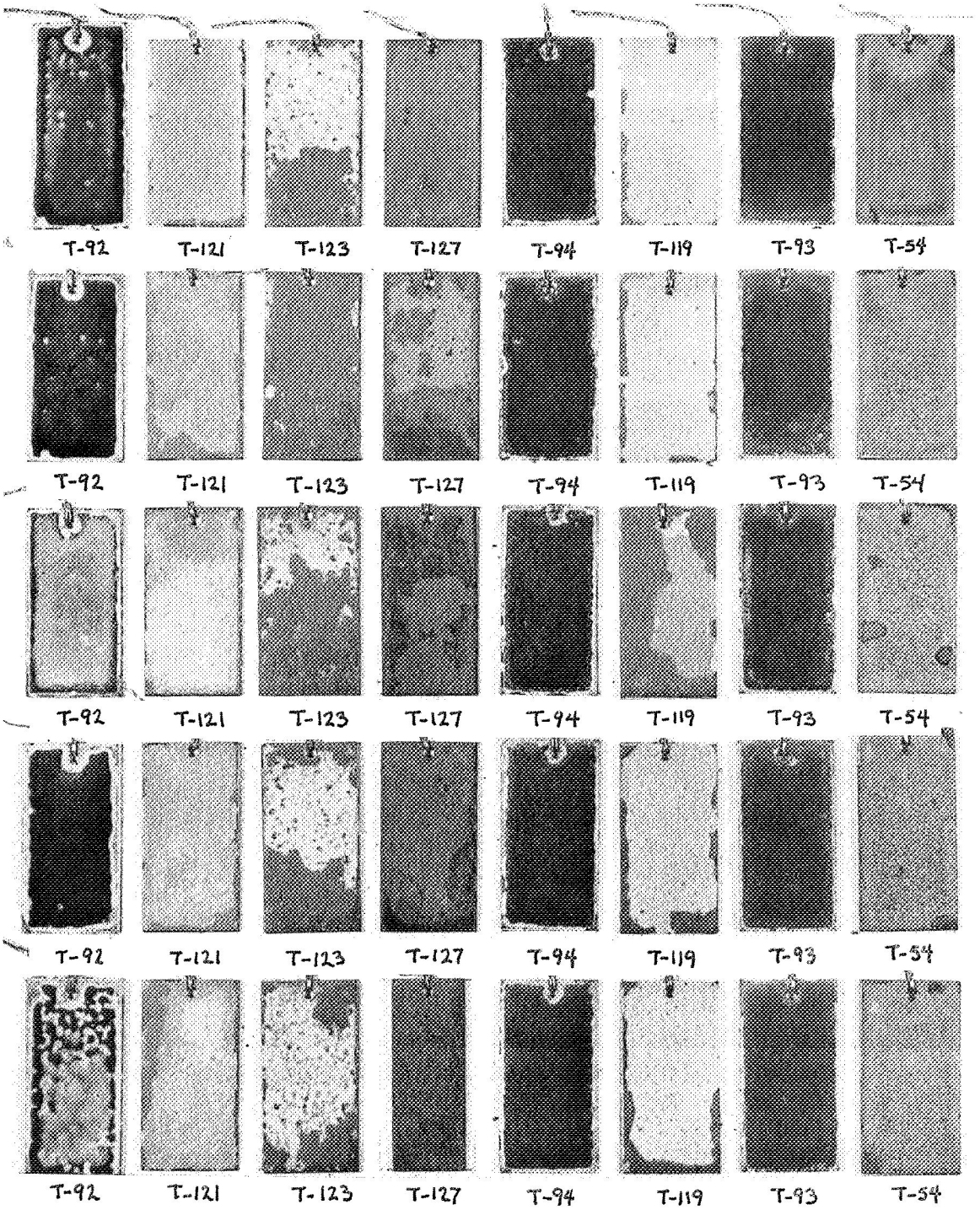

Fig. 16—Selected system after 20 one-hour cycles

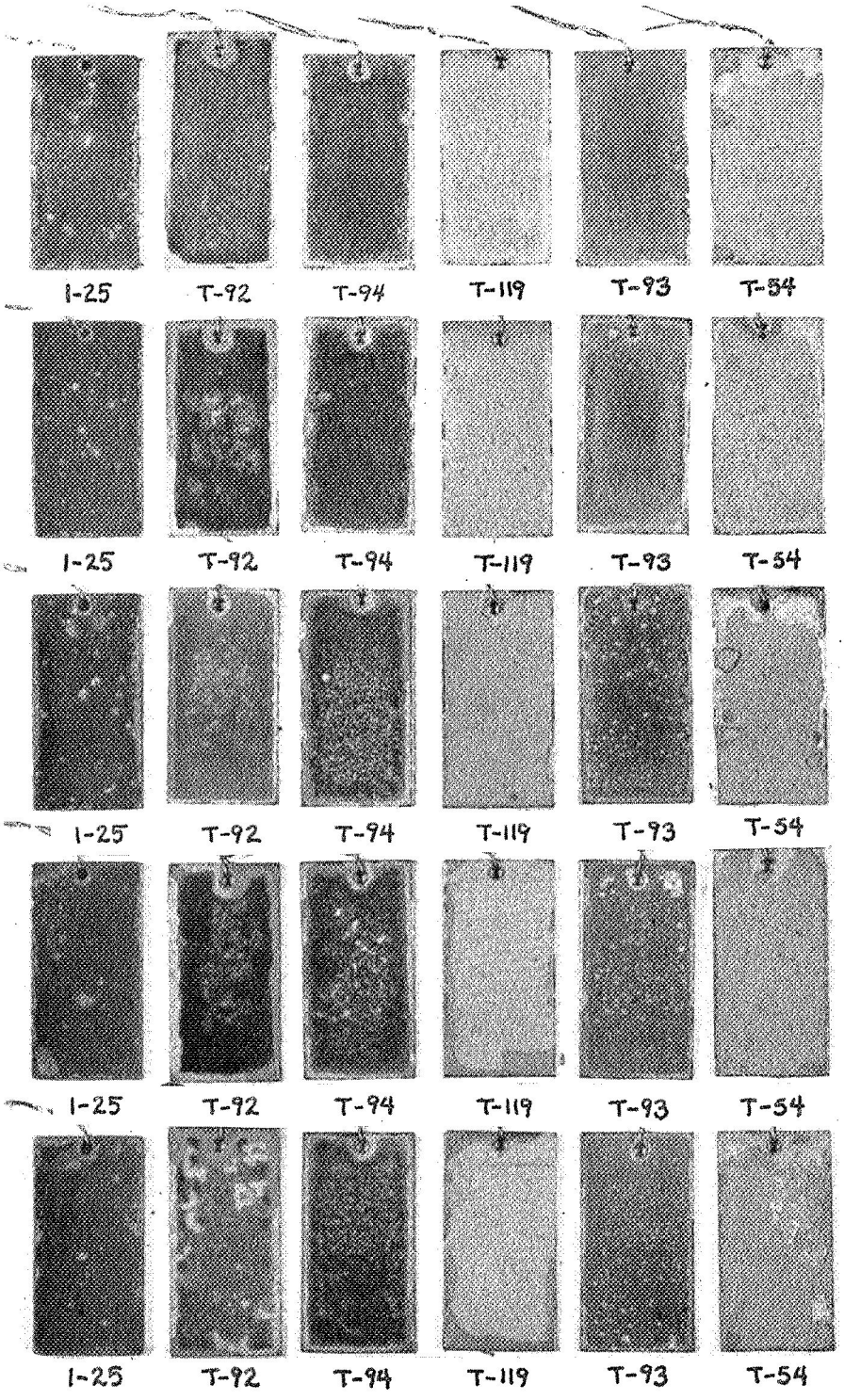

Fig. 17—Combined test after 1st 20 hour cycle

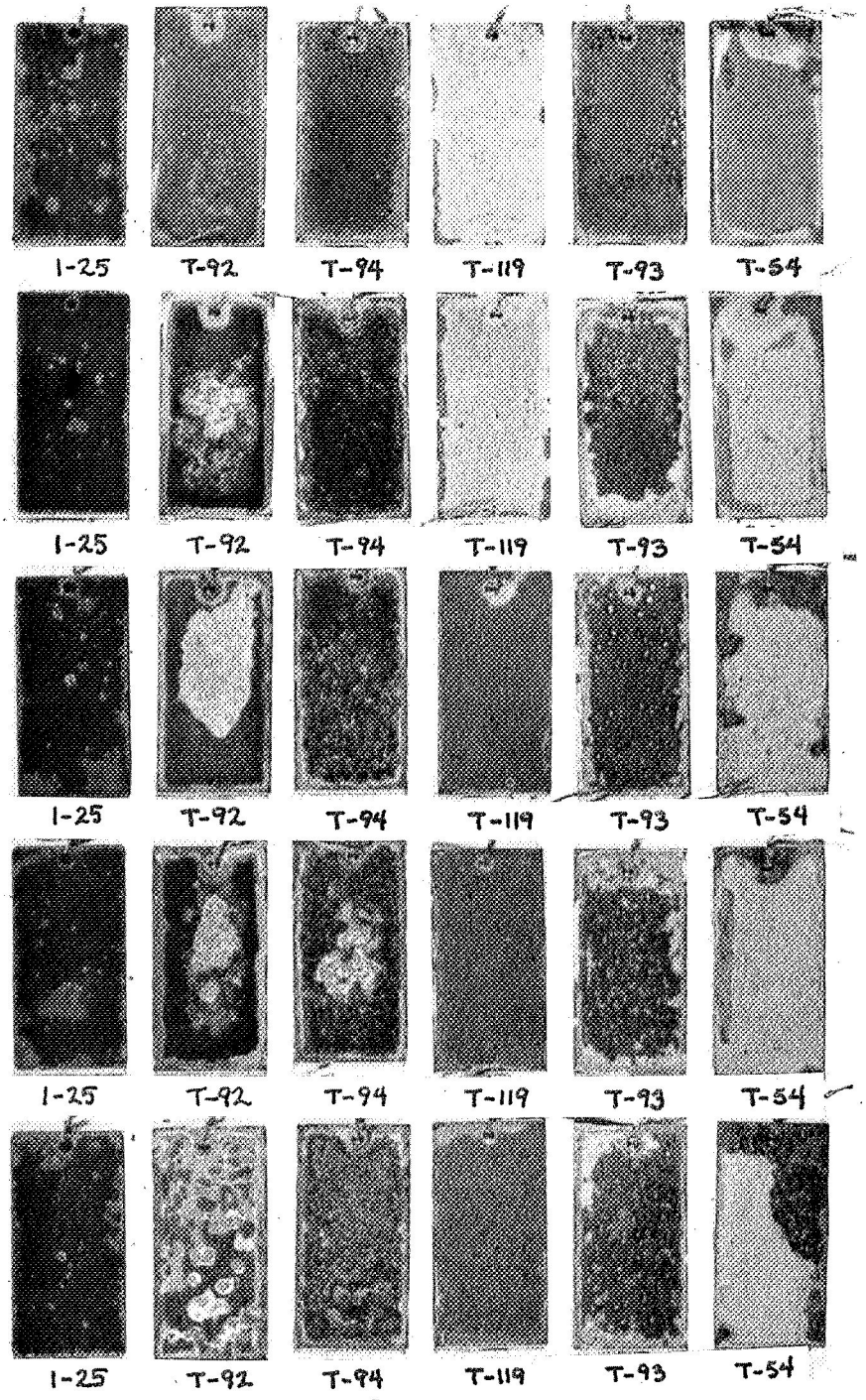

Fig. 18—Combined test after 2nd 20 hour cycle

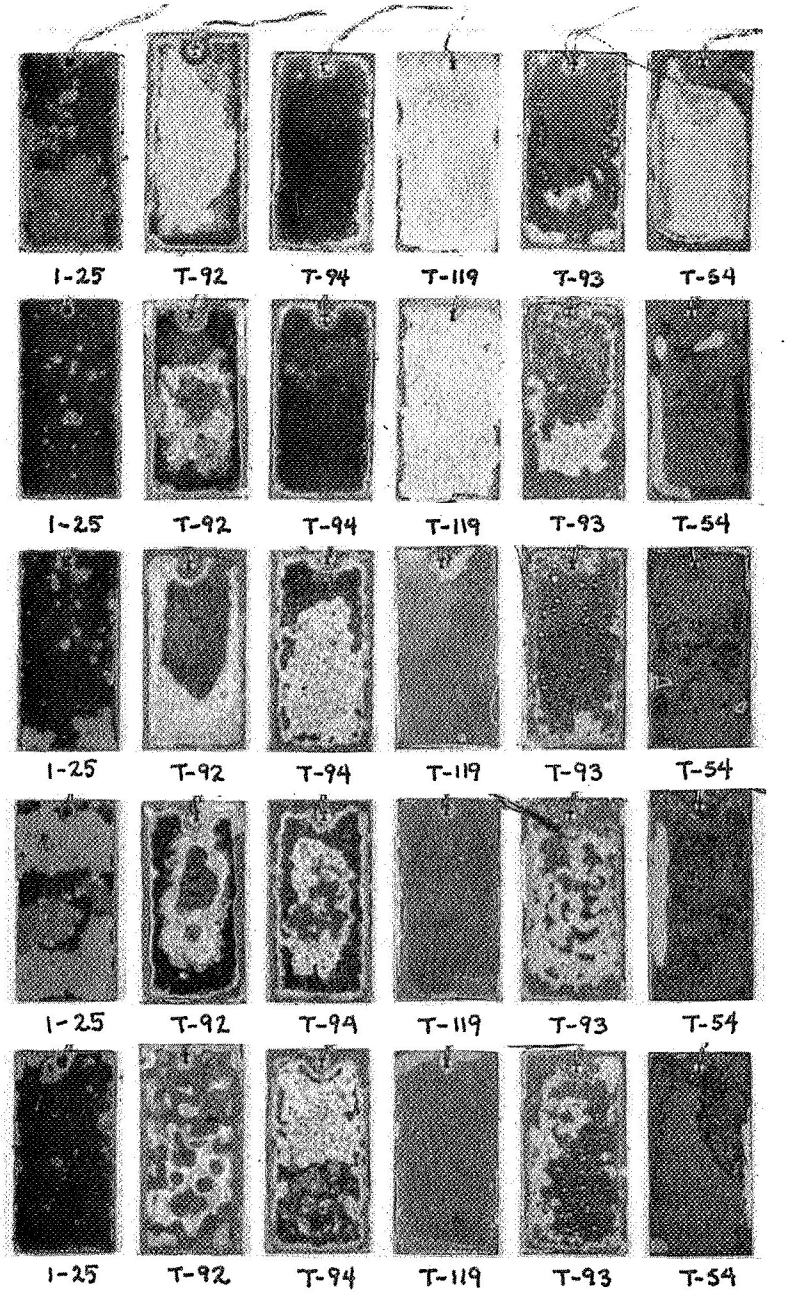

Fig. 19—Combined test after 3rd 20 hour cycle

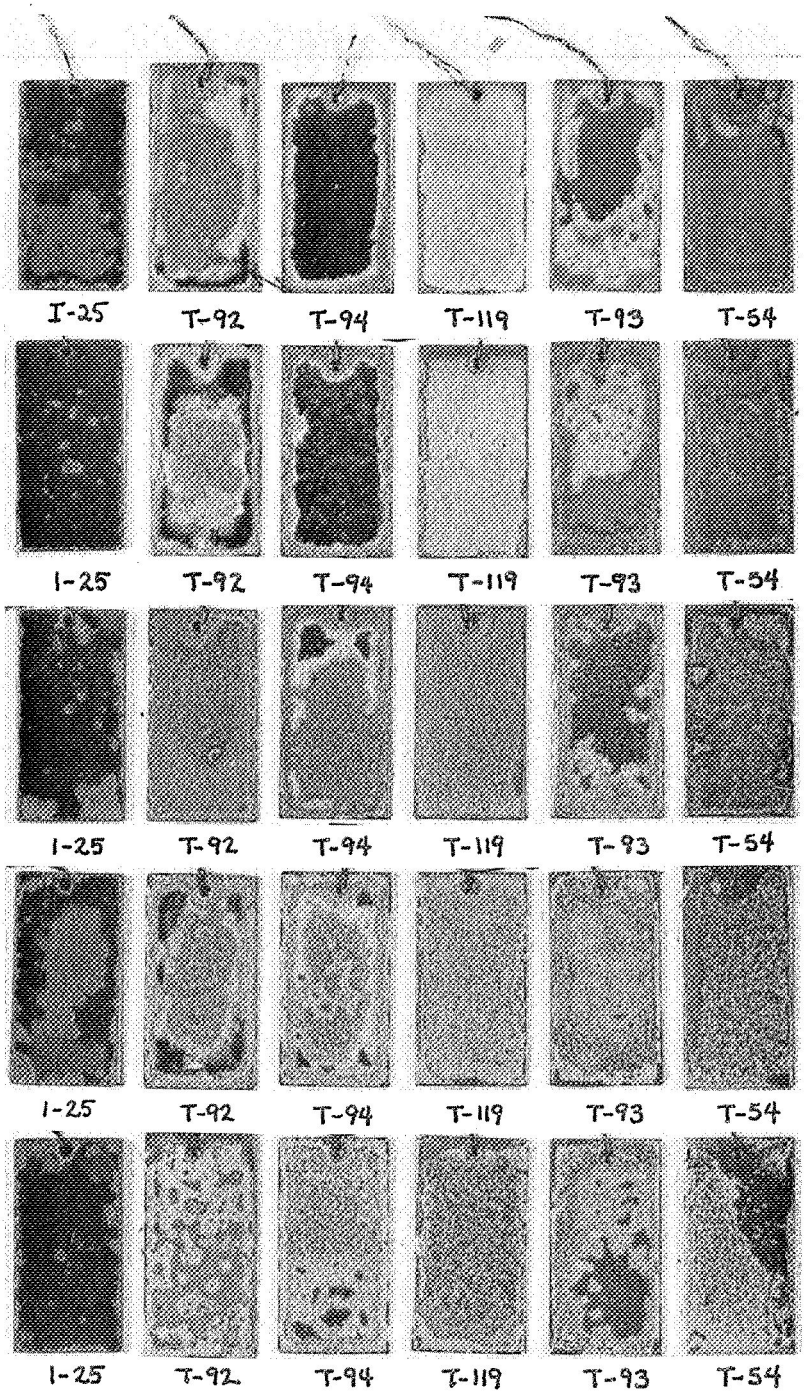

Fig. 20—Combined test after 4th 20 hour cycle

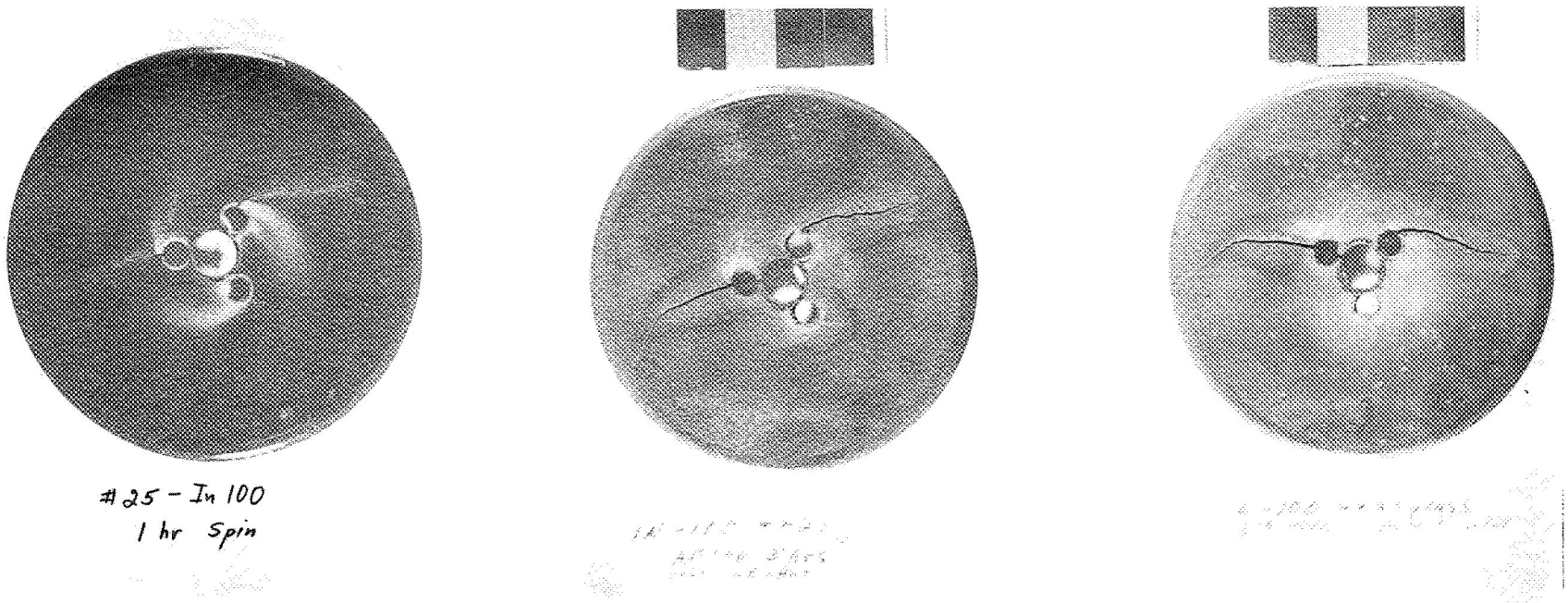

After 1 Hour | After 5 Hours, Ballistically Impacted | After 6 Hours

Fig. 21—Progressive deterioration of I-25 specimen during 6—one-hour centrifugal spin tests at 1149°C

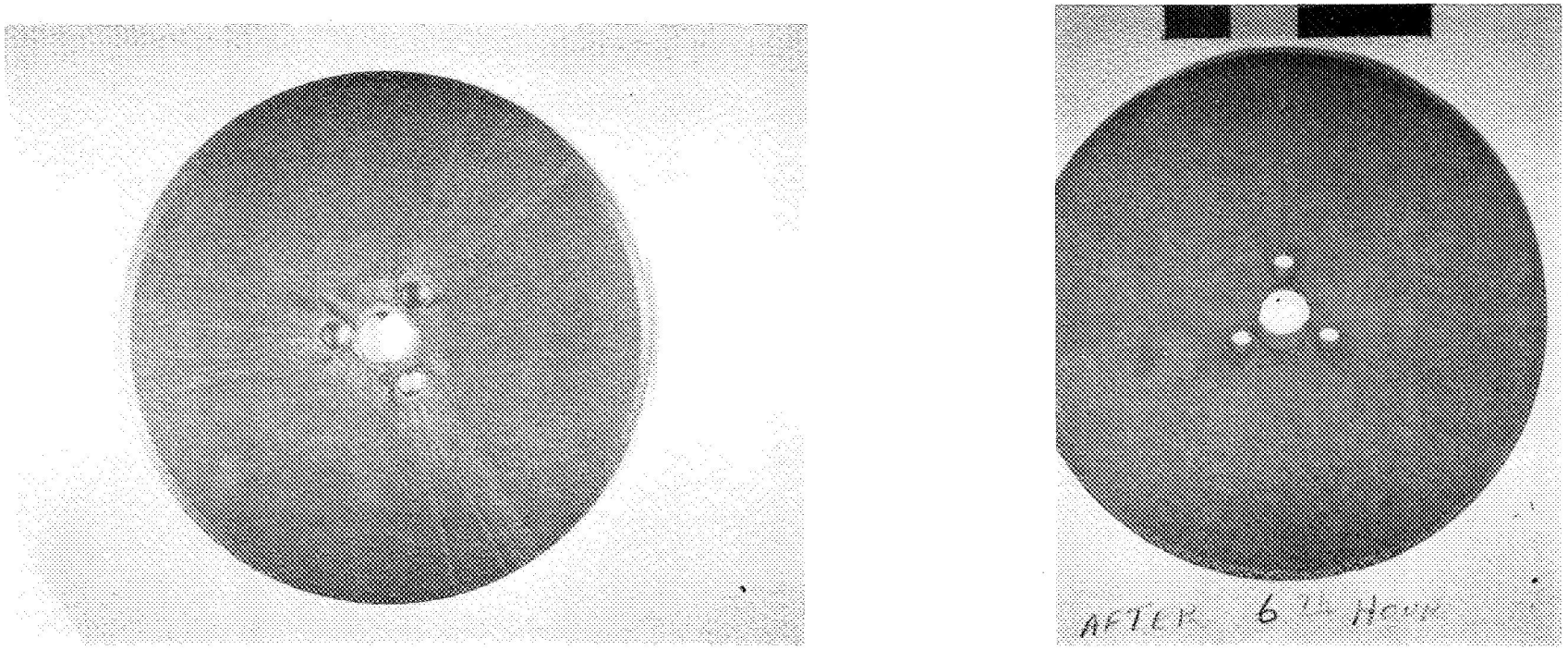

After 1 Hour

After 6 Hours

Fig. 22—Effect of 6—one-hour centrifugal spin tests on T-94 specimen at 1149°C

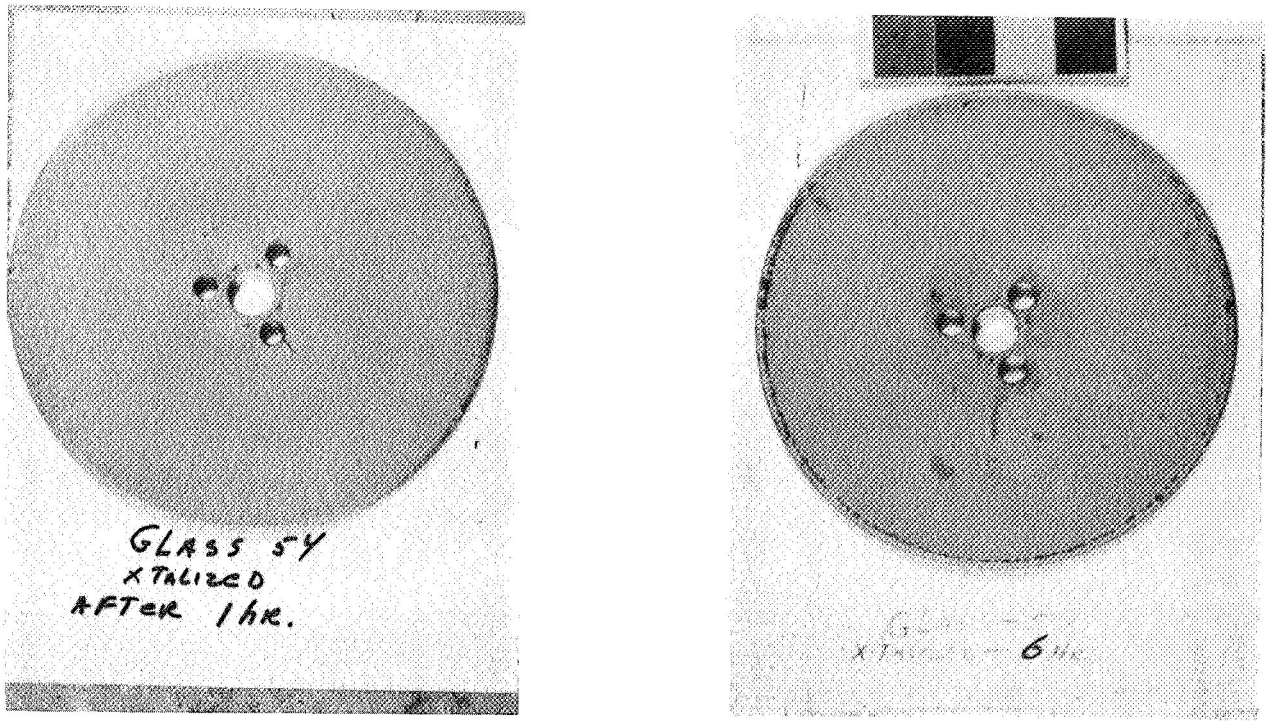

After 1 Hour

After 6 Hours

Fig. 23—Effect of 6—one-hour centrifugal spin tests on T-54 specimen at 1149°C

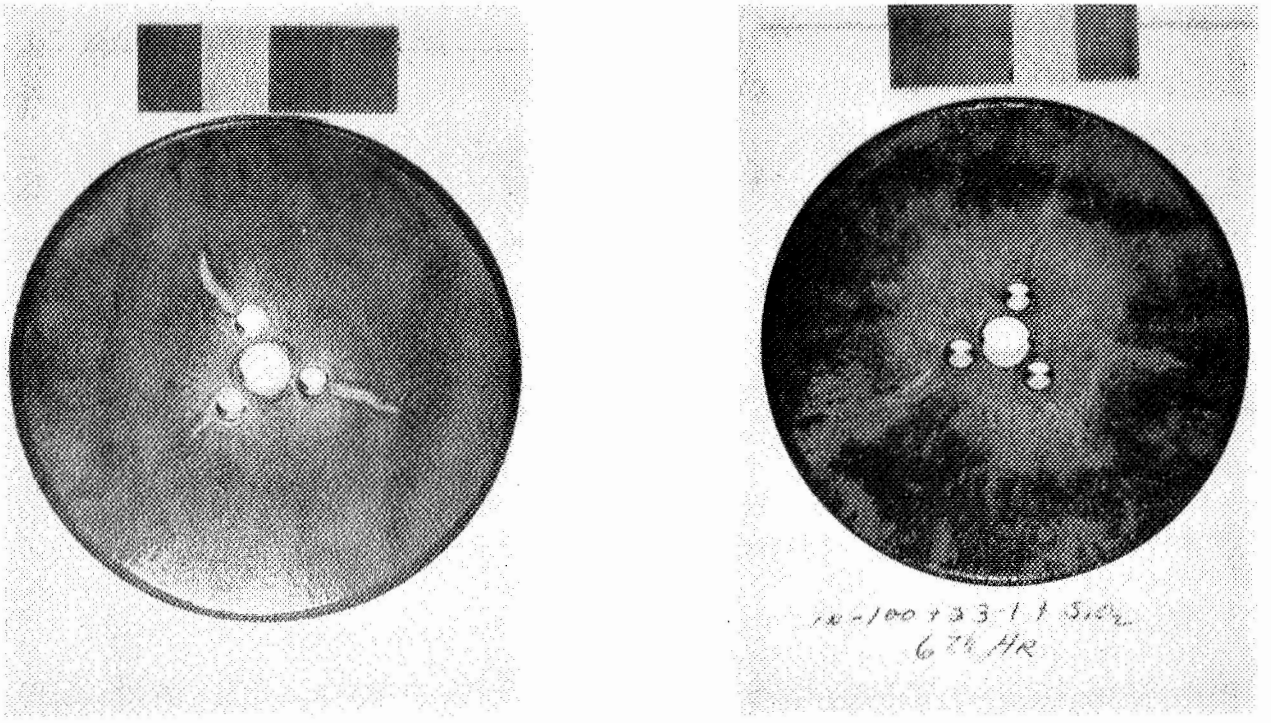

After 1 Hour

After 6 Hours

Fig. 24—Effect of 6—one-hour centrifugal spin tests on I-119 specimen at 1149°C

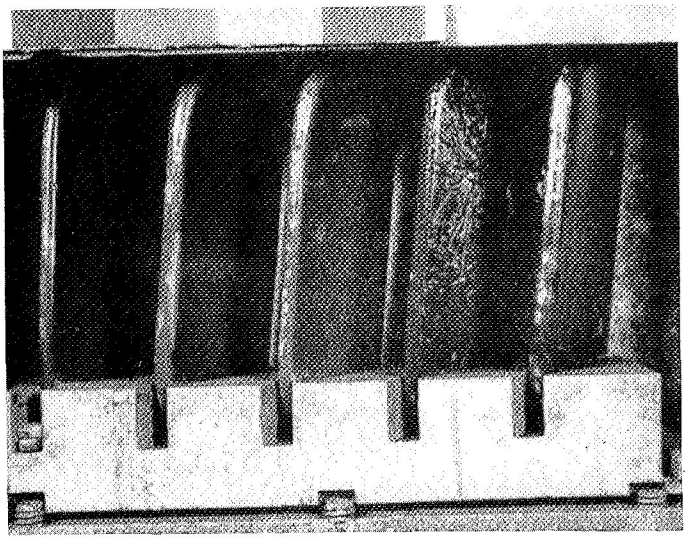

Fig. 25—Simulator Test No. 1 after 6 hours (back)
Results of 6 one-hour turbine simulator tests of
I-25 (1, 2, 3 in picture) and I-94 (4, 5) specimens
at 1038°C (back)

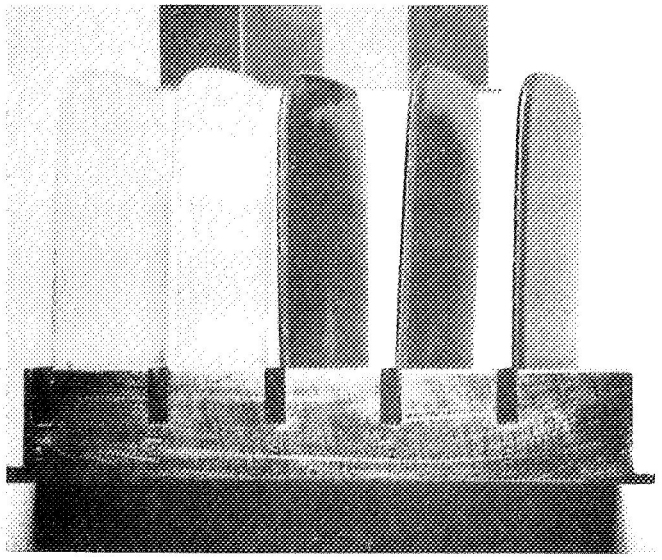

Fig. 26(a)—Sample T-54 (1, 2), T-94 (3, 4, 5) before turbine simulator testing

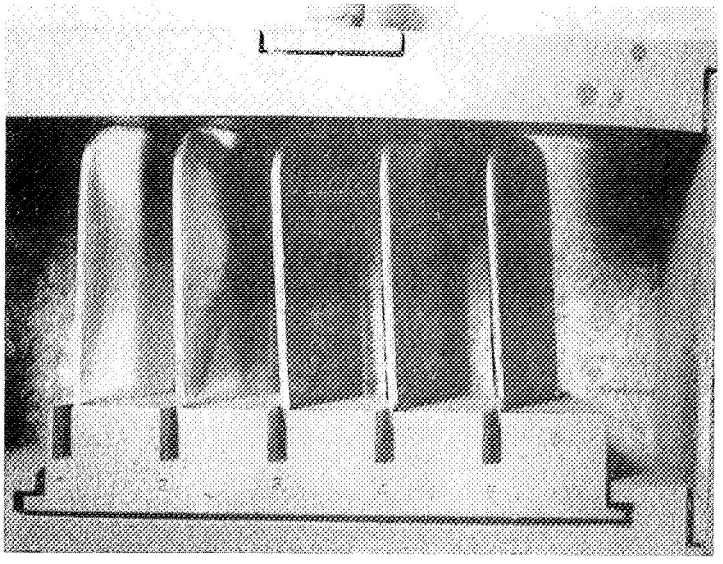

Fig. 26(b)—One hour turbine simulator testing at 1038°C of above specimens

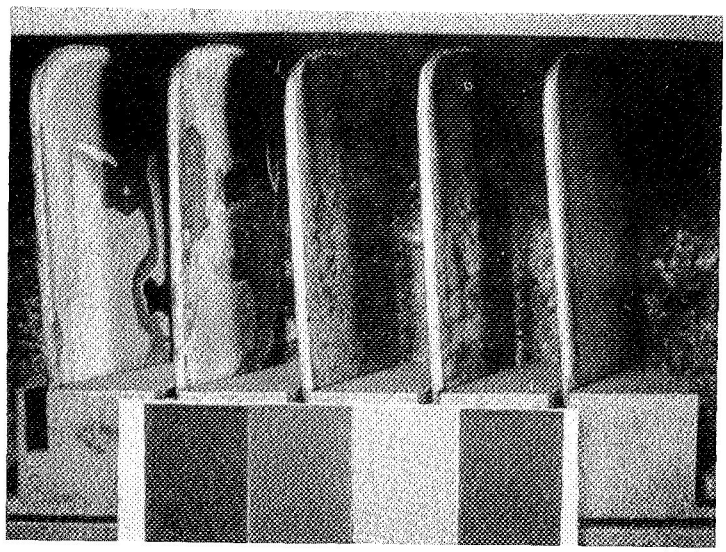

Fig. 27(a)—Sample T-54 (1, 2) and I-94 (3, 4, 5) after 4 one hour turbine simulator tests 1038°C (front)

Dummy Samples
X X

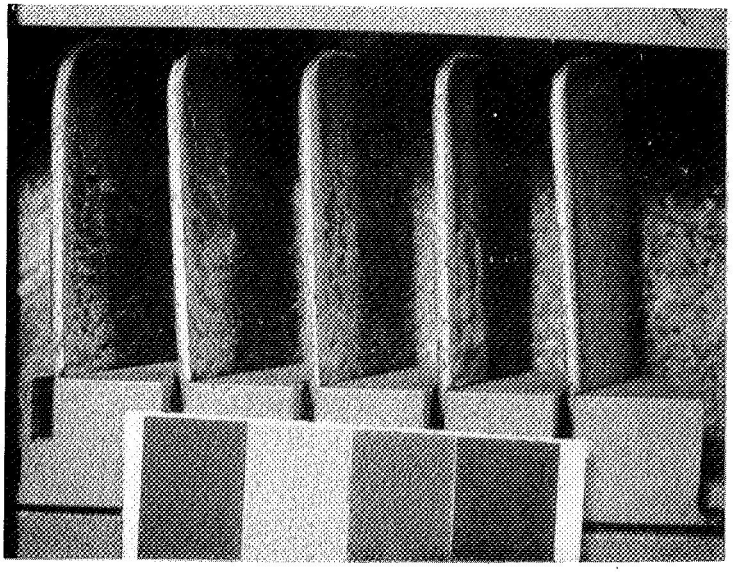

Fig. 28—Results of 6 one-hour turbine simulator tests on T-94 specimens at 1038°C (front)

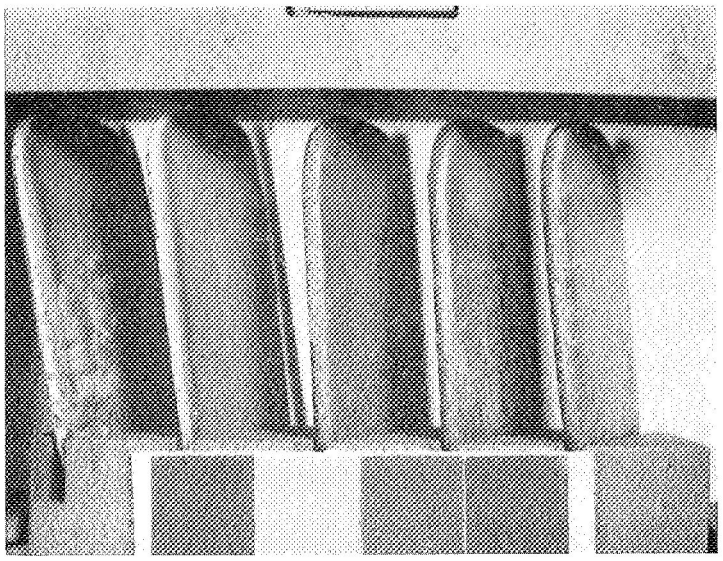

Fig. 29(a) —Results of first 6-hour turbine simulator test at 1038°C on T-94 (1, 2) and I-25 (3, 4, 5) (front)

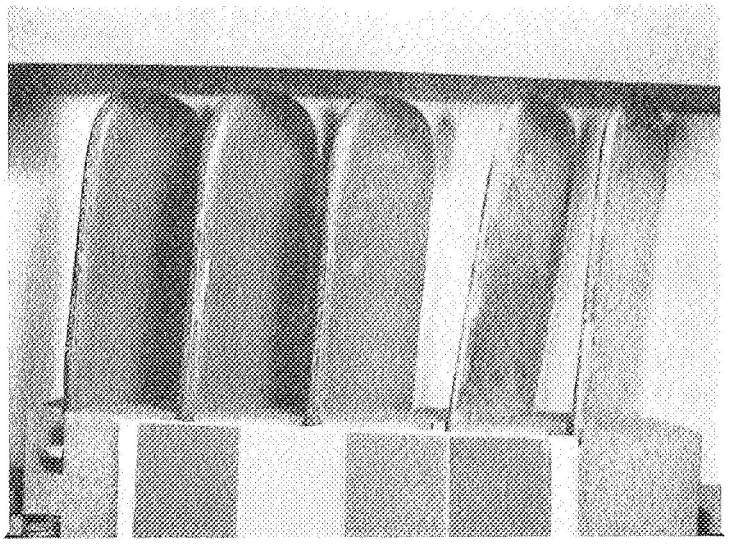

Fig. 29(b)—Back view of above

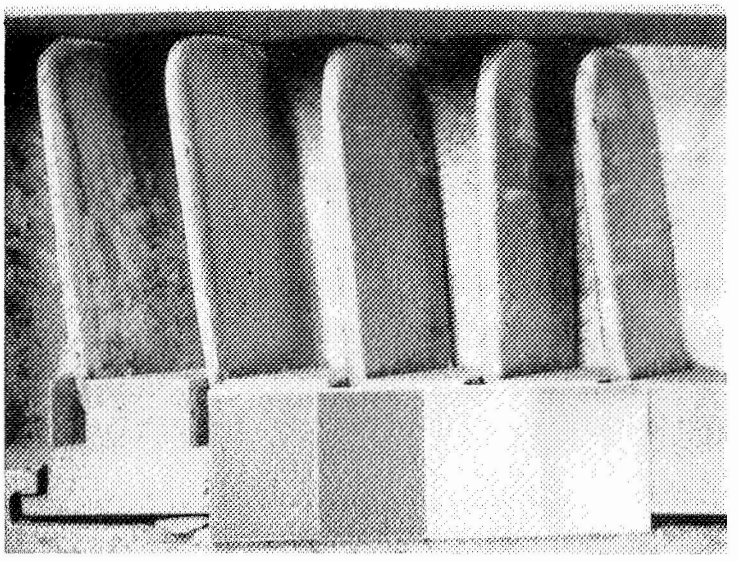

Fig. 30(a) —Results of third 6-hour turbine simulator test at 1038°C on T-94 (1, 2) and I-25 (3, 4, 5) (front)

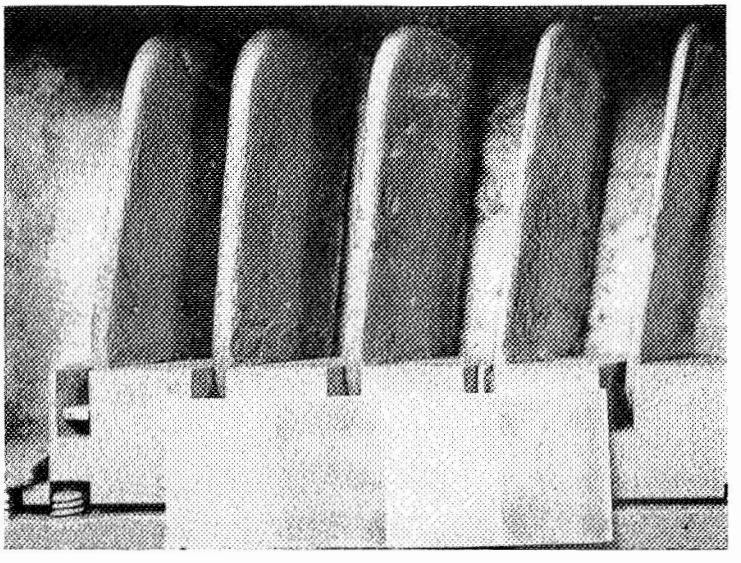

Fig. 30(b)—Back view of above

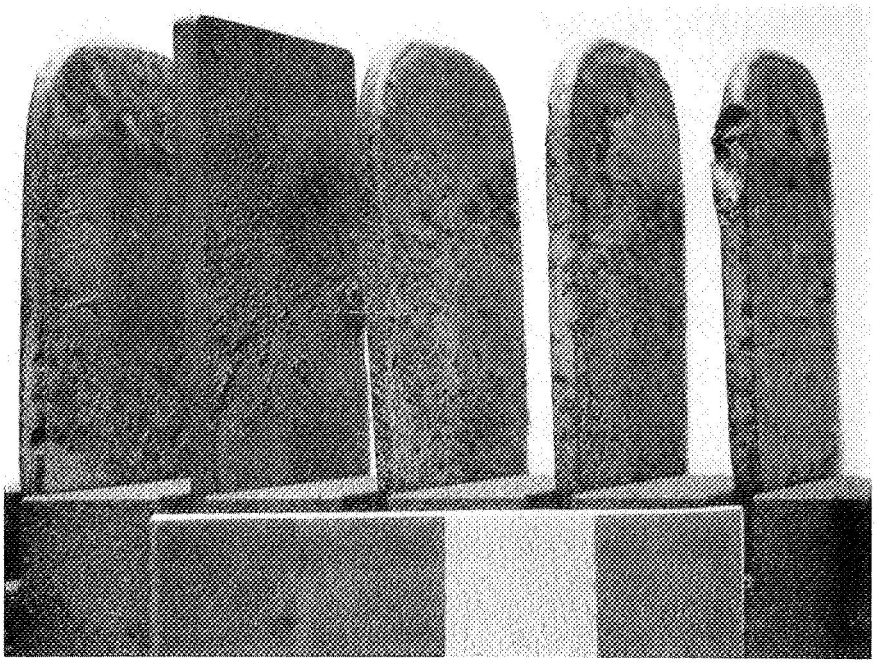

Fig. 31(a) —Results of 100 hour turbine simulator test of I-25 (3, 4, 5) at 1038°C. First two specimens of I-25 and IN-100 were only tested for 76 hours (front)

Fig. 31—Back view of above specimens

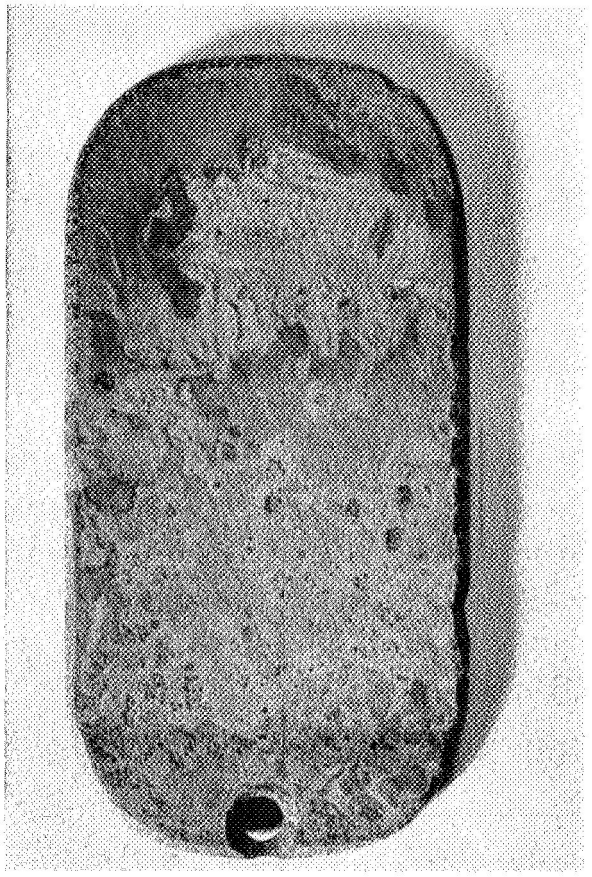

Fig. 32—Front of specimen I-25 after 100 total hours of turbine simulator test 1038°C

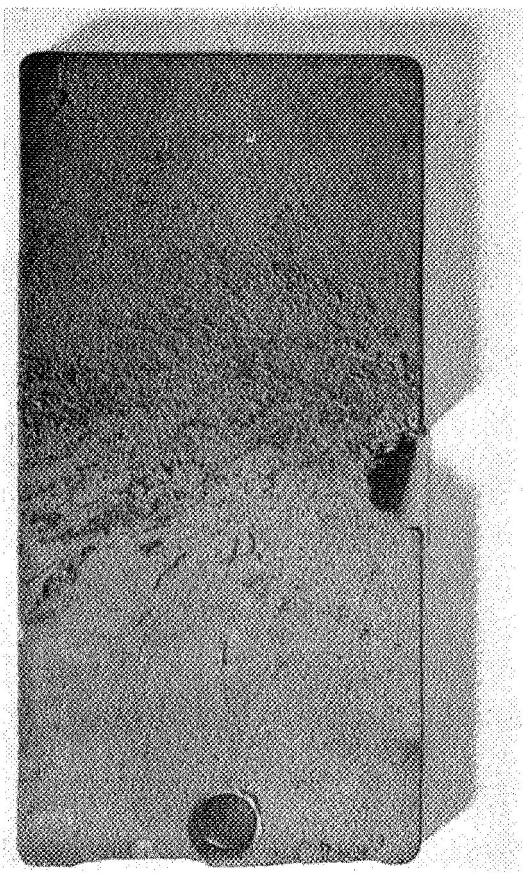

Fig. 33 —Front of specimen IN-100 after 76 total hours of turbine simulator test at 1038°C

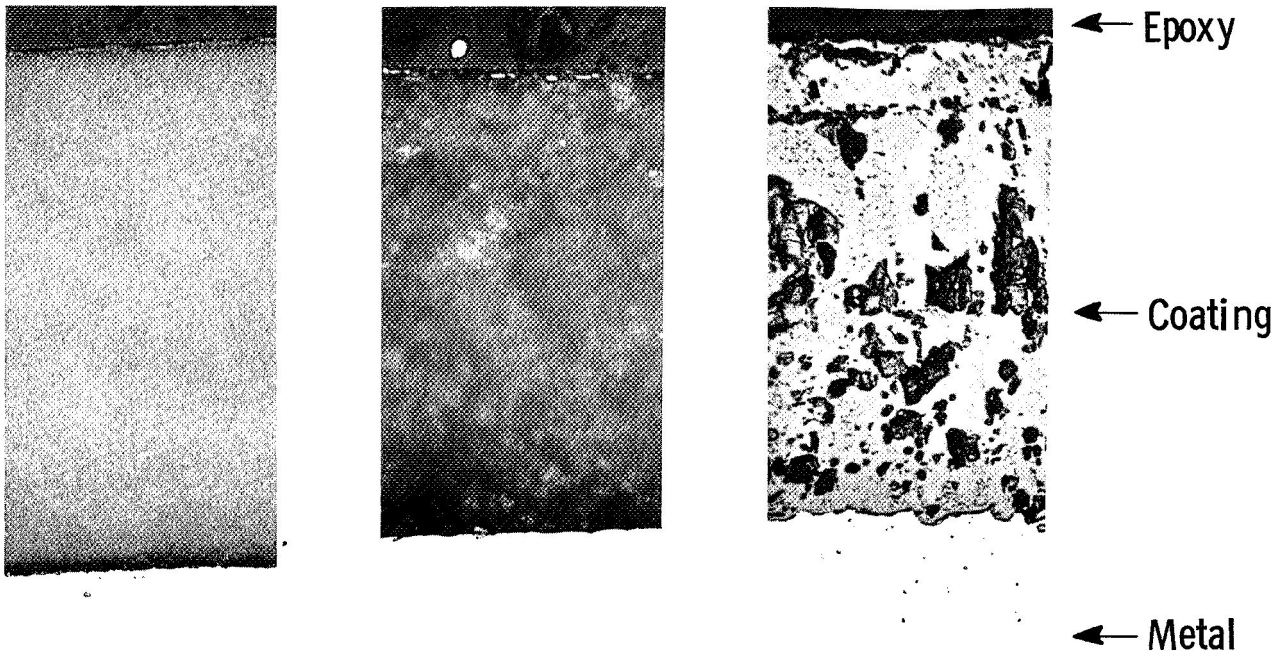

As Crystallized | 6 Hours Oxidation (1149°C) | 100 Hours Oxidation (1149°C)

Fig. 34—Deterioration of glass 54 on TD-Ni (T-54) - As crystallized at 900°C (500X)

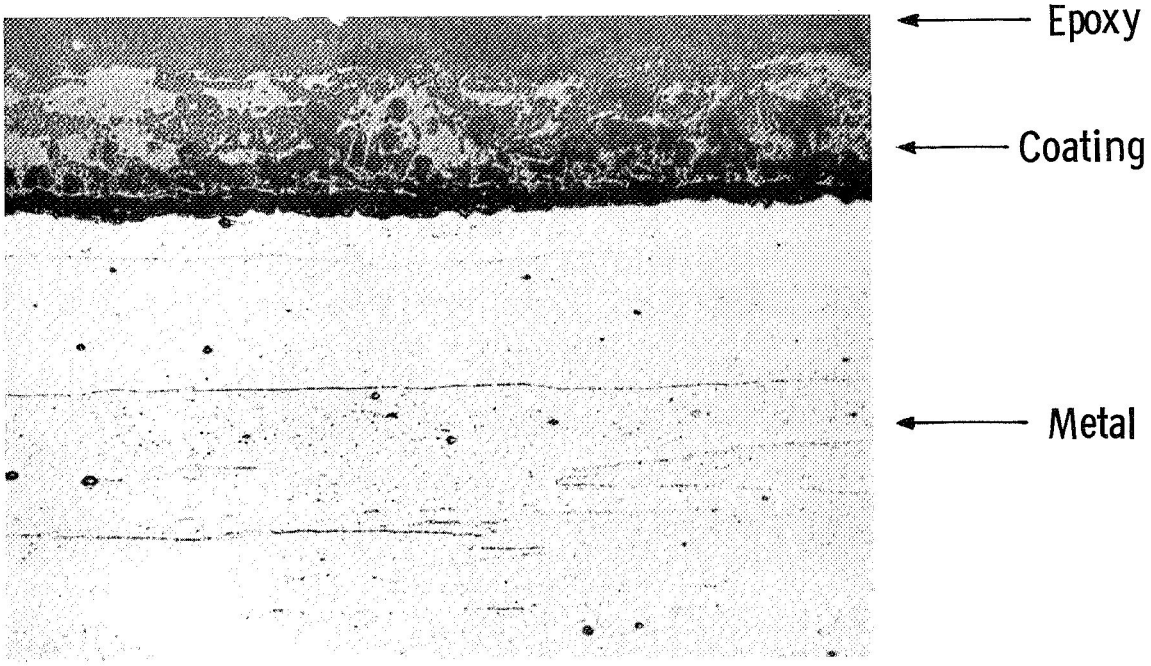

Fig. 35(a) —900°C crystallized glass T-54 - 6 hours cyclic spin (1149°C) 500X

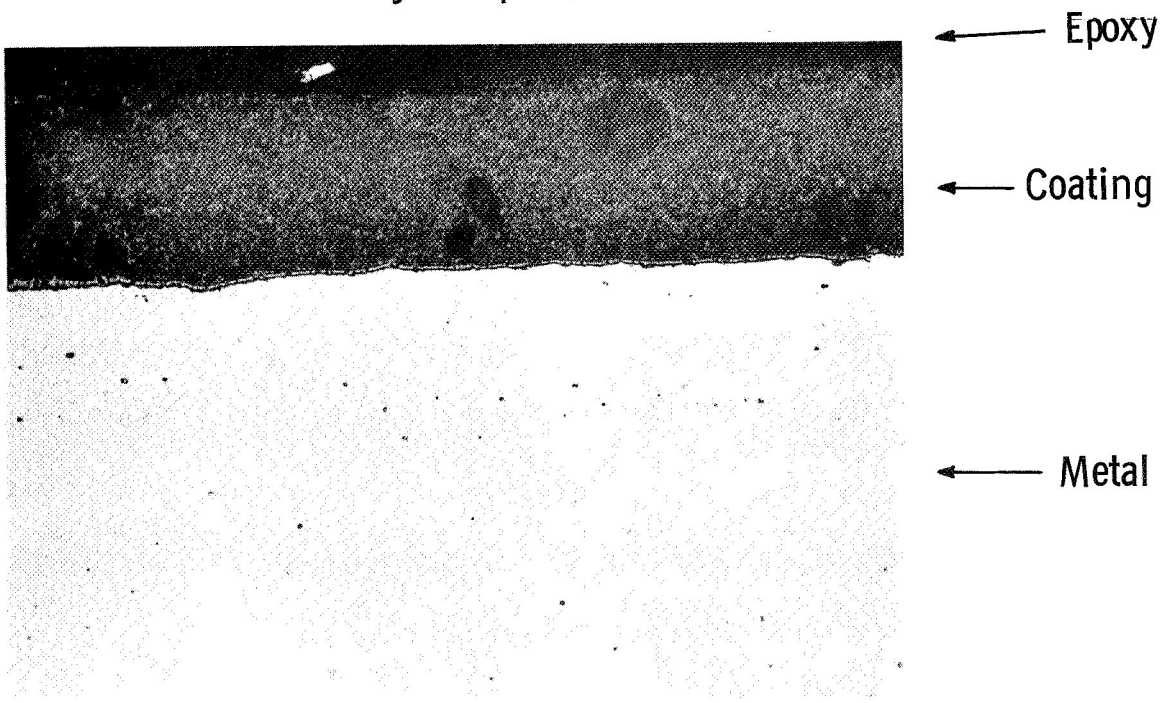

Fig. 35(b) —900°C crystallized glass T-54 - 4 hours turbine simulator (1038°C) 500X

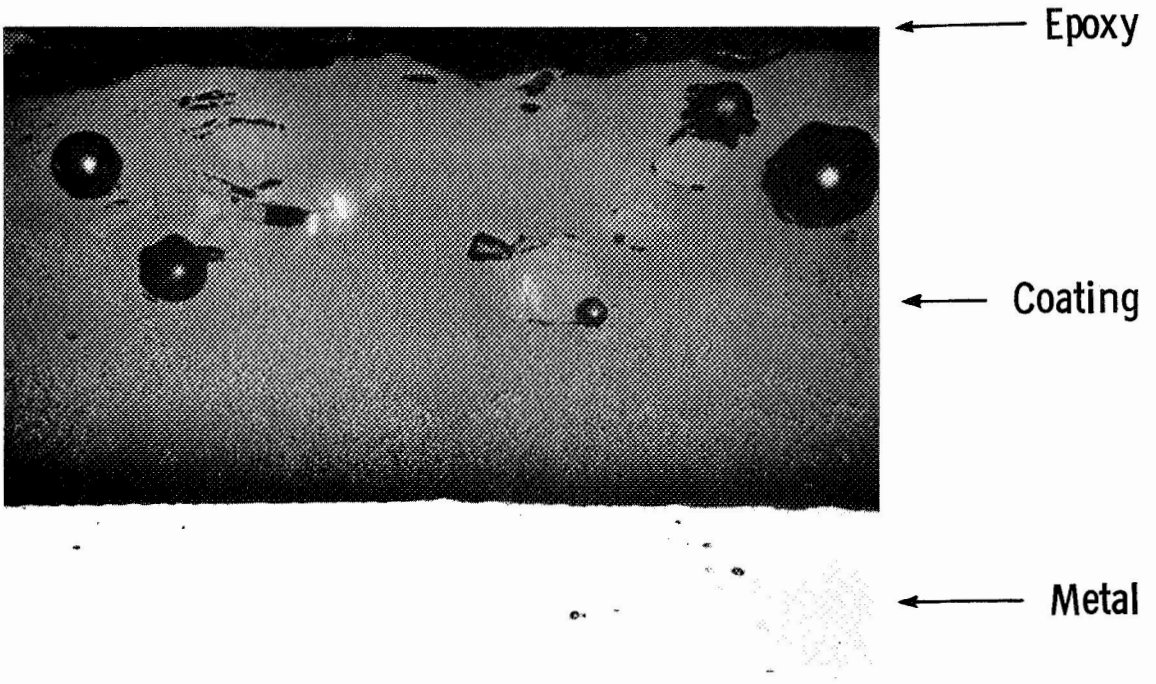

Fig. 36(a) – 50% SiO_2 on GC TD-Ni (T-94) - As coated (500X)

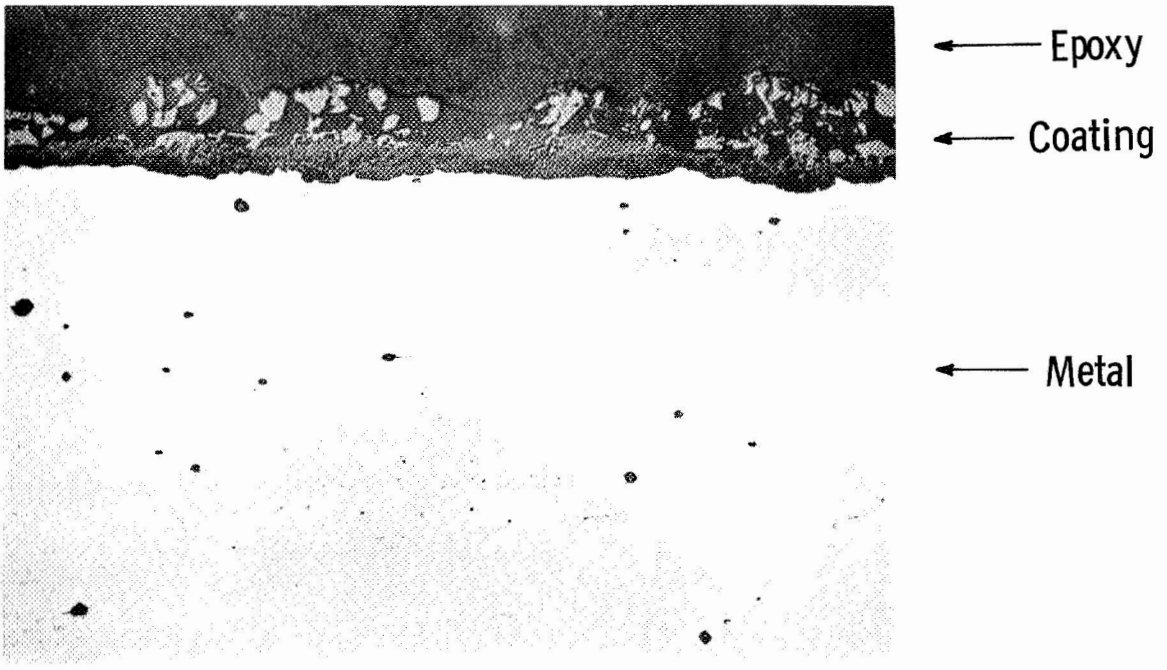

Fig. 36(b) – 50% SiO_2 on GC TD-Ni (T-94) - 6 hours cyclic spin (1149°C) 500X

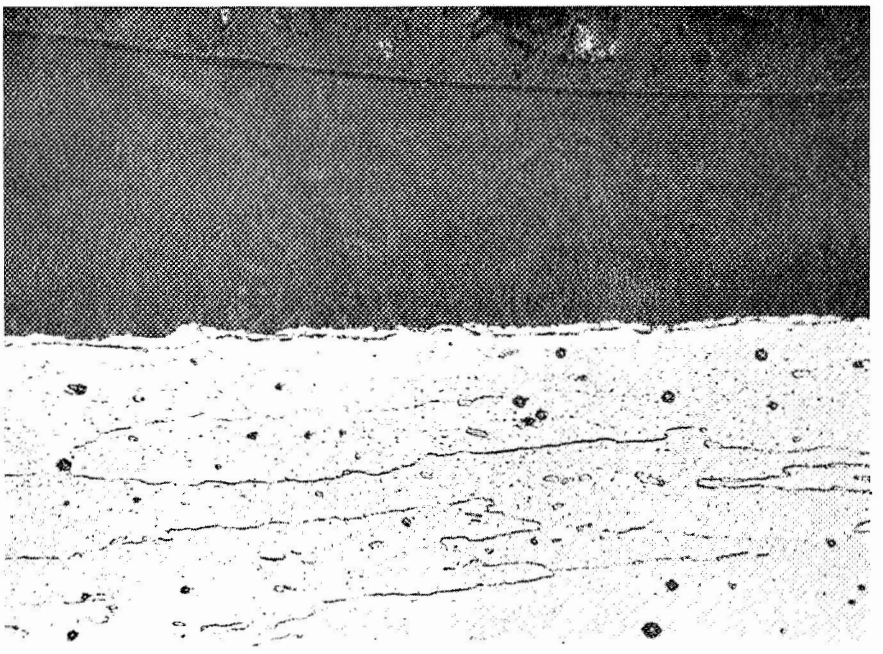

Fig. 37(a) – 50% SiO_2 on GC TD-Ni (T-94) - 2 hours turbine simulator 1038°C (500X)

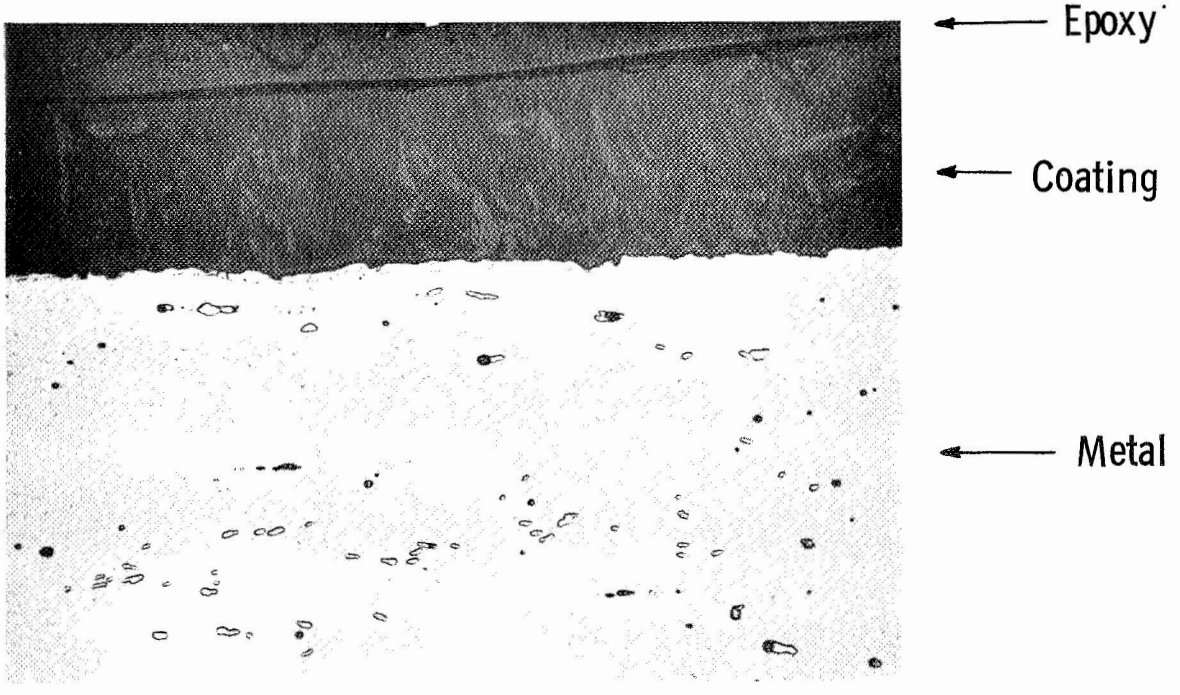

Fig. 37(b) – 50% SiO_2 on GC TD-Ni (T-94) - 24 hours turbine simulator 1038°C (500X)

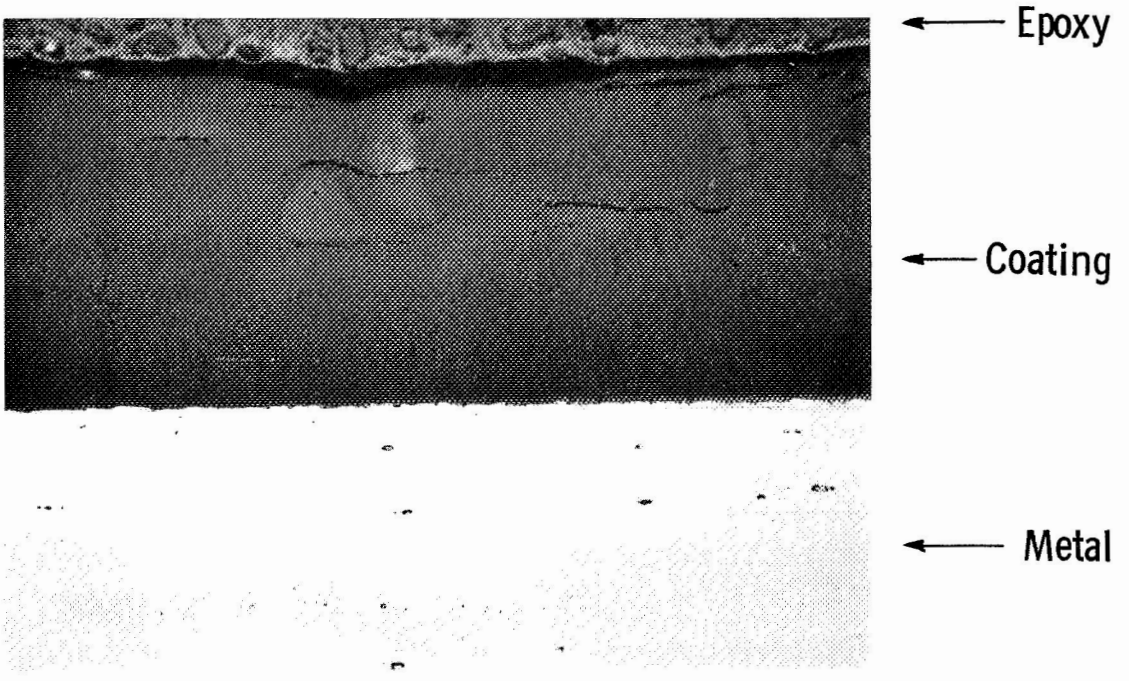

Fig. 38(a) – 50% SiO_2 on GC TD-Ni (T-94) - 6 hour oxidation 1149°C (500X)

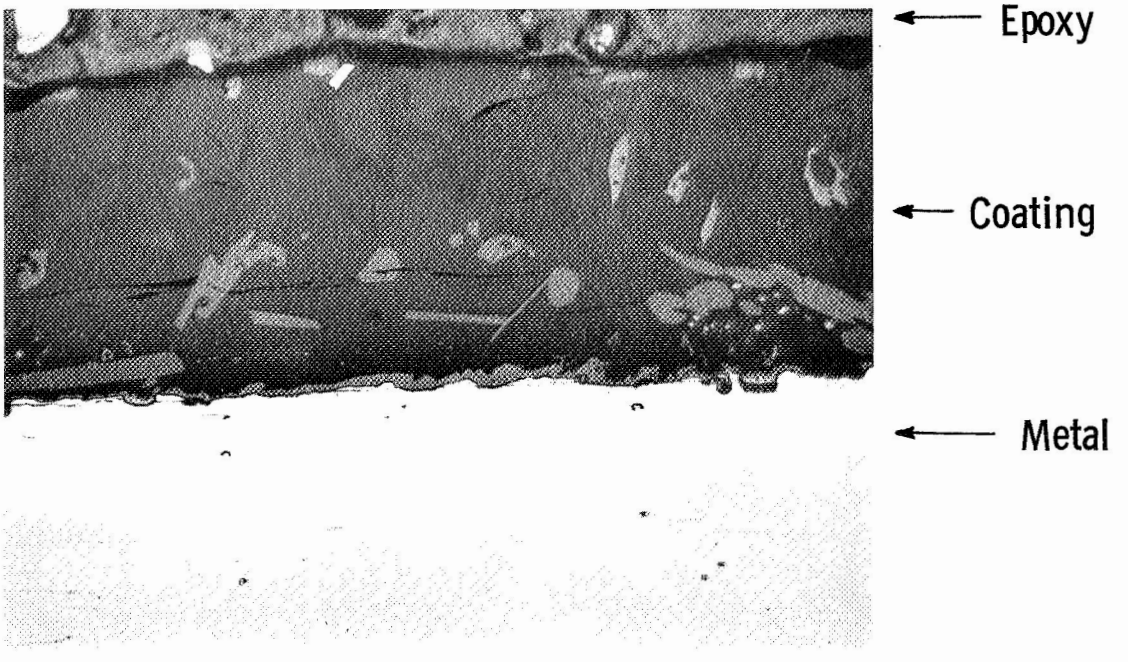

Fig. 38(b) – 50% SiO_2 on GC TD-Ni (T-94) - 100 hours oxidation 1149°C (500X)

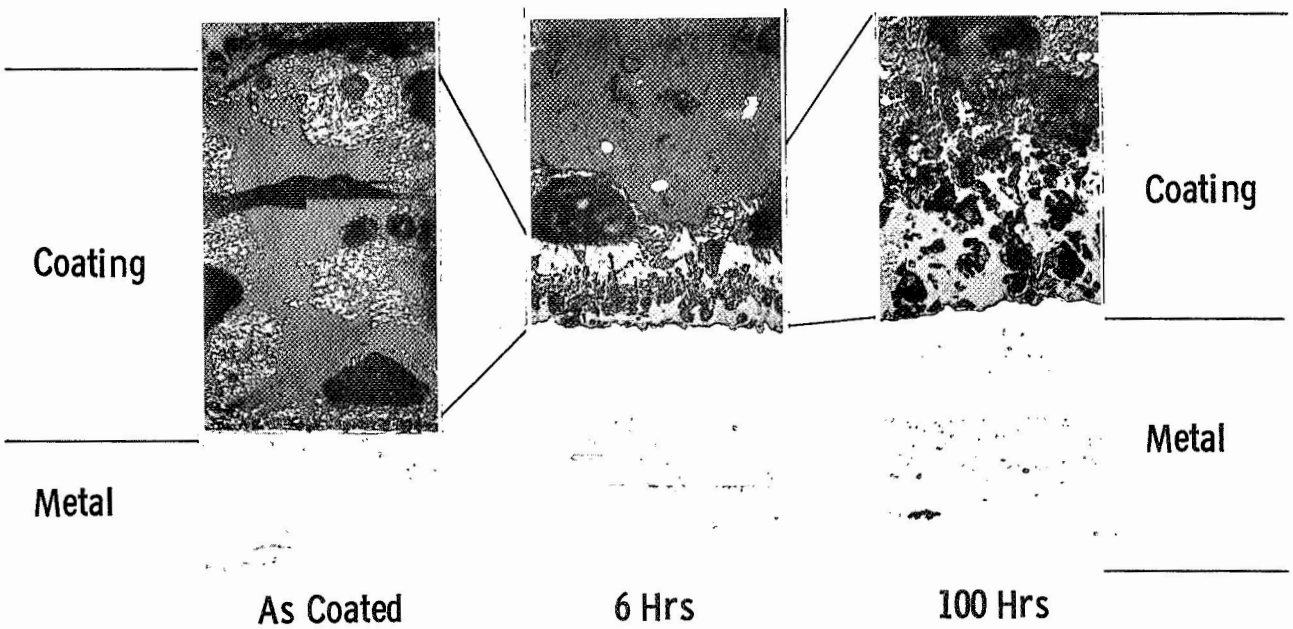

Fig. 39—Oxidation of 25% NiO in glass 23-1 on NGC TD-Ni (T-119) at 1149°C (500X)

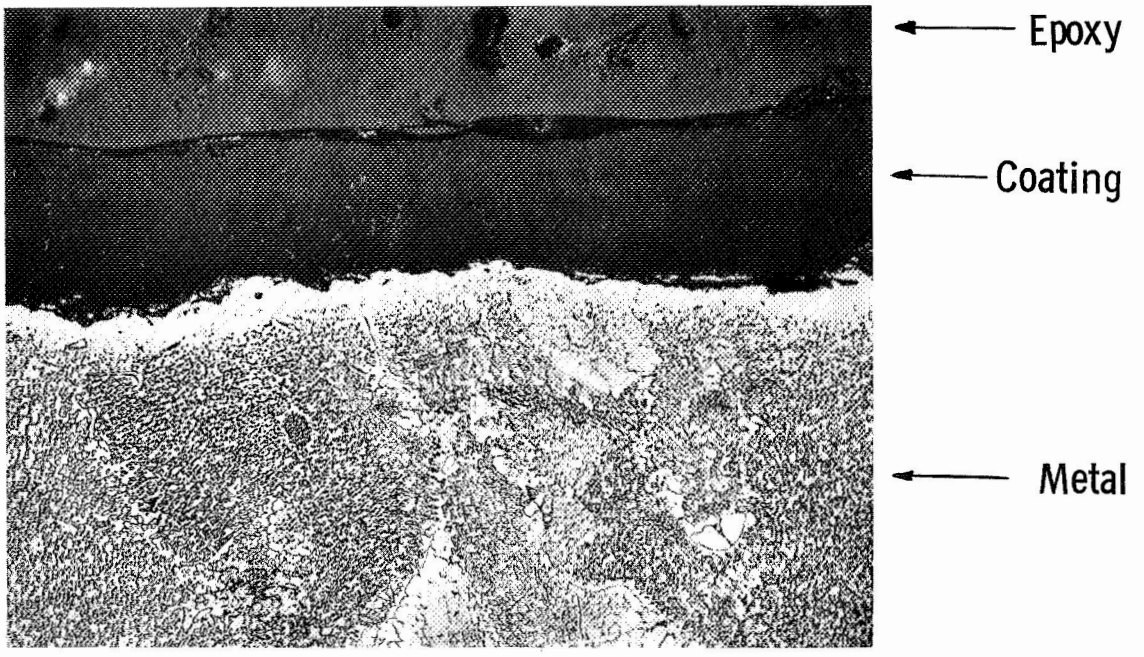

Fig. 40(a) —Glass 23-1 on IN-100 (I-23) - As coated (500X)

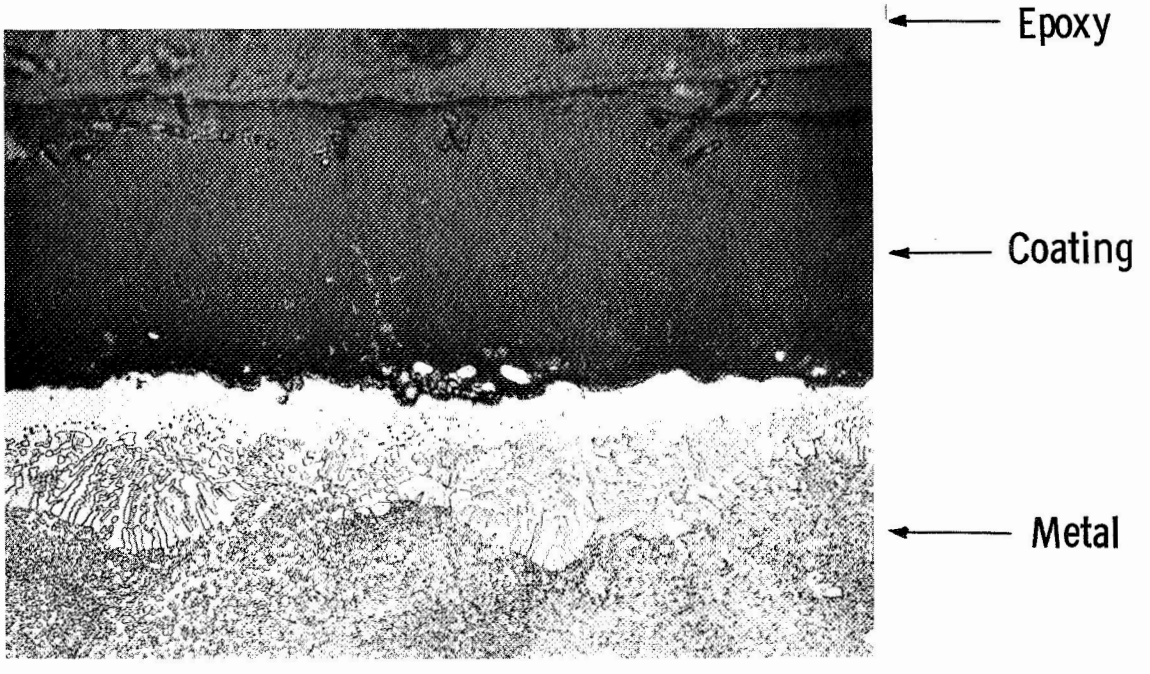

Fig. 40(b) —Glass 23-1 on IN-100 (I-23) - 20 hours cyclic oxidation 1149°C (500X)

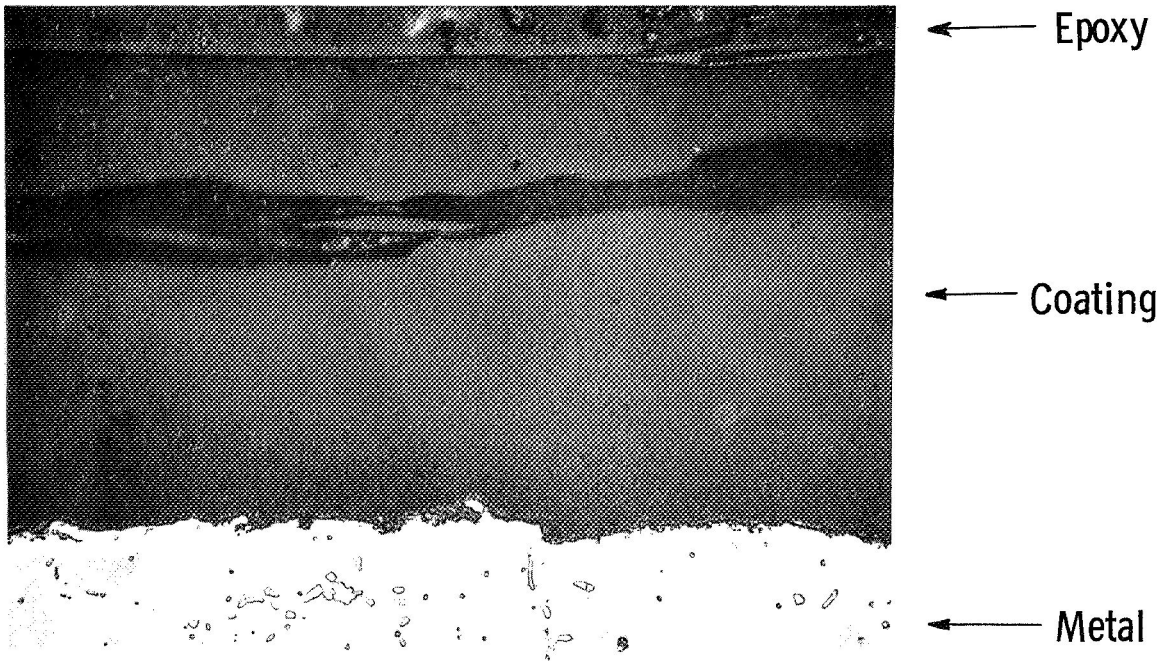

Fig. 41(a)—Glass 25 on IN-100 (I-25) - As coated (500X)

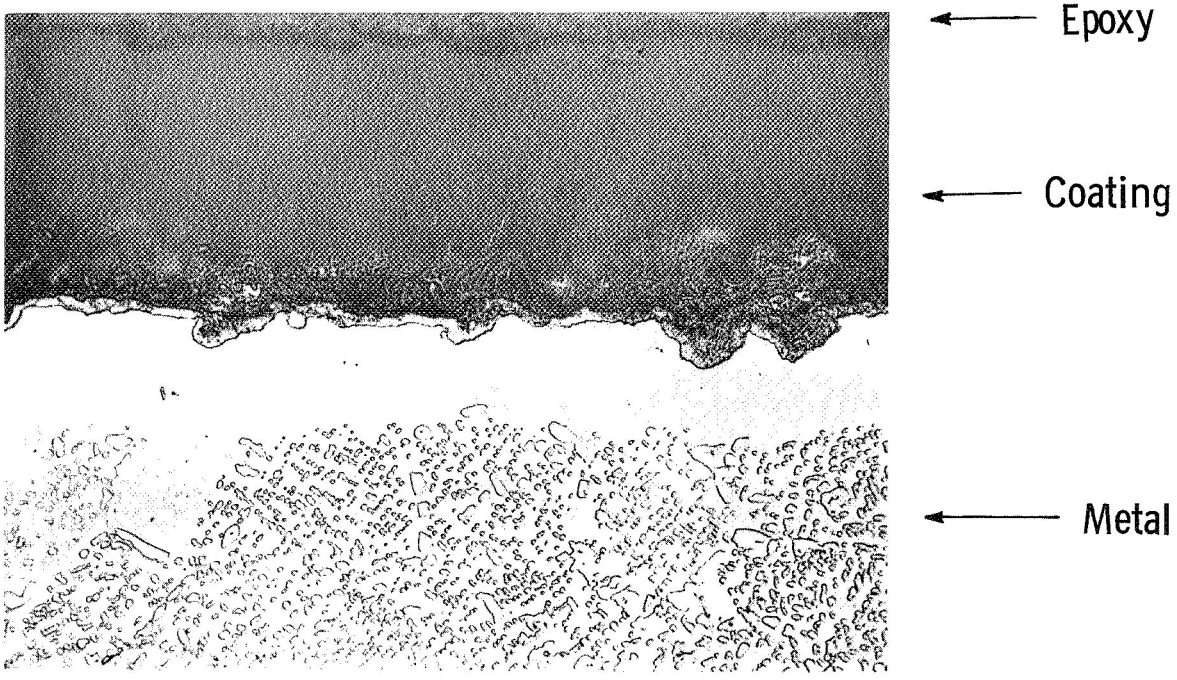

Fig. 41(b)—Glass 25 on IN-100 (I-25) - 100 hours cyclic oxidation 1149°C (500X)

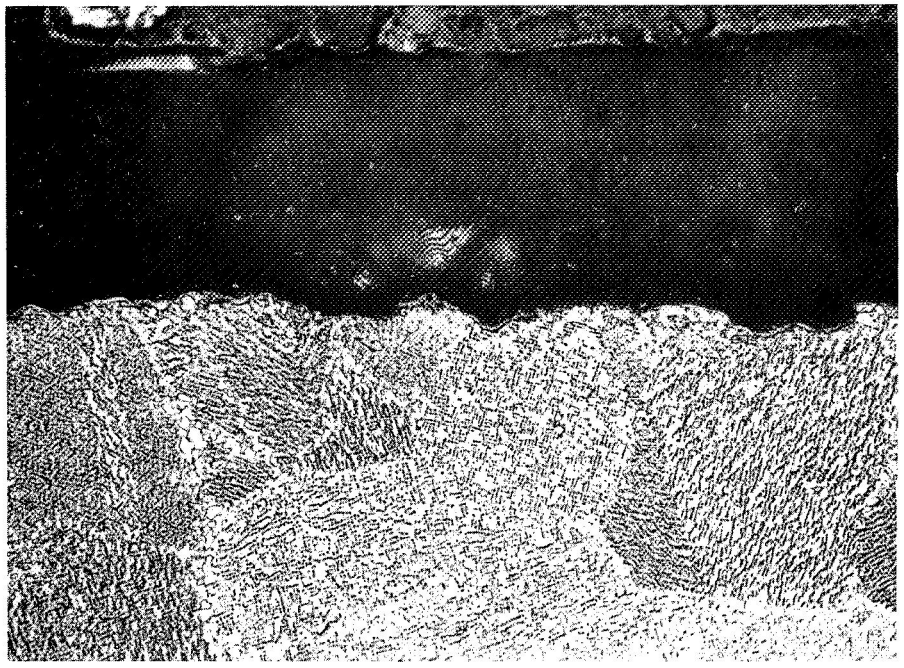

Fig. 42(a)—Glass 25 on IN-100 (I-25) - 6 hours cyclic spin 1149°C (500X)

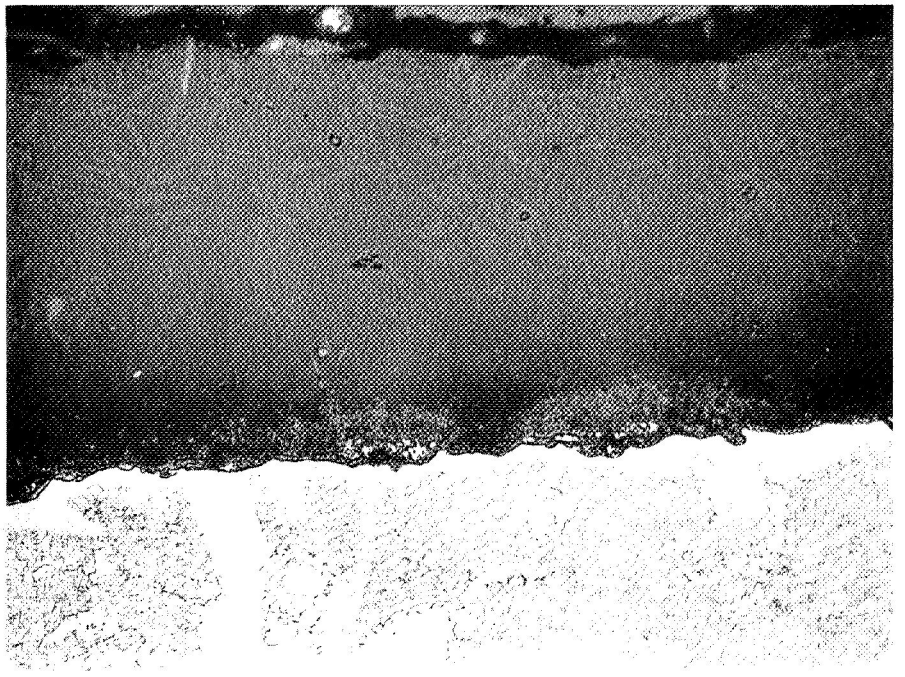

Fig. 42(b)—Glass 25 on IN-100 Front - After 100 hours turbine simulator 1038°C (500X)

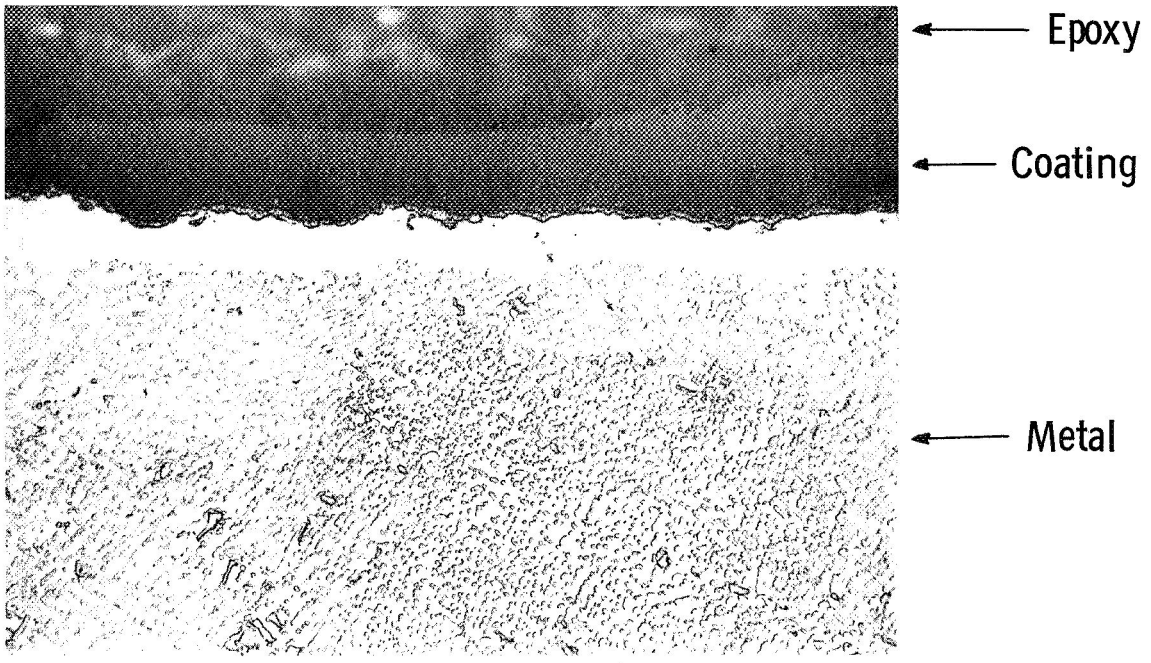

Fig. 43(a) —50% of SiO_2 on GC IN-100 (I-94) - 6 hours cyclic spin 1149°C (500X)

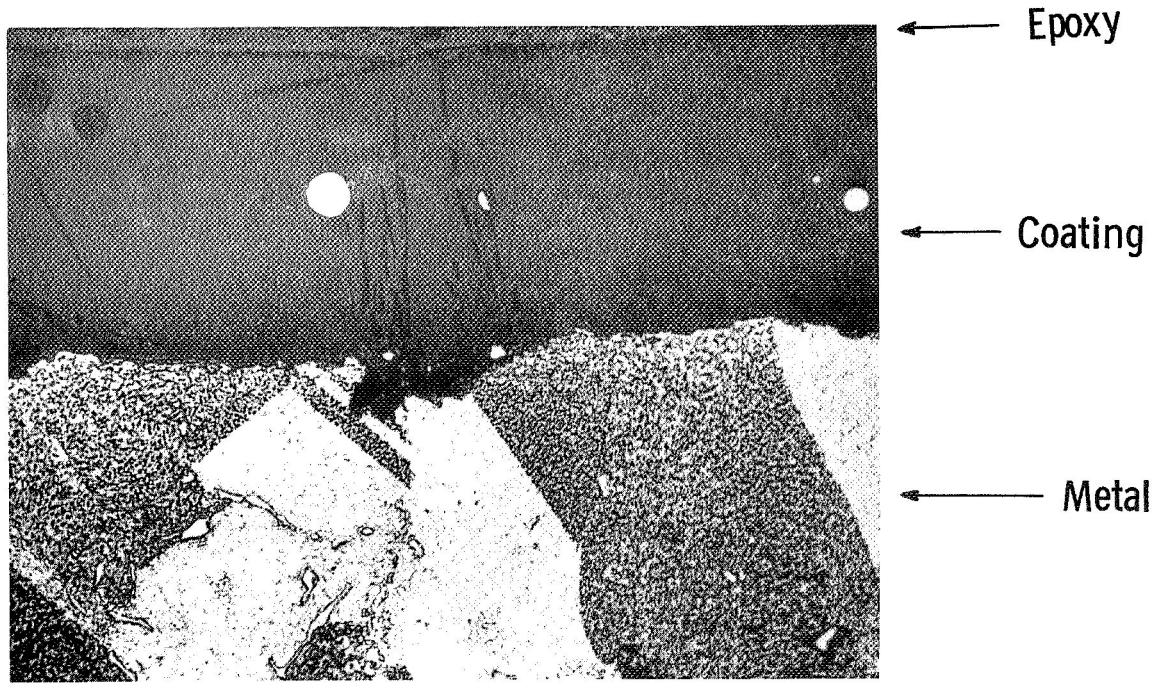

Fig. 43(b) —50% of SiO_2 on GC IN-100 (I-94) - 6 hours turbine simulator 1038°C (500X)

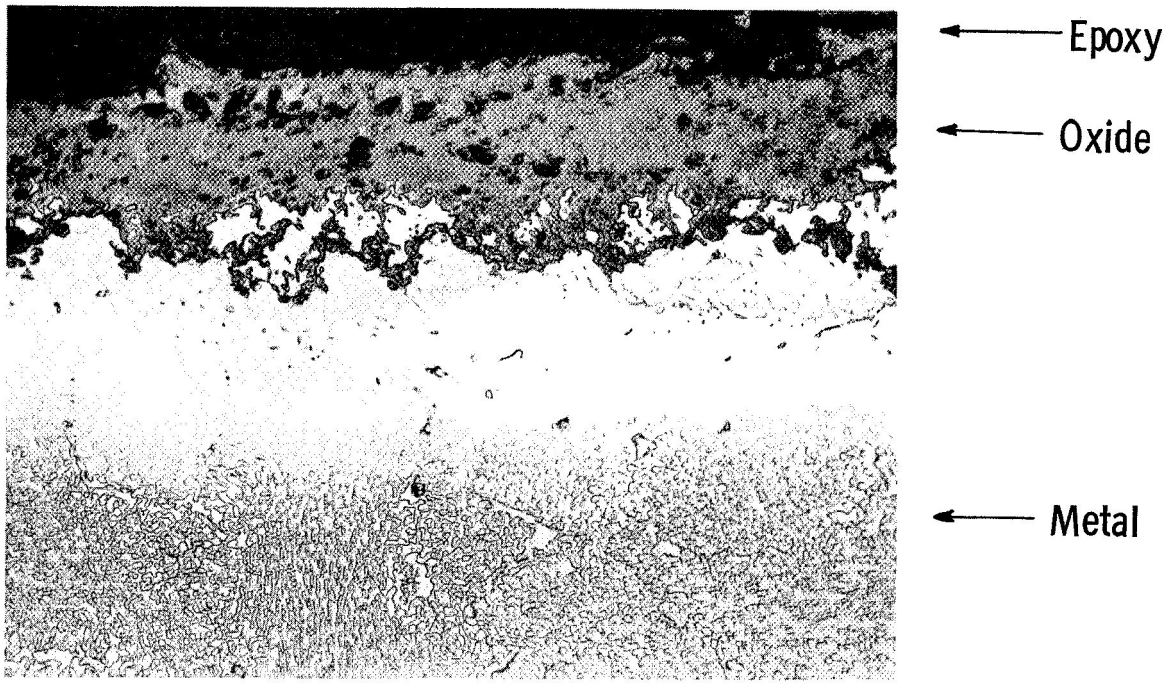

Fig. 44—Uncoated IN-100 - Front - After 76 hours turbine simulator 1038°C (500X)

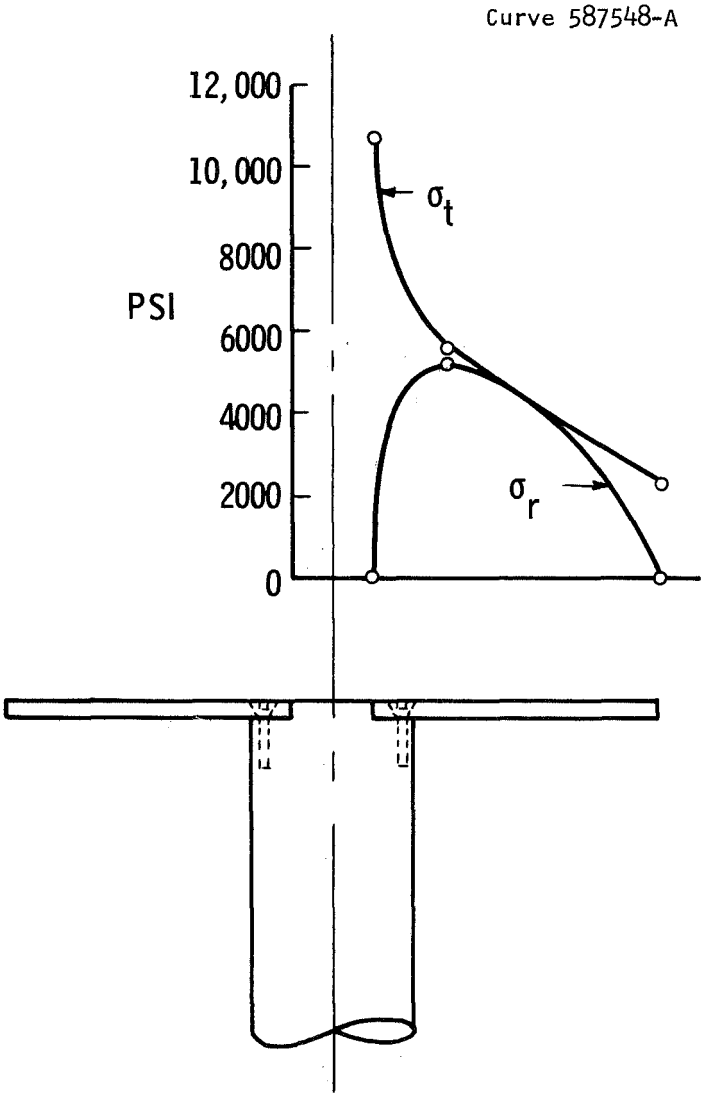

Fig. 45—Tangential and radial stresses in a rotating disk

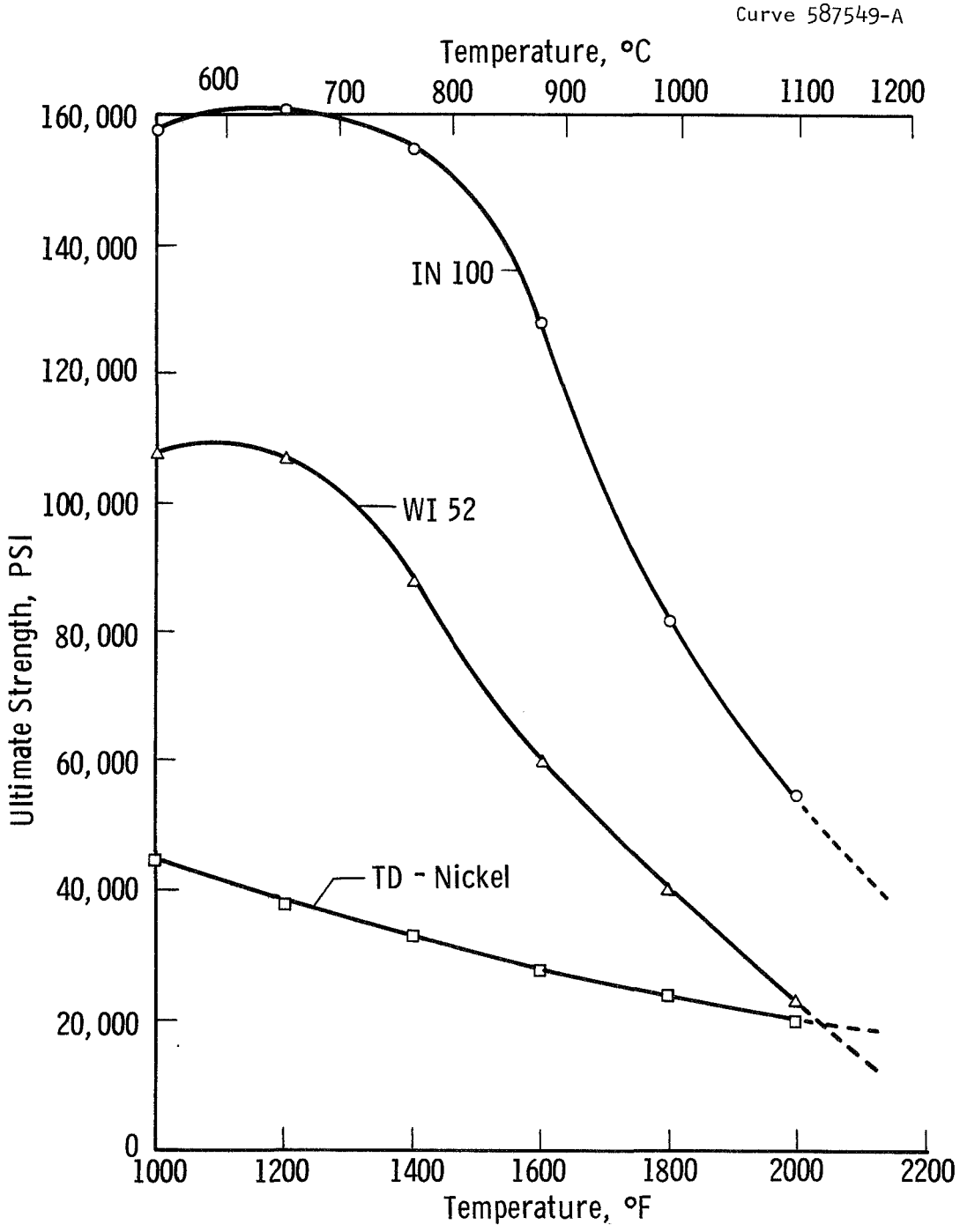

Fig. 46—Ultimate strengths

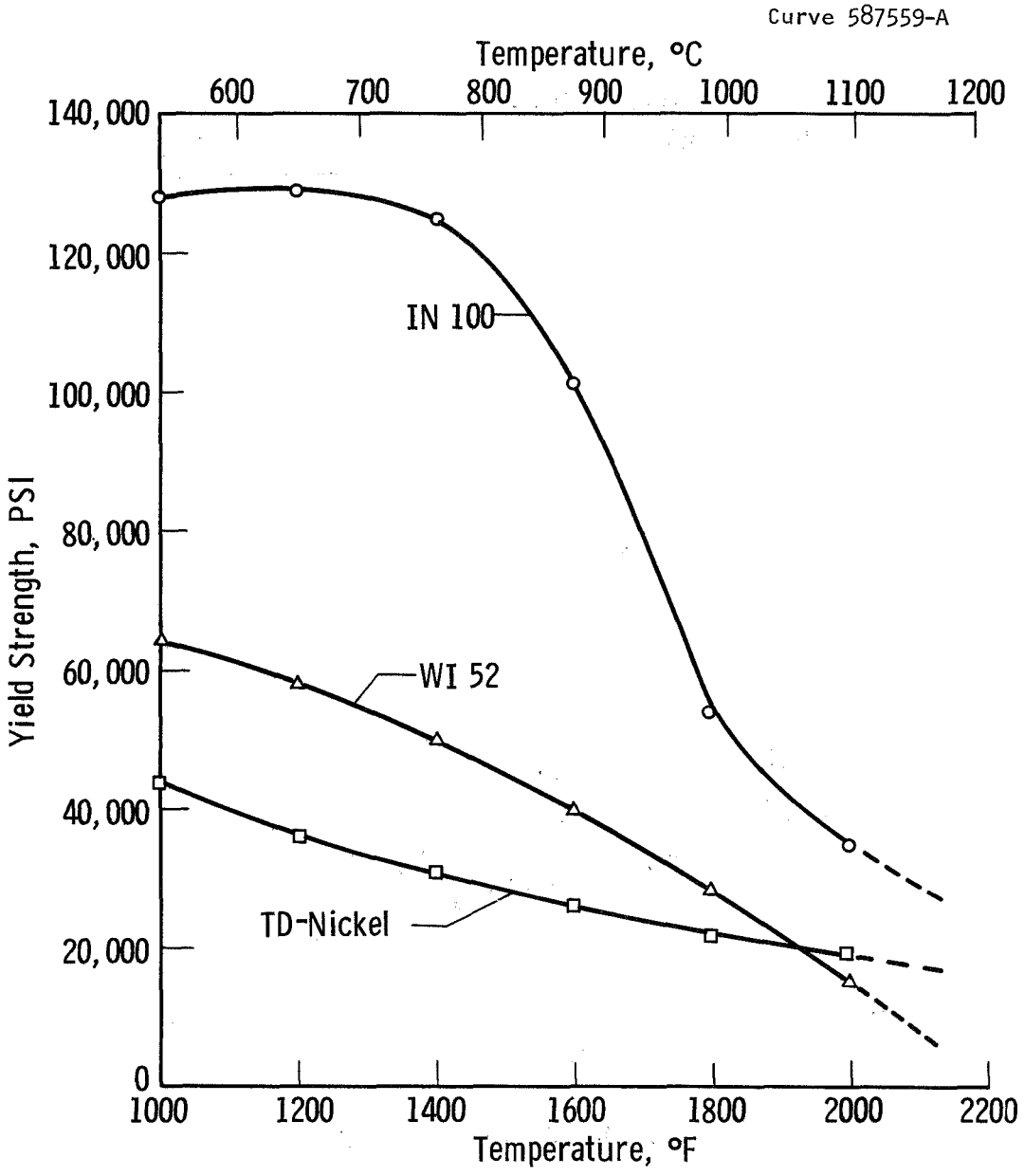

Fig. 47—Yield strengths

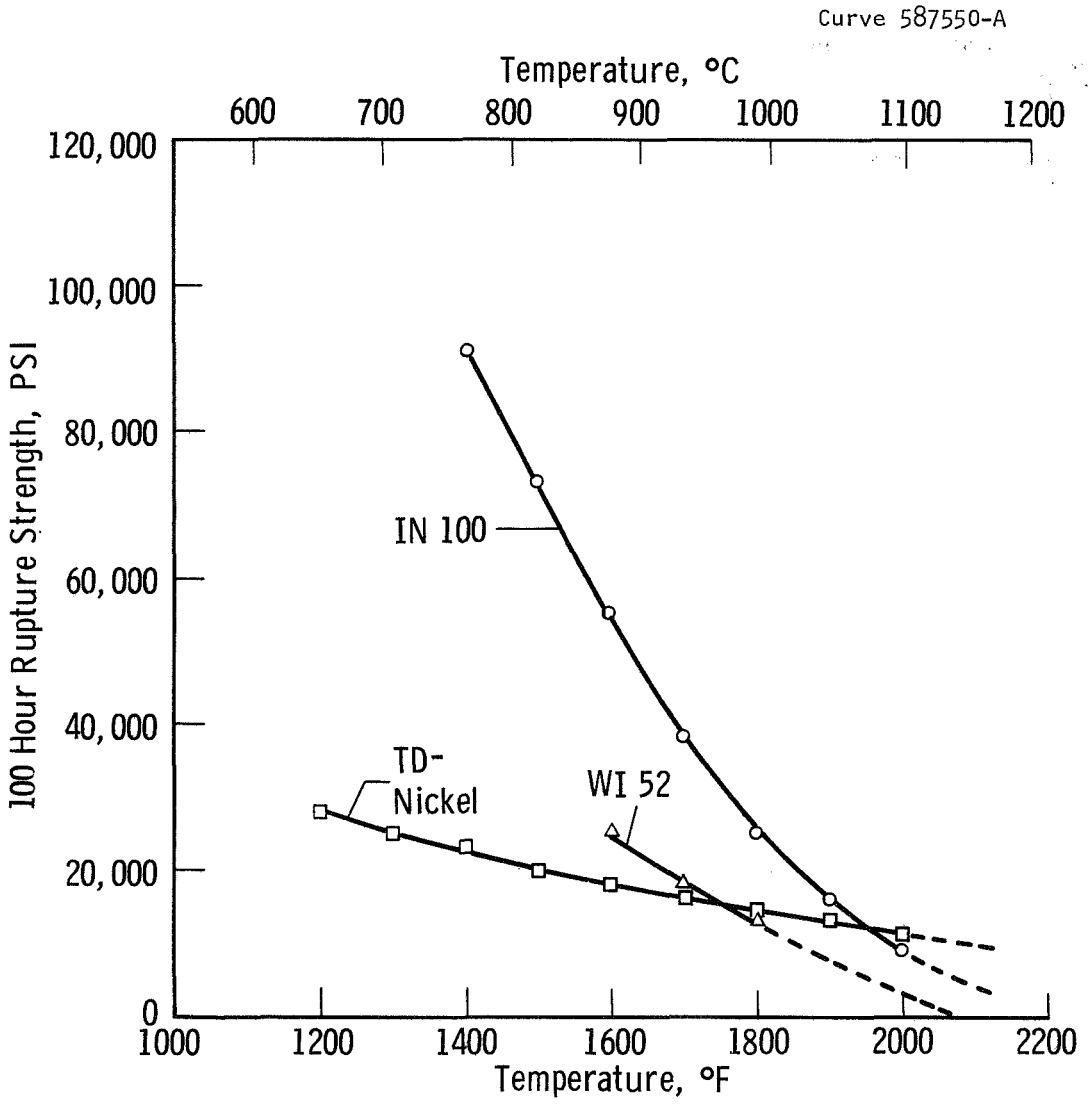

Fig. 48 —100 hour rupture strength

FINAL REPORT - DISTRIBUTION LIST
CONTRACT NAS3-10486

(The number in parentheses is the number of copies sent to each addressee)

NASA Headquarters
600 Independence Avenue
Washington, D.C. 20546

Attention: RAP/N. F. Rekos (1)
RRM/G. C. Deutch (1)
RRM/R. H. Raring (1)

NASA-Ames Research Center
Moffett Field, California 94035
Attention: Library (1)

NASA-Flight Research Center
P.O. Box 273
Edwards, California 93523
Attention: Library (1)

NASA-Goddard Space Flight Center
Greenbelt, Maryland 20771
Attention: Library (1)

Jet Propulsion Laboratory
4800 Oak Grove Drive
Pasadena, California 91102
Attention: Library (1)

NASA-Langley Research Center
Langley Field, Virginia 23365
Attention: 214/Irvin Miller (1)
Library (1)

NASA-Manned Space Flight Center
Houston, Texas 77058
Attention: Library (1)

NASA-Marshall Space Flight Center
Huntsville, Alabama 35812
Attention: Library (1)

Air Force Office of Scientific Research
Propulsion Research Division
USAF Washington, D.C. 20525
Attention: Library (1)

Defense Documentation Center (DDC)
Cameron Station (1)
5010 Duke Street
Alexandria, Virginia 22314

NASA-Lewis Research Center
21000 Brookpark Road
Cleveland, Ohio 44135

Attention: 105-1/G. M. Ault (1)
3-19/Technology Utilization Office (1)
49-1/S. Grisaffe (2)
105-1/N. T. Saunders (1)
60-3/Library (2)
5-5/Report Control Office (1)
106-1/R. E. Oldrieve (10)
106-1/A. E. Anglin (1)
77-3/Aeronautics Procurement Soc. (1)
5-3/A. Ginsburg (1)
60-4/J. Howard Childs (1)
105-1/W. D. Klopp (1)
105-1/R. W. Hall (1)
49-1/J. C. Freche (1)
49-1/H. B. Probst (1)

NASA Scientific and Technical Information Facility
P.O. Box 33
College Park, Maryland 20740 (6)

FAA Headquarters
800 Independence Avenue, S.W.
Washington, D.C. 20553

Attention: Brig. Gen. J. C. Maxwell (1)
SS/210/F. B. Howard (1)

U.S. Atomic Energy Commission
Washington, D.C. 20545
Attention: Technical Reports Library (1)

Oak Ridge National Laboratory
Oak Ridge, Tennessee 37830
Attention: Technical Reports
Library (1)

Department of the Navy (1)
ONR
Code 429
Washington, D.C. 20525

Headquarters
Wright-Patterson AFB, Ohio 45433
Attention: MAMP (1)
MATB (1)
MAAM/Technical
Library (1)
AFSC-FTDS (1)
AFML:MAM (1)
MAG/Directorate of
Materials (1)

U.S. Army Aviation Materials
Laboratory
Fort Eustis, Virginia 23604
Attention: SMOFE-APG/John White
Chief (1)

Bureau of Naval Weapons
Department of the Navy
Washington, D.C. 20525
Attention: RRMA-2/T. F. Kearns
Chief (1)

Army Materials Research Agency
Watertown Arsenal
Watertown, Massachusetts 02172
Attention: Director (1)

Battelle Memorial Institute
505 King Avenue
Columbus, Ohio 43201
Attention: Defense Metals
Information Center
(DMIC)(1)
Dr. R. I. Jaffee (1)

Aerospace Corporation (1)
Reports Acquisition
P.O. Box 95085
Los Angeles, California 90045

Advanced Metals Research Corporation
149 Middlesex Turnpike
Burlington, Massachusetts 01804
Attention: J. T. Norton (1)

Allegheny Ludlum Steel Corporation
Research Center
Alabama and Pacific Avenues
Brackenridge, Pennsylvania 15014
Attention: Library (1)

American Society for Metals
Metals Park
Novelty, Ohio 44073
Attention: Library (1)

Avco Space Systems Division
Lowell Industrial Park
Lowell, Massachusetts 01851
Attention: Library (1)

The Bendix Corporation
Research Laboratories Division
Southfield, Michigan 48075
Attention: Library (1)

Boeing Company
P.O. Box 733
Renton, Washington 98055
Attention: SST Unit Chief
W. E. Binz (1)

Case Western Reserve University
University Circle
Cleveland, Ohio 44106
Attention: Library (1)

Chromalloy Corporation
169 Western Highway
West Nyack, New York 10994
Attention: Mr. L. Maisel (1)

Denver Research Institute
University Park
Denver, Colorado 80210
Attention: Library (1)

Douglas Aircraft Company MFSD
3000 Ocean Park Blvd.
Santa Monica, California 90406
Attention: Library (1)

Fansteel Metallurgical Corporation
Number One Tantalum Place
North Chicago, Illinois 60064
Attention: Library (1)

Ford Motor Company
Materials Development Department
20000 Rotunda Drive
P.O. Box 2053
Dearborn, Michigan 48123
Attention: Mr. Y. P. Telang (1)

Firth Sterling, Inc.
Powder Metals Research
P.O. Box 71
Pittsburgh, Pennsylvania 15230
Attention: Library (1)

General Electric Corporation
Advanced Technology Laboratory
Schenectady, New York 12305
Attention: Library (1)

General Electric Corporation
Materials Development Lab. Oper.
Advance Engine and Tech. Dept.
Cincinnati, Ohio 45215

General Motors Corporation
Allison Division
Indianapolis, Indiana 46206
Attention: Mr. D. K. Hanink (1)
Materials Lab

General Technologies Corporation
708 North West Street
Alexandria, Virginia 22314
Attention: Library (1)

E. I. DuPont de Nemours and Co., Inc.
Pigments Dept. Metal Products
Wilmington, Delaware 19898
Attention: Library (1)

IIT Research Institute
Technology Center
Chicago, Illinois 60616
Attention: Mr. V. Hill (1)
Library (1)

Ilikon Corporation
Natick Industrial Center
Natick, Massachusetts
Attention: Library (1)

International Nickel Company
P. D. Merica Research Lab
Sterling Forest
Suffern, New York 10901
Attention: Library (1)

Arthur D. Little, Inc.
20 Acorn Park
Cambridge, Massachusetts
Attention: Dr. J. D. Berkowitz (1)

Lockheed Palo Alto Research Labs
Material and Science Lab 52-30
3251 Hanover Street
Palo Alto, California 94304
Attention: Mr. R. Perkins (1)

Massachusetts Institute of Tech.
Metallurgy Dept., RM 8-305
Cambridge, Massachusetts 02139
Attention: Library (1)

Narmco Research & Development Div.
Whittacker Corporation
3540 Aero Court
San Diego, California 92123
Attention: Library (1)

Nuclear Materials Company
West Concord, Massachusetts 01781
Attention: Library (1)

Ohio State University
Columbus, Ohio 43210
Attention: Library (1)

Rensselaer Polytechnic Institute
Troy, New York 12180
Attention: Library (1)

Sherritt Gordon Mines, Ltd.
Research and Development Division
For Saskatchewan, Alberta, Canada
Attention: Library (1)

Solar Division
International Harvester Corporation
San Diego, California 92112
Attention: Mr. A. R. Stetson (1)

Stanford Research Institute
Menlo Park, California
Attention: Library (1)

Stanford University
Palo Alto, California 94305
Attention: Library (1)

Westinghouse Electric Corporation
Westinghouse Astronuclear Lab
P.O. Box 10864
Pittsburgh, Pennsylvania 15236
Attention: D. Goldberg (1)

TRW Electromechanical Division
TRW Inc.
23555 Euclid Avenue
Cleveland, Ohio 44117
Attention: Mr. J. Gadd (1)
Dr. J. Sawyer

Union Carbide Corporation
Stellite Division
Technology Department
Kokomo, Indiana 46901
Attention: Technical Library (1)

United Aircraft Corporation
400 Main Street
East Hartford, Connecticut 06108
Attention: Research Library (1)
E. F. Bradley, Chief (1)
Materials Engineering
Frank Talboom (1)

United Aircraft Corporation
Pratt and Whitney Division
West Palm Beach, Florida 33402
Attention: D. Maxwell (1)

Universal-Cyclops Steel Corporation
Bridgeville, Pennsylvania 15017
Attention: Library (1)

Spartan Aviation
Tulsa, Oklahoma
Attention: Mr. M. Ortner (1)

Wah Chang Corporation
Albany, Oregon 97321
Attention: Library (1)

COATINGS ADDENDUM

AFML (MAMP)
Wright-Patterson AFB, Ohio 45433
Attention: Mr. N. Geyer (1)

Bureau of Naval Weapons
Department of the Navy
Washington, D.C. 20525
Attention: Mr. I. Machlin (1)

Alloy Surfaces, Inc.
100 South Justison Street
Wilmington, Delaware 19899
Attention: Mr. George H. Cook (1)

Battelle Memorial Institute
505 King Avenue
Columbus, Ohio 43201
Attention: Mr. E. Bartlett (1)

City College of New York
Department of Chemical Engineering
New York, New York 10031
Attention: Mr. R. A. Graff (1)
Mr. M. Kolodney (1)

E. I. DuPont de Nemours and Co.
1007 Market Street
Wilmington, Delaware 19898
Attention: Dr. Warren I. Pollack (1)

General Electric Company
Materials Development Lab Oper.
Advance Engine and Tech. Dept.
Cincinnati, Ohio 45215
Attention: Mr. J. Levinstein (1)
Mr. J. W. Clark (1)

Howmet Corporation
Misco Division
One Misco Drive
Whitehall, Michigan 49461
Attention: Mr. S. Wolosin (1)

Pratt & Whitney Division of (1)
United Aircraft Corporation
Manufacture Engineering
Aircraft Road
Middletown, Connecticut 06457

Sylvania Electric Products
Sylcor Division
Cantiague Road
Hicksville L.I., New York 11802
Attention: Mr. L. Sama (1)

Texas Instruments, Inc.
Materials and Controls Division
P.O. Box 5474
Dallas, Texas 75222
Attention: Mr. Gene Wakefield (1)

U.S.A.F.
San Antonio Air Material Area
Kelly Air Force Base, Texas 78241
Attention: SANEPJ/A. E. Wright, Chief
Jet Engine Section (1)

University of Dayton
Research Institute
300 College Park Avenue
Dayton, Ohio 45409
Attention: Library (1)

University of Illinois
Department of Ceramic Engineering
Urbana, Illinois 61801
Attention: Mr. J. Wurst (1)

University of Pittsburgh
Center for Study of Thermodynamic
Properties of Materials
409 Engineering Hall
Pittsburgh, Pennsylvania 15213
Attention: Dr. G. R. Fitterer (1)

University of Washington
Ceramics Department
Seattle, Washington 98101
Attention: Dr. J. Mueller (1)

Westinghouse Electric Corporation
Research Laboratories
Beulah Road, Churchill Boro
Pittsburgh, Pennsylvania 15235
Attention: Mr. R. Grekila (1)

Whitfield Laboratories (1)
P.O. Box 287
Bethel, Connecticut 06801